Electroweak Phase Transition in the Standard Model and its Inert Higgs Doublet Extension

vorgelegt von

Manuel Meyer

von Ohmstal LU

Supervisor:
Prof. Dr. Mikko Laine
Albert Einstein Center for Fundamental Physics
Institute for Theoretical Physics, Universität Bern

Co-Supervisor:
Dr. Germano Nardini
Albert Einstein Center for Fundamental Physics
Institute for Theoretical Physics, Universität Bern

Electroweak Phase Transition in the Standard Model and its Inert Higgs Doublet Extension

Inauguraldissertation
der Philosophisch-naturwissenschaftlichen Fakultät
der Universitat Bern

vorgelegt von

Manuel Meyer

von Ohmstal LU

Supervisor:
Prof. Dr. Mikko Laine
Albert Einstein Center for Fundamental Physics
Institute for Theoretical Physics, Universität Bern

Co-Supervisor:
Dr. Germano Nardini
Albert Einstein Center for Fundamental Physics
Institute for Theoretical Physics, Universität Bern

Von der Philosophisch-naturwissenschaftlichen Fakultät angenommen.

Bern, 31.08.2017   Der Dekan:

Prof. Dr. Gilberto Colangelo

to Larissa

May you live forever in our thoughts and hearts.

Abstract

The origin of the asymmetry between matter and anti-matter is an interesting but yet unresolved problem of modern physics. To realize a net production of more baryons than anti-baryons a system has to depart from thermal equilibrium. A first order electroweak phase transition in the evolution of the early universe could account for a stage of non-equilibrium. This thesis is meant to examine this transition within the Standard Model and its inert Higgs doublet extension. The main parts of this thesis are chapters 2 and 3 which are based on our papers [1] and [2] respectively.

Even though there is no electroweak phase transition within the Standard Model, its thermodynamics across the crossover shows interesting features at temperatures around $T \sim 160$ GeV. Although the system does not leave thermal equilibrium its dynamics deviate from ideal gas thermodynamics. The Standard Model, lacking a first order phase transition, cannot account for the baryon asymmetry of the universe but its background can still have an impact on non-equilibrium physics taking place at temperatures around $T \sim 160$ GeV. We study the relevant thermodynamical functions across the electroweak crossover in a perturbative three-loop computation and by making use of results from lattice simulations based on a dimensionally reduced effective theory.

Many extensions of the Standard Model include an extended Higgs sector where scalar couplings are faced with conflicting requirements. Small couplings are needed to predict the measured dark matter relic abundance, whereas large couplings strengthen a first order phase transition. Large couplings, however, can compromise perturbative studies and spoil the high-temperature expansion needed for dimensionally reduced lattice simulations. Within the Inert Doublet Model we compute the resummed two-loop effective potential and we compare physical parameters related to the electroweak phase transition, e.g. the latent heat, the critical temperature and the discontinuity of the transition, with the high-temperature expansion. We also provide master integral functions for a model independent computation of a two-loop potential.

Acknowledgements

First and foremost I thank my supervisor, Mikko Laine, for his support, advise, guidance and fruitful discussions in the past years. It was an exceptional experience to learn and work with him and to benefit from his expertise and knowledge.

I also thank Germano Nardini for his co-supervision of my thesis. I cherished all the discussions and talks we had and I am grateful that he always showed me where to put my finger on by asking the right questions.

I thank Kimmo Kainulainen for being the co-referee of my thesis and the external expert on the defense committee.

For interesting conversations and discussions about various topics in physics I thank my fellow graduate students Stephan Caspar and Jason Aebischer. I also enjoyed our talks and activities beyond physics.

I thank my parents, Sepp and Vreni and my brother Philipp for their love and support throughout all these years. I thank my roommates Bä, Marc, Stylo and Brönni for putting up with me at all times and for providing distractions from continuous calculations. Never forget the simple truth that more gratinity equals more happiness. Of all my friends I especially thank Paikea for her support during difficult times and good ones. I also thank Gion for his relentless teasing to get my Ph.D. and helping me improve my cooking skills.

For discussions about life, the universe and everything and for the diversion from sitting in the office all day long I thank my dancing partner Niki.

This thesis is dedicated to my best friend Larissa. You will forever be kept in our hearts as if you never left.

Contents

Notations

In this thesis we use natural units where the speed of light c, the Boltzmann constant k_B as well as the reduced Planck constant $\hbar$ are set to unity. Furthermore, there are a couple of definitions and notations we list here.

For estimations of a certain scale we use a generic coupling constant

$$g^2 \in \{g_1^2, g_2^2, g_3^2, \lambda, h_t^2\} \; ,$$

where the couplings g_1, g_2 and g_3 are the gauge couplings of the gauge groups $U(1), SU(2)$ and $SU(3)$ respectively. The Higgs scalar self coupling is λ and h_t is the top Yukawa coupling. We consider all other fermions to be massless.

We use the $\overline{\text{MS}}$ renormalization scheme at the scale $\bar{\mu}$ and dimensional regularization in $D = d + 1 = 4 - 2\epsilon$ dimensions. Integrals over four-dimensional momentum space are depicted as

$$\int_K \equiv \left(\frac{e^{\gamma_E} \bar{\mu}^2}{4\pi} \right)^\epsilon \int \frac{d^{4-2\epsilon} k}{(2\pi)^{4-2\epsilon}} \; ,$$

where γ_E is the Euler-Mascheroni constant. At finite temperature, we introduce Matsubara frequencies for the temporal component k_0 of the momentum

$$K = (k_0, \vec{k}) \quad \Rightarrow \quad K^2 = k_0^2 + k^2 \; .$$

Therefore, an integration over $(4-2\epsilon)$-dimensional momentum space is expressed via the sum-integral

$$\sum\!\!\!\!\!\!\int_K = T \sum_{k_0} \int_k \; , \qquad \int_k \equiv \left(\frac{e^{\gamma_E} \bar{\mu}^2}{4\pi} \right)^\epsilon \int \frac{d^{3-2\epsilon} k}{(2\pi)^{3-2\epsilon}} \; .$$

Introducing the inverse temperature $\beta = 1/T$, the integration over space-time in position space is

$$\int_X = \int_0^\beta d\tau \int_x \; , \qquad \int_x \equiv \left(\frac{e^{\gamma} \bar{\mu}^2}{4\pi} \right)^{-\epsilon} \int d^{3-2\epsilon} x \; .$$

The Matsubara frequencies are sometimes denoted ω_n corresponding to their respective mode for bosons $\omega_n = 2\pi n T$ or fermions $\omega_n = (2n+1)\pi T$, with $n \in \mathbb{Z}$. This should not be confused with the energy $\omega_i^k = \sqrt{k^2 + m_i^2}$. Propagators can then equivalently be written as

$$\frac{1}{K^2 + m_i^2} = \frac{1}{k_0^2 + k^2 + m_i^2} = \frac{1}{\omega_n^2 + (\omega_i^k)^2} \; .$$

Chapter 1

Introduction

The universe and our physical description thereof is fascinating on all length scales, ranging from cosmological large scale structures like galaxy clusters to subatomic particles and their elementary constituents. In the very early universe, those scales were close to each other but through the expansion of the universe they have diverged significantly. Objects at a cosmological scale are described by the theory of general relativity, whereas the theory of subatomic particles and their interactions is described by the Standard Model.

The Standard Model of particle physics (SM) is a gauge theory that incorporates the theory of electromagnetism as well as the weak and strong interactions. The quantum field theory of electromagnetism is described by quantum electrodynamics (QED) through the gauge group $U(1)$ and the gauge group of the weak interactions is $SU(2)$. The mediators of electroweak gauge group $SU(2) \times U(1)$ are the massless photon and the massive $W^\pm$ and Z bosons. Quantum chromodynamics (QCD) is the theory of strong interactions with symmetry group $SU(3)$ and its gauge fields are the gluons. The gauge group of the Standard Model is then written as

$$G_{\mathrm{SM}} = SU(3) \times SU(2) \times U(1) \ .$$

The three gauge groups all have different couplings which depend on the energy scale. This dependence is also called the running of the couplings and it is described by beta-functions in renormalization group equations.

If we run the couplings to a higher temperature scale, it is like going backward in time to the early universe. And if the couplings were to meet in one point, it could give rise to a unified description in a so called Grand Unified Theory (GUT). Unfortunately, within the Standard Model this is not the case. The introduction of supersymmetry potentially solves this unification but there are also other models with different higher gauge groups claiming to explain grand unification. The idea in all these models is a theory with more symmetries that are then broken through multiple steps to ultimately reproduce the Standard Model symmetry group.

One such symmetry breaking pattern, or restoration if we consider going from low to high temperatures, has been described a long time ago. The theory of the unification of the electromagnetic and the weak force was originally described by Glashow, Weinberg and Salam [3–5]. However, in this model, the two couplings of the electromagnetic and the weak interactions do not combine

into one single coupling at some high scale but are rather a different set of couplings related through the Weinberg angle. As the plasma of the early universe cooled down, the electroweak symmetry was spontaneously broken to give rise to the weak and the electromagnetic forces. The theoretical description of the breaking of this symmetry that is now called the Higgs mechanism, where the Higgs field acquires a non-zero vacuum expectation value, has been around for quite a while [6, 7].

The scale at which the transition from the symmetric phase to the broken Higgs phase takes place is called the electroweak scale. The interest in physics at this scale has been around for a long time and has not yet diminished. The topic of this thesis is to study this transition within the Standard Model and within a simple extension thereof.

The ultimate goal of theoretical physics would of course be to also include gravitational interactions into a theory of quantum field theory. Although attempts are made to give a description of such a theory of quantum gravity or Theory Of Everything, e.g. string theory, this holy grail of particle physics remains to be found.

In this introductory chapter, we first take a look at baryogenesis in section 1.1, which is the reason we study the electroweak phase transition in the first place. Such transitions and especially cosmological phase transitions are described in section 1.2. We then provide a brief introduction into some relevant features of thermal field theory in section 1.3.

The outline of this thesis is as follows. After the introduction, we study in chapter 2 the thermodynamics across the electroweak crossover within the Standard Model. In chapter 3 we extend the Standard Model by a second scalar doublet and compare its two-loop effective potential with the high-temperature expansion. We then conclude in chapter 4 and give a brief outlook into current and future experiments. We provide derivations of vacuum integral functions and a summary of the master integrals as well as their high-temperature expansions in Appendix A. For the Inert Doublet Model we list the results of all diagrams contributing to the potential at two-loop order in Appendix B and give the expressions for the counterterms and pole masses in Appendix C.

1.1   Baryogenesis

Physics and especially our mathematical description thereof is built on symmetries. The principle of reproducibility of an experiment states that physicists all over the world or even in space can conduct the same experiments at any time and should get the same results. This universality of physical laws is one among many such symmetries.

As the universe was created in the big bang, matter, but also anti-matter, was produced and in a world governed by symmetries one would expect this creation to be symmetric. What we observe however, is that this symmetry is broken in our universe and that a small part of baryonic matter survived up until today which builds up all the planets, stars and galaxies. The creation of this baryon asymmetry of the universe, i.e. the excess of baryons over anti-baryons, is called baryogenesis.

The other possibility, the asymmetric case of the big bang where there is a net

baryon number in the plasma of the very early universe, is spoiled by inflation. The theory of inflation was developed in the early 1980s as a possible solution to the horizon and flatness problems and as an explanation to homogeneity and isotropy of our universe [8–10]. During inflation, a short period of time where the expansion of the universe is exponentially fast, all initial irregularities, e.g. a baryon excess, are diluted (for a review of inflation, see e.g. ref. [11]). Therefore, we consider an initially matter anti-matter symmetric universe.

A particle will annihilate with its anti-particle and produce two photons in the process. Therefore, a measurement of photons is needed to deduce the ratio between photons and baryonic matter. The measurement of these photons, i.e. the Cosmic Microwave Background (CMB), was carried out by Penzias and Wilson in 1964 [12] for the first time and many times ever since, with the most accurate data coming from the two satellites WMAP (Wilkinson Microwave Anisotropy Probe) [13, 14] and Planck [15, 16].

Not only are the results from these two satellites for the fluctuations of the cosmic microwave background extremely accurate and can resolve temperature differences of $10^{-3}K$, but they also agree beautifully with Big Bang Nucleosynthesis (BBN, see [17] and references therein). Big bang nucleosynthesis [18, 19] tells us about the abundance of light elements created in the early universe and thus gives the second ingredient for the aforementioned fraction of photons to baryons. This ratio of baryons to photons is [15]

$$\eta = \frac{n_B}{n_\gamma} = 6.05(7) \times 10^{-10} \ . \tag{1.1.1}$$

From this we learn that even though there is an enormous number of stars and galaxies in our universe, the initial discrepancy between matter and anti-matter was tiny.

On the other hand, one could also think of a universe with no net baryon number where different regions are either dominated by matter or anti-matter. However, on the surface where a matter-domain borders an anti-matter domain, large amounts of photons would be produced through annihilation of matter and anti-matter particles. There is good evidence that this is not the case [20].

A theory that wants to explain baryogenesis has to fulfill the three Sakharov conditions [21]. These conditions are:

- Violation of baryon number. Obviously to evolve from a symmetric state in the very early universe with $\Delta B = 0$ to a state where $\Delta B \neq 0$ non-conservation of baryon number is inevitable.

- Violation of charge conjugation C and simultaneous charge conjugation and parity CP. Violation of C symmetry is needed because otherwise an interaction which produces more baryons than anti-baryons would be counterbalanced through its charge conjugate process. Similarly, CP symmetry has to be violated to prevent the production of the same amount of left-handed baryons and right-handed anti-baryons and vice versa.

- Departure from thermal equilibrium. In thermal equilibrium and with CPT symmetry in place, even CP violating interactions would be countered by the equal and opposite back-reaction. Thus the system has to be out of equilibrium to produce a net baryon excess.

The aim of this thesis is to address the third Sakharov condition. As we will see in the next section, during a first order phase transition the system is not in equilibrium and thus meets the third Sakharov condition. A first order phase transition is therefore a good starting point for baryogenesis. If this transition is the one at the electroweak scale we speak of electroweak baryogenesis for which good reviews can be found in the literature, e.g. [22, 23].

There are, however, a lot of other scenarios addressing the issue of baryogenesis. As alluded to above, there might be more gauge symmetries at high temperatures described in a grand unified theory. GUT baryogenesis then corresponds to the breaking of this symmetry through a first order phase transition just like in the electroweak case.

By adding right-handed neutrinos to the Standard Model one could not only provide neutrino masses through the see-saw mechanism [24], but also spontaneously generate leptons from decays of these neutrinos. In this leptogenesis model [25] the produced lepton asymmetry could then be converted into a baryon asymmetry through electroweak sphalerons, which are introduced in the next section.

The last model we want to mention here originates from the supersymmetric extension of the Standard Model. It makes use of additional scalar fields in supersymmetry which have a shallow potential. During the inflationary epoch, a condensate can form along a so called flat direction and its non-zero vacuum expectation value can spontaneously break C and CP. If this direction has in addition a non-zero baryon number, this asymmetry remains when the condensate decays. This scenario is called the Affleck-Dine mechanism [22, 26].

1.2 Phase Transitions

Phase transitions occur in a wide range of different physical systems. What makes the study so interesting is the fact that these transitions are characterized through a handful of parameters which are universal and thus allow us to use one description for several apparently completely unrelated systems.

Phase transitions can either be of first or of second order and if no such transition occurs when the system changes from one phase to another we speak of a crossover. Latent heat is involved in a first order transition where the system absorbs or releases energy without changing its temperature. In such a transition both phases are present simultaneously in different parts of the system. This is not the case in a second order transition which is also called a continuous phase transition. In a phase diagram there is usually a first order transition line eventually ending at a critical point where a second order transition takes place. This leaves the rest of the parameter space open for a crossover from one phase to another.

The most intuitive phase transitions to us are transitions between different phases of matter, namely solids, liquids and gases. As an example of a first order phase transition we consider boiling water in a pan where at one point we can observe the creation of bubbles of water vapor at the bottom of the pan. These bubbles then rise to the water surface where the vapor is released. During this time of bubble nucleation there coexist both the liquid and the gaseous phase inside the pan and the temperature does not rise above the boiling temperature until all the water has evaporated. The amount of absorbed energy divided by
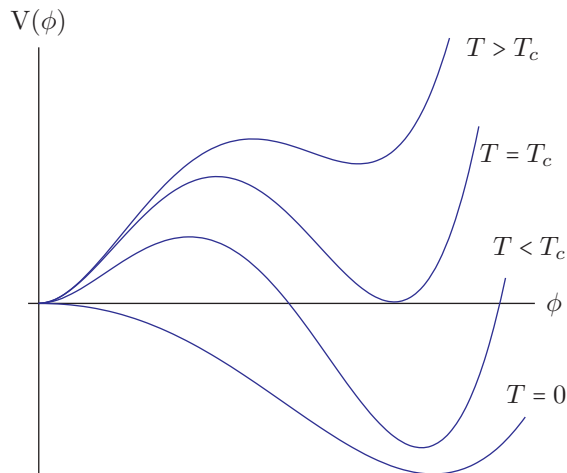
Figure 1.1: Schematic temperature evolution of a generic potential with a phase transition.

the mass of the water is exactly the latent heat.

However, we can also have a phase transition in a system that moves from a symmetric to a broken phase or vice versa. Such a transformation is usually attributed to a change in temperature such that broken symmetries are restored at high temperatures. Figure 1.1 shows a temperature-dependent potential at different temperatures where the symmetry is restored at high temperatures, i.e. with $\phi = 0$ being the global minimum for temperatures above some critical temperature T_c. This phenomenon is called symmetry restoration at high temperatures and can give rise to phase transitions [27].

The critical temperature T_c is defined in the case of a first order phase transition as the temperature where the two minima are degenerate. In a second order transition it is the temperature at which the second derivative of the potential vanishes at $\phi = 0$, i.e. $V''(0) = 0$. The discontinuity in the entropy during a first order phase transition results in energy that has to be released which is done in the form of latent heat. Latent heat is thus a good measure for the strength of the transition.

A phase transition like the electroweak transition is described through a temperature-dependent potential as shown in figure 1.1, where going to high temperatures corresponds to going to earlier times in the thermal evolution of the universe. The QCD phase transition where the quark-gluon plasma goes into the confined hadronic phase at $T \sim 100$ MeV is another cosmological phase transition. The electroweak phase transition taking place at $T \sim 100$ GeV originates from the already mentioned spontaneous symmetry breaking of the Standard Model Higgs field, where the scalar Higgs field acquires a vacuum expectation value. The system goes from a symmetric phase to a "Higgs phase", giving non-thermal masses through the Higgs mechanism to all known massive particles. Fortunately for us and our theoretical models, energies of the order $\mathcal{O}(100$ GeV) are accessible with particle accelerators such as the Large Hadron Collider (LHC) and thus these models can be tested.

Yang-Mills theories and especially the non-abelian $SU(2)$ gauge theory have an infinite number of degenerate vacua [28] which are distinguished by their

Chern-Simons number [28–30]. A change in Chern-Simons number through a sphaleron process is related to a change in baryon number [31]. A sphaleron is a solution of the electroweak theory at the saddle point between two neighboring vacuum states and its energy E_{sph} corresponds to the height of the barrier. A sphaleron process is the transition between two vacua which in case of a system with energy $E < E_{\mathrm{sph}}$ becomes a tunneling transition and the tunneling rate in the broken phase is exponentially suppressed by a factor of $\exp[-E_{\mathrm{sph}}(T)/T]$.

In order for the electroweak phase transition to be the origin of baryogenesis one has to make sure that a created net baryon number is not washed out again, e.g. through sphaleron processes. Constraints on the washout rate, such that the measured baryon fraction remains, are also constraints for the ratio $E_{\mathrm{sph}}(T_c)/T_c$. The lowest and most restrictive bound then translates to the well known constraint for a first order phase transition [32]

$$\frac{\phi(T_c)}{T_c} \gtrsim 1 \; . \tag{1.2.1}$$

Thus, at the critical temperature T_c the two degenerate vacua of the scalar potential have to be far enough apart to prevent a washout through sphaleron processes. From the requirement of non-equilibrium it is not surprising that a second order transition with $\phi(T_c) \simeq 0$ could not generate a baryon asymmetry. For the Standard Model to have a strong enough first order electroweak phase transition, this constraint leads to a bound on the Higgs mass.

The constraint usually used $\phi(T_c)/T_c \gtrsim 1$ for a first order phase transition is gauge-dependent [33, 34]. This dependence originates from the truncation of the perturbative series such that the critical temperature T_c gets gauge-dependencies even though it is determined from stationary points where the potential is gauge-independent. Nevertheless, applying Nielsen's identity [35,36] this problem can be circumvented and the critical temperature can be computed in a gauge-independent way (see Appendix D of [34]).

In an idealized description of a phase transition we can write the corresponding temperature dependent scalar potential, making use of the notation of Quiros (p. 43 in ref. [37]), as

$$V(\phi, T) = D(T^2 - T_c^2)\phi^2 - ET\phi^3 + \frac{\lambda}{4}\phi^4 \; . \tag{1.2.2}$$

The three terms describe the three parts marked in figure 1.2. To strengthen the transition, i.e. to increase the height of the barrier separating the two minima and thus the distance of those two minima, new degrees of freedom are needed. We will see later on in section 1.3.1 that only bosonic degrees of freedom contribute to the part ϕ^3.[1]

To study thermal phase transitions we need a quantum field theory at finite temperatures. This theory is called thermal field theory.

1.3   Thermal Field Theory

In theoretical calculations of processes or decays for particle accelerators like the LHC, computations are usually done at zero-temperature. There is of course

---

[1]It is not to say that fermionic particles have no impact on the potential. On the contrary, it is the Yukawa coupling of the top quark which is mainly responsible for the shape of the Higgs potential at large ϕ in the Standard Model.
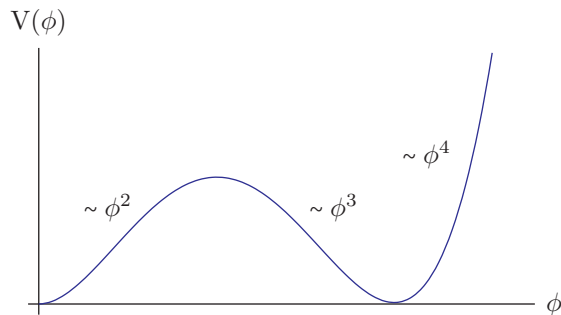
Figure 1.2: The form of the potential in eq. (1.2.2) at the critical temperature.

a good reason for that. We live *at late times* in the evolution of the universe, meaning that even the cosmic background radiation has cooled down to 2.725 K which is of the order of 10^{-4} eV. And even if energies in the TeV range are accessed in particle accelerators, very accurate predictions can still be made using techniques like parton distribution functions for the unknown internal structure of, say, a proton.

However, there are cases, where it is inevitable to include thermal effects to get an accurate picture of the physical processes. One such system is the point of collision in a particle accelerator where very high energy densities and thus temperatures are set free. These also include macroscopic cases of very high densities, e.g. in white dwarfs or neutron stars. Furthermore, thermal phase transitions like the one under study in this thesis are amongst them. Thus we have to understand how to handle perturbative calculations in quantum field theory at finite temperature, i.e. thermal field theory.

To understand some of the techniques and technicalities covered in this thesis we want to give a brief introduction of thermal field theory. This introduction does by no means claim to cover all the relevant topics of finite temperature field theories but only the most relevant aspects for this thesis. For a more thorough and complete introduction see [37–39].

Here we want to cover the basics of thermal sum-integrals, the emergence of thermal mass terms and explain the concept and the necessity of resummation.

1.3.1 Thermal Integrals

Consider a scalar field $\phi(\vec{x}, t)$. We can write it in a Fourier representation

$$\phi(\vec{x}, t) = T \sum_{n=-\infty}^{\infty} \tilde{\phi}(\vec{x}, \omega_n) e^{i\omega_n t} \ , \tag{1.3.1}$$

where we have introduced the Matsubara modes $\omega_n = 2\pi nT$, $n \in \mathbb{Z}$ [40]. The Kubo-Martin-Schwinger relations [41, 42] imply periodic boundary conditions on the Matsubara modes.

This then corresponds to compactifying the time, or rather temperature, direction. Thus performing an integration over all of space-time is no longer just a four dimensional integration but an integration over three spatial dimensions and an infinite sum over all Matsubara modes. We express this with the sum-

integral

$$\oint_K = T \sum_{\omega_n} \int \frac{d^3 k}{(2\pi)^3} \ . \tag{1.3.2}$$

We define the one-loop integral functions as

$$J(m,T) = \bigcirc \quad , \qquad I(m,T) = \frac{1}{m} \frac{d}{dm} J(m,T) = \bigcirc \quad , \tag{1.3.3}$$

and we split them up into a zero-temperature and a finite-temperature part as

$$J(m,T) = J_{\text{vac}}(m) + J_T(m) \ , \qquad I(m,T) = I_{\text{vac}}(m) + I_T(m) \ . \tag{1.3.4}$$

The function $J_{\text{vac}}(m)$ corresponds to the well known one-loop Coleman-Weinberg potential form

$$J_{\text{vac}}(m) = -\frac{m^4}{64\pi^2} \left[\frac{1}{\epsilon} - \ln \frac{m^2}{\bar{\mu}^2} + \frac{3}{2} + \mathcal{O}(\epsilon) \right] \ . \tag{1.3.5}$$

Taking the derivative with respect to m as in eq. (1.3.3) gives us the function $A(m)$, given in Appendix A.1, which reads

$$I_{\text{vac}}(m) = A(m) = -\frac{m^2}{16\pi^2} \left[\frac{1}{\epsilon} - \ln \frac{m^2}{\bar{\mu}^2} + 1 + \mathcal{O}(\epsilon) \right] \ . \tag{1.3.6}$$

The thermal parts of the functions J and I are

$$J_T(m) = \frac{T^4}{2\pi^2} \int_0^\infty dx \ x^2 \ln \left[1 \pm e^{-\sqrt{x^2+y^2}} \right] \ , \tag{1.3.7}$$

$$I_T(m) = \frac{T^2}{2\pi^2} \int_0^\infty dx \ \frac{x^2}{\sqrt{x^2+y^2}} \frac{1}{e^{\sqrt{x^2+y^2}} \pm 1} \ , \tag{1.3.8}$$

where the signs correspond to bosons $(-)$ and fermions $(+)$ respectively and $y = m/T$. These integrals cannot be computed analytically, however, they can be expressed as a sum over modified Bessel functions of the second kind $K_\alpha(z)$. To do so we first change variables $x = y \sinh t \ \Rightarrow \ dx = y \cosh t \ dt$, such that

$$\frac{T^4}{2\pi^2} \int_0^\infty dx \ x^2 \ln \left[1 \pm e^{-\sqrt{x^2+y^2}} \right] = \frac{T^4}{2\pi^2} \int_0^\infty dt \ y^3 \sinh^2 t \cosh t \ln \left[1 \pm e^{-y \cosh t} \right] \ . \tag{1.3.9}$$

Now we have to distinguish between the bosonic and the fermionic case since the logarithm can be written as

$$\ln(1-z) = -\sum_{n=1}^\infty \frac{z^n}{n} \ , \quad \ln(1+z) = \sum_{n=1}^\infty (-1)^{n+1} \frac{z^n}{n} \ . \tag{1.3.10}$$

However, we see that the difference between the bosonic and fermionic sum is just a factor of $(-1)^n$. We can then write

$$J_T(m) = -\frac{T^4}{2\pi^2} \int_0^\infty dt \ y^3 \sinh^2 t \cosh t \sum_{n=1}^\infty (\pm 1)^n \frac{e^{-yn \cosh t}}{n}$$

$$= -\frac{T^4}{2\pi^2} \int_0^\infty dt \; \frac{y^3}{2} \sinh t \sinh 2t \sum_{n=1}^\infty (\pm 1)^n \frac{e^{-yn\cosh t}}{n} \; , \qquad (1.3.11)$$

where we have used the identity $\sinh 2t = 2\sinh t \cosh t$ and the signs now correspond to bosons $(+)$ and fermions $(-)$ respectively. We then integrate by parts using $de^{-bf(a)}/da = -bf'(a)e^{-bf(a)}$, where the boundary term vanishes. This is true since $\sinh 2t \; e^{-\cosh t}|_{t=0} = \sinh 2t \; e^{-\cosh t}|_{t=\infty} = 0$. We then get

$$J_T(m) = -\frac{y^2 T^4}{2\pi^2} \int_0^\infty dt \; \cosh 2t \sum_{n=1}^\infty (\pm 1)^n \frac{e^{-yn\cosh t}}{n^2} \; . \qquad (1.3.12)$$

Interchanging the sum and the integral as well as using the integral representation of the modified Bessel function

$$K_\alpha(z) = \int_0^\infty dt \; e^{-z\cosh t} \cosh \alpha t \qquad (1.3.13)$$

and inserting $y = m/T$ we get

$$J_T(m) = -\frac{m^2 T^2}{2\pi^2} \sum_{n=1}^\infty \frac{(\pm 1)^n}{n^2} K_2\left(\frac{nm}{T}\right) \; , \qquad (1.3.14)$$

where the signs again correspond to bosons $(+)$ and fermions $(-)$. The computation of the sum-integrals of the functions J and I without the Bessel function representation is presented in the next chapter in section 3.2.1 and the results are summarized in Appendix A.2. However, we are often interested in evaluating these functions in the high-temperature limit, i.e. at small $y = m/T$. Taking this limit allows us to have an analytical expression and furthermore we can give physical meaning to different terms in the high-temperature expansion.

For the expansion of the bosonic I-function we split it up into two parts, namely the zero-mode Matsubara contribution and the non-zero mode Matsubara contribution. Using the expression for a standard integral given in eq. (A.0.5) we can immediately determine the zero-mode part

$$I_{n=0}(m) = T \int_k \frac{1}{k^2 + m^2} = -\frac{mT}{4\pi} + \mathcal{O}(\epsilon) \; . \qquad (1.3.15)$$

For the second part we first have to Taylor-expand before applying eq. (A.0.5). We then use the alternating geometric series

$$\sum_{i=0}^\infty \frac{(-1)^i m^i}{A^{i+1}} = \frac{1}{A+m} \qquad (1.3.16)$$

to get

$$I_{n\neq 0}(m) = T \sum_{\omega_n \neq 0} \int_k \frac{1}{\omega_n^2 + k^2 + m^2} = 2T \sum_{n=1}^\infty \int_k \sum_{\ell=0}^\infty (-1)^\ell \frac{m^{2\ell}}{\left[(2\pi nT)^2 + k^2\right]^{\ell+1}}$$

$$= \frac{T^{2-2\epsilon}}{2\pi^{\frac{1}{2}+\epsilon}} \sum_{\ell=0}^\infty \left(-\frac{m^2}{(2\pi T)^2}\right)^\ell \frac{\Gamma\left(\ell - \frac{1}{2} + \epsilon\right)}{\Gamma(\ell+1)} \zeta(2\ell - 1 + 2\epsilon) + \mathcal{O}(\epsilon) \; , \quad (1.3.17)$$

where $\Gamma(z)$ is the Euler gamma function and $\zeta(s)$ the Riemann zeta function. The sum over ℓ lists the terms in the m^2/T^2 expansion. We consider only the first three terms $\ell = 0, 1, 2$ and expand up to $\mathcal{O}(\epsilon^0)$ to get

$$I_{n\neq0}(m) = \frac{T^2}{12} - \frac{2m^2}{(4\pi)^2}\left[\frac{1}{2\epsilon} + \ln\left(\frac{\bar{\mu}e^{\gamma_E}}{4\pi T}\right)\right] + \frac{2m^4\zeta(3)}{(4\pi)^4 T^2} + \mathcal{O}\left(\frac{m^6}{T^6}\right) + \mathcal{O}(\epsilon) \ . \quad (1.3.18)$$

To get the temperature-dependent part only, we subtract the vacuum contribution $I_{\text{vac}}(m)$ from eq. (1.3.6). The divergence, which is temperature-independent and in a full computation will be canceled by a counterterm, as well as the dependence on the renormalization scale $\bar{\mu}$ are thus subtracted. Adding the contribution from the zero-mode and omitting higher-order terms, the result reads

$$I_T(m) = \frac{T^2}{12} - \frac{mT}{4\pi} - \frac{2m^2}{(4\pi)^2}\left[\ln\left(\frac{me^{\gamma_E}}{4\pi T}\right) - \frac{1}{2}\right] + \frac{2m^4\zeta(3)}{(4\pi)^4 T^2} \ . \quad (1.3.19)$$

We can now use the relation

$$I(m,T) = \frac{1}{m}\frac{d}{dm}J(m,T) \quad \Rightarrow \quad J(m,T) = \int dm\ m I(m,T) \quad (1.3.20)$$

to get the high-temperature expansion for the J-function. We again omit terms of order $\mathcal{O}(\epsilon)$ and $\mathcal{O}(m^6/T^2)$ and get

$$J_T(m) = -\frac{\pi^2 T^4}{90} + \frac{m^2 T^2}{24} - \frac{m^3 T}{12\pi} - \frac{m^4}{2(4\pi)^2}\ln\left(\frac{me^{\gamma_E}}{4\pi T}\right) \ . \quad (1.3.21)$$

The fermionic counterpart can be calculated similarly and the resulting expansion to the same order is

$$J_T^{\text{fermion}}(m) = \frac{7}{8}\frac{\pi^2 T^4}{90} - \frac{m^2 T^2}{48} - \frac{m^4}{2(4\pi)^2}\ln\left(\frac{me^{\gamma_E}}{\pi T}\right) \ . \quad (1.3.22)$$

Applying the relation (1.3.20) to the zero-mode contribution (1.3.15) we get

$$J_{n=0}(m) = -\frac{m^3 T}{12\pi} + \mathcal{O}(\epsilon) \ . \quad (1.3.23)$$

We see that the term $\sim m^3 T$, related to the zero-mode contribution, is absent in the fermionic expansion in eq. (1.3.22) as it should be, since there are no fermionic zero-modes. This is true more generally for all terms of odd powers of m. In higher-order perturbative calculations, these terms lead in the small mass limit to $1/m$ divergences which have to be taken care of. The cure for this infrared problem is resummation. This term in the expansion is the reason we need bosonic degrees of freedom to strengthen a phase transition as alluded to in section 1.2.

Before we tackle the problem of resummation, however, we take a look at the term $\sim m^2 T^2$ in the expansions (1.3.21) and (1.3.22) which can be interpreted as a thermal mass term.
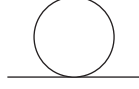
Figure 1.3: Diagram contributing to the thermal mass at one-loop in the ϕ^4 toy-model.

1.3.2 Thermal Masses

We have seen above that there is a term $\sim T^2$ in the high-temperature expansions of the J-function for bosons (1.3.21) and fermions (1.3.22). This term, i.e. the leading term in the expansion, since the one $\sim T^4$ is constant, or rather the coefficient multiplying m^2 can be interpreted as a thermal mass term. The effective mass parameter of a particle then not only gets contributions from the zero-temperature loop expansion but also from thermal loops.

To demonstrate how this works in a simple theory, we consider a scalar ϕ^4 toy-model with the Lagrangian

$$\mathcal{L}_{\phi^4} = \frac{1}{2}\partial_\mu\phi\partial^\mu\phi + \frac{m_\phi^2}{2}\phi^2 + \frac{\lambda}{4}\phi^4 \ . \tag{1.3.24}$$

Writing the bare Lagrangian as $\mathcal{L}_B = \mathcal{L}_{\phi^4} + \delta\mathcal{L}_{\phi^4}$, where $\delta\mathcal{L}_{\phi^4}$ contains the vacuum counterterms, we can add and subtract a thermal mass term [43, 44]. The bare Lagrangian is then written as

$$\mathcal{L}_B = \mathcal{L}_{\phi^4} + \frac{\delta m_T^2}{2}\phi^2 + \delta\mathcal{L}_{\phi^4} - \frac{\delta m_T^2}{2}\phi^2 \ . \tag{1.3.25}$$

The term $+\delta m_T^2$ is then included in the calculation along with the vacuum masses while the term $-\delta m_T^2$ is treated as an additional, i.e. thermal, counterterm.

We now want to compute the effective mass parameter which at tree-level is $m_{\text{eff}}^2 = m_\phi^2 + 3\lambda\phi^2$. For the calculation of the thermal mass term we consider the high-temperature regime and neglect external momenta. In this simple model, there is only one contributing diagram, which is shown in figure 1.3. It can be expressed in terms of the master integral function

$$I(0) = \frac{T^2}{12} \ . \tag{1.3.26}$$

The thermal mass contribution to the mass of the scalar is then

$$\delta m_T^2 = 3\lambda I(0) = \frac{\lambda T^2}{4} \ , \tag{1.3.27}$$

and the effective mass parameter becomes

$$\widetilde{m}_{\text{eff}}^2 = m_{\text{eff}}^2 + \delta m_T^2 = m_\phi^2 + 3\lambda\phi^2 + \delta m_T^2 \ , \tag{1.3.28}$$

where we have introduced the notation $\widetilde{m}$ for masses including their thermal mass terms.

We now turn to the issue of the infrared divergences mentioned at the end of section 1.3.1. The solution to this problem is called resummation.
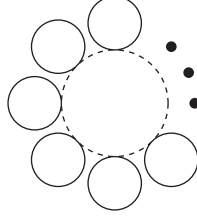
Figure 1.4: Generic ring or daisy diagram. The dashed line is a zero-mode propagator and solid lines are non-zero mode propagators.

1.3.3 Resummation

The problematic terms in the small mass limit of the perturbative expansion are those from the Matsubara zero-mode. To get rid of the infrared divergences one has to resum so called ring or daisy diagrams to all orders [45]. Ring diagrams as shown in figure 1.4 consist of one zero-mode propagator dressed with N non-zero mode loops, where then the sum over all N is taken.

To demonstrate how resummation is implemented we again consider the simple ϕ^4 toy-model Lagrangian given in eq. (1.3.24). The unresummed one-loop potential only includes the vacuum blob

$$V_{\phi^4,\mathrm{unres}}^{\text{one-loop}} = \bigcirc = J(m_{\mathrm{eff}}) \ . \tag{1.3.29}$$

As we have mentioned at the end of section 1.3.1, it is necessary to resum the Matsubara zero-modes to ensure infrared finiteness. We therefore subtract the unresummed zero-mode contribution from the potential and add the resummed expression which includes the thermal mass contribution. The resummed potential is then written as

$$V_{\phi^4,\mathrm{res}}^{\text{one-loop}} = J(m_{\mathrm{eff}}) - J_{n=0}(m_{\mathrm{eff}}) + J_{n=0}(\widetilde{m}_{\mathrm{eff}}) \ . \tag{1.3.30}$$

Even though it is necessary to resum the zero-modes, to spare us from having to implement three J-functions we choose to resum all modes instead. This is an alternative resummation prescription with its own drawbacks as described below. To emphasize the different resummation prescription we denote the potential by $V_{\mathrm{res'}}$. It takes the simple form

$$V_{\phi^4,\mathrm{res'}}^{\text{one-loop}} = J(\widetilde{m}_{\mathrm{eff}}) \ . \tag{1.3.31}$$

We now look at the divergent part of this potential which comes from the zero-temperature part in eq. (1.3.5) and reads

$$V_{\phi^4,\mathrm{res'},1/\epsilon}^{\text{one-loop}} = -\frac{\widetilde{m}_{\mathrm{eff}}^4}{64\pi^2\epsilon} = \frac{m_\phi^4 + 9\lambda^2\phi^4 + 6\lambda m_\phi^2\phi^2 + 2\delta m_T^2(m_\phi^2 + 3\lambda\phi^2) + (\delta m_T^2)^2}{64\pi^2\epsilon} \ . \tag{1.3.32}$$

The temperature-independent parts get canceled by the vacuum counterterms of lower order as usual ($\delta\mathcal{L}_{\phi^4}$ in eq. (1.3.25)). However, the temperature-dependent parts only get canceled by terms of higher order. The term $\sim \delta m_T^2$
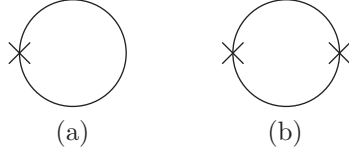
Figure 1.5: Topologies canceling the temperature-dependent divergences of the one-loop potential. The cross denotes a contribution from an insertion of δm_T^2.

gets canceled by a contribution from the diagram (a) in figure 1.5 which is part of the two-loop potential. The last term $\sim \delta m_T^4$ is canceled by a one-loop topology with two thermal mass insertions as shown in diagram (b) in figure 1.5 which is counted as of three-loop order.

The fact that ultraviolet divergences do not cancel order by order is the prize to pay for the simplicity of the alternative resummation prescription introduced in eq. (1.3.31). In practice, computations are only performed up to a certain order in perturbation theory and thus some temperature-dependent divergences remain uncanceled. In our calculations we remove these divergences, that are formally of higher order, by hand.

Chapter 2

Phase Transition in the Standard Model

The Standard Model of particle physics has proven to be very accurate and data from the Large Hadron Collider suggest that it represents a precise description of nature up to energy scales of several hundred GeV. However, since the discovery of the Higgs boson at the LHC [46,47] we know that its mass of $m_h = 125.09 \pm 0.24$ GeV [48] is too high to meet the bounds mentioned in section 1.2. The line of first order transitions has a second order transition endpoint at $m_h \sim m_W$ [49–52] and for heavier Higgs masses the transition is a crossover.

Therefore, within the Standard Model the spontaneous symmetry breaking at the electroweak scale did not occur through a phase transition, but was a smooth crossover [49, 53–57]. This means that as the universe cooled down to temperatures below this crossover, the plasma did not depart from thermal equilibrium. Since the third Sakharov condition is not met, the Standard Model cannot explain baryogenesis at the electroweak scale.

Nevertheless, even without a thermal phase transition at the electroweak scale there is still some interesting physics going on at temperatures around $T \sim 160$ GeV. These SM background effects could potentially have an imprint on some Beyond the Standard Model non-equilibrium physics. Even small features in the equation of state could have an impact on dark matter decoupling in this temperature range [58] or some $B + L$ violating rate that is switched off rapidly [59, 60]. The Standard Model background could then determine the fraction of a given lepton number produced around this scale, that is converted into baryons [61].

To describe this background we need to study the SM equation of state around the crossover. We do this through a perturbative three-loop computation where we use existing data within a dimensionally reduced effective theory on the lattice. We then integrate across the crossover and calculate different thermodynamic functions. The anticipated order is $\mathcal{O}(g^5)$ where g is some generic coupling constant.

We start off by deriving a master equation for the pressure, or rather its logarithmic temperature derivative, in section 2.1. We then treat each of the three terms arising in the master equation individually in sections 2.2, 2.3 and 2.4 before presenting our results in section 2.5. The possible implications of

these results are described in section 2.6.

2.1   Master Equation

The first step in our study is to derive a master equation whose parts we then compute individually. We consider the Standard Model with the scalar part of the Euclidean Lagrangian

$$\delta \mathcal{L}_E = -\nu_B^2 \phi^\dagger \phi + \lambda_B (\phi^\dagger \phi)^2 \ . \tag{2.1.1}$$

The renormalized parameters corresponding to the bare ones ν_B^2 and λ_B are denoted by ν^2 and λ. In our study we are considering the temperature range

$$T^2 \gtrsim \frac{\nu^2}{g^2} \ , \tag{2.1.2}$$

where g^2 is some generic coupling constant $g^2 \in \{\lambda, h_t^2, g_1^2, g_2^2, g_3^2\}$. Looking at the lower edge of this range, the effective Higgs mass parameter of the dimensionally reduced theory, $\bar{m}_3$ [62] satisfies

$$|\bar{m}_3^2| \sim |-\nu^2 + g^2 T^2| \lesssim \frac{g^3 T^2}{\pi} \ . \tag{2.1.3}$$

If the sign is negative we are in a Higgs phase where the Higgs field has an expectation value $v^2 \sim -\bar{m}_3/\lambda > 0$. This expectation value is small ($v \lesssim \sqrt{g}T$) in our parameter range since $\lambda \sim g^2$ for a Higgs mass $m_h \simeq 125$ GeV.

The dynamics of the system is non-perturbative if momenta in the range $|\bar{m}_3^2| \sim (g^2 T/\pi)^2$ are considered [63, 64] and thus they have to be treated with lattice simulations. However, the non-perturbative nature is associated with particular modes and can thus be described by a dimensionally reduced effective theory [65, 66]. Such a theory is constructed perturbatively but nevertheless the accuracy is expected to be at the percent level. This estimate is based on the analysis of higher-order operators that are truncated in this theory [62], and on a comparison of lattice results in the dimensionally reduced theory with a full 4-dimensional simulation [52, 67].

The basic observable we are considering is the thermodynamic pressure $p_B(T)$ which only depends on one thermodynamic variable, namely the temperature, since we set chemical potentials associated with conserved charges such as $B - L$ or the hypercharge magnetic flux to zero.

Following [68, 69], where the parameter ranges $\bar{m}_3 \sim g^2 T$ and $\bar{m}_3 \sim g^3 T/\pi$ respectively have already been considered, we rewrite the pressure as

$$p_B(T) = p_E(T) + p_M(T) + p_G(T) \ . \tag{2.1.4}$$

The three parts collect contributions from different momentum scales. While the hard scales $k \sim \pi T$ contribute to p_E, the soft scales $k \sim gT$ contribute to p_M and the ultrasoft scales $k \sim g^2 T/\pi$ to p_G. We use the terminology from QCD where the effective theory contributing to p_M is called the Electrostatic Standard Model (ESM) while the one contributing to p_G Magnetostatic Standard Model (MSM).

We do not present here the full three-loop calculation performed for the different contributions of the thermodynamic pressure. The explicit result in
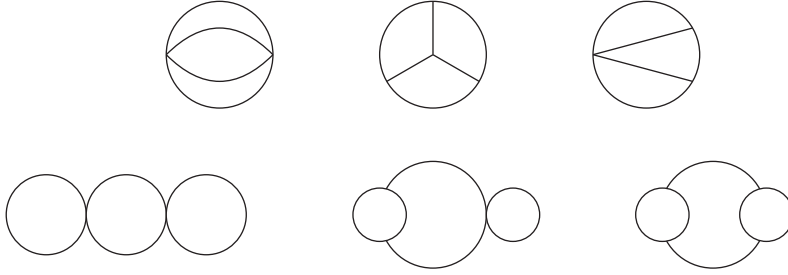
Figure 2.1: Vacuum three-loop topologies.

terms of master integral functions of all the contributing diagrams or family of diagrams can be found in [68] with typos and corrections listed in the Appendix of [1]. We only want to show the relevant topologies and the corresponding master integrals.

At one-loop there is only one diagram which is related to the J-function given in the next chapter in section 3.2.1, that is

$$\bigcirc \sim J(m) \ . \tag{2.1.5}$$

At two-loop we have contributions from the topologies

$$\bigcirc\bigcirc \sim I(m)^2 \ , \qquad \ominus \sim H(m) \ , \tag{2.1.6}$$

where the functions $I(m)$ and $H(m)$ are given in sections 3.2.1 and 3.2.2 in the next chapter. The sum-integral functions in these sections refer to the full theory. However, here we also need the three-dimensional integrations for the contributions to p_M and p_G. An example of such a computation is given in section 2.3. At three-loop there are six different topologies contributing which are shown in figure 2.1.

The calculation of the pressure can then be carried out both in the full 4-dimensional theory as well as in the dimensionally reduced effective theory. The particle content in the reduced 3d-theory is different from the full theory. After the first reduction step, i.e. in the ESM, there are no longer any fermions, since they all have masses of the order $\sim \pi T$ and only Matsubara zero-modes remain. Furthermore, we distinguish between the spatial and temporal parts of the gauge bosons since the latter get a Debye screening mass contribution [68] of order $m_E \sim gT$. The theory can then be viewed as a 3d-theory with a fundamental scalar, i.e. the Higgs, and adjoint scalars, i.e. the temporal components of the gauge fields. The next reduction step to the MSM leaves us with a 3d-theory where the temporal parts of the gauge fields have been integrated out.

Using dimensional reduction gives us a new set of parameters, couplings and masses, we can then relate to the ones of the full theory by matching coefficients of Green's functions in either theory. These parameters themselves are then expressed in terms of physical parameters, like pole masses and the

muon lifetime. This is presented in [62] and for the couplings used in the next chapter the procedure is described in section 3.3.

The pressure in eq. (2.1.4) has to be renormalized and we do so by assuming that it vanishes at $T = 0$. We then write

$$p(T) = p_B(T) - p_B(0) \ . \tag{2.1.7}$$

Now rather than calculating the pressure itself we are interested in the dimensionless ratio $p(T)/T^4$. As alluded to above, we want to integrate the pressure across the electroweak crossover. If, on either side, we are far from the crossover, say $T_0 \ll 160$ GeV and $T_1 \gg 160$ GeV, we can determine the pressure by a direct perturbative computation. The integration to be determined then reads

$$\frac{p(T_1)}{T_1^4} - \frac{p(T_0)}{T_0^4} = \int_{T_0}^{T_1} \frac{dT}{T} \, T \frac{d}{dT} \left[\frac{p(T)}{T^4} \right] \ . \tag{2.1.8}$$

We need to compute the logarithmic temperature derivative of the dimensionless ratio p/T^4. Since scale invariance is broken explicitly by the Higgs mass term and by quantum corrections the result is non-zero. The integrand of (2.1.8) can be expressed in terms of the energy density $e(T)$ as

$$\Delta(T) = T \frac{d}{dT} \left[\frac{p(T)}{T^4} \right] = \frac{e(T) - 3p(T)}{T^4} \ . \tag{2.1.9}$$

We again use a terminology known from QCD where $\Delta(T)$ is referred to as the trace anomaly. Now since in (2.1.7) all $1/\epsilon$ divergences cancel we can replace the bare pressure by the renormalized one, denoted by p_R. Furthermore, for dimensional reasons we may write the dimensionless ratio $\hat{p} = p/T^4$ as

$$\frac{p(T)}{T^4} = \hat{p}_R \left(\frac{\bar{\mu}}{T}, \frac{\nu^2(\bar{\mu})}{T^2}, g^2(\bar{\mu}) \right) - \frac{p_{0R}(\bar{\mu}, \nu^2(\bar{\mu}), g^2(\bar{\mu}))}{T^4} \ , \tag{2.1.10}$$

where p_{0R} is the renormalized pressure at zero-temperature.

The bare pressure can be written in terms of the grand canonical partition function, which is defined through the thermodynamical limit

$$\mathcal{Z} = \lim_{V \to \infty} \exp \left[\frac{p_B(T)V}{T} \right] \ . \tag{2.1.11}$$

The partition function relates to the Euclidean path integral as

$$\mathcal{Z} = \int \mathcal{D}A\mathcal{D}\psi\mathcal{D}\bar{\psi}\mathcal{D}\phi \, \exp \left[- \int_X \mathcal{L}_E \right] \ , \tag{2.1.12}$$

where in our case the path integral includes integrations over all gauge fields A, fermion and anti-fermion fields ψ and $\bar{\psi}$ and the Higgs field ϕ. The integral $\int_X = \int_0^\beta d\tau \int_x$ is defined in the notations in the preface of this thesis. We can then write the pressure as

$$p_B(T) = \lim_{V \to \infty} \frac{T}{V} \ln \left\{ \int \mathcal{D}A\mathcal{D}\psi\mathcal{D}\bar{\psi}\mathcal{D}\phi \, \exp \left[- \int_X \mathcal{L}_E \right] \right\} \ . \tag{2.1.13}$$

To calculate the trace anomaly we need to take the derivative with respect to the Higgs mass parameter $\nu^2(\bar{\mu})$, or rather the dimensionless ratio $\nu^2(\bar{\mu})/T^2$

of $\hat{p}_R$. To do so, we first write $\nu_B^2 = \mathcal{Z}_m \nu^2(\bar{\mu})$, where $\mathcal{Z}_m$ is the renormalization factor which always appears in the combination $\mathcal{Z}_m \langle \phi^\dagger \phi \rangle$, in the part of the Lagrangian given in eq. (2.1.1). Even though they are not explicitly needed here, we also replace the other bare couplings with the renormalized ones. The derivative of the renormalized pressure, i.e. the renormalized expression of eq. (2.1.13), is then

$$
\begin{aligned}
\frac{\partial \hat{p}_R}{\partial(\nu^2/T^2)} &= \frac{1}{T^4} \frac{\partial}{\partial(\nu^2/T^2)} \lim_{V\to\infty} \frac{T}{V} \ln \left\{ \int \mathcal{D}[\ldots] \, C \exp\left[T^2 \int_X \frac{\mathcal{Z}_m \nu^2}{T^2} \phi^\dagger \phi \right] \right\} \\
&= \lim_{V\to\infty} \frac{T}{V} \frac{1}{\mathcal{Z}_0 T^4} \int \mathcal{D}[\ldots] e^{-S_E} T^2 \int_X \mathcal{Z}_m \phi^\dagger \phi \\
&= \lim_{V\to\infty} \frac{T}{V} \frac{1}{T^2} \int_X \mathcal{Z}_m \langle \phi^\dagger \phi \rangle
\end{aligned} \tag{2.1.14}
$$

where $\mathcal{D}[\ldots]$ is the path integration measure for all the fields, C includes all ν^2-independent terms in the action and $\mathcal{Z}_0 = \int \mathcal{D}[\ldots] e^{-S_E}$, where S_E is the Euclidean action. In the last step we have changed the order of the integration and used the definition of the expectation value $\langle A \rangle = \mathcal{Z}_0^{-1} \int \mathcal{D}[\ldots] A e^{-S_E}$. Since the integration $\int_X = V\beta = V/T$, the factor T/V is canceled and the limit can be taken. We can then write

$$
\frac{\partial \hat{p}_R}{\partial(\nu^2(\bar{\mu})/T^2)} = \frac{[\mathcal{Z}_m \langle \phi^\dagger \phi \rangle]_R}{T^2} \ , \tag{2.1.15}
$$

where we have added the subscript R to indicate that renormalized quantities are used.

We can now take the logarithmic temperature derivative of eq. (2.1.10) and thus the trace anomaly can be written as

$$
\begin{aligned}
T\frac{d}{dT}\left[\frac{p(T)}{T^4}\right] &= T\frac{\partial(\bar{\mu}/T)}{\partial T}\frac{\partial \hat{p}_R}{\partial(\bar{\mu}/T)} + T\frac{\partial(\nu^2(\bar{\mu})/T^2)}{\partial T}\frac{\partial \hat{p}_R}{\partial(\nu^2(\bar{\mu})/T^2)} + T\frac{4p_{0R}}{T^5} \\
&= -\frac{\partial \hat{p}_R}{\partial \ln[\bar{\mu}/T]} - \frac{2\nu^2(\bar{\mu})[\mathcal{Z}_m \langle \phi^\dagger \phi \rangle]_R}{T^4} + \frac{4p_{0R}}{T^4} \ .
\end{aligned} \tag{2.1.16}
$$

This is our master equation whose three parts correspond to three different contributions. The first term collects the explicit logarithms appearing in $\hat{p}_R$ which correspond to the breaking of scale invariance by quantum corrections. The second part grasps the temperature evolution of the Higgs condensate where the vacuum expectation value introduces an explicit breaking of scale invariance. The last term is the vacuum renormalization. We want to study each of these terms individually.

Although we checked and corrected (see Appendix of [1]) the calculation of the pressure in both the full and the reduced effective theory, we do not want to list all the various coefficients again here. They can be found in the Appendices of [68] and can with minor changes in notation directly be used here.[1]

2.2   Scale violation by Quantum Corrections

There are two ways to collect the logarithms appearing in the loop corrections in our perturbative study needed for evaluating the first term in the master equa-

---

[1]The changes are $g'^2 \to g_1^2$, $g^2 \to g_2^2$, $g_Y^2 \to h_t^2$, $\Lambda \to \bar{\mu}$ and $\gamma \to \gamma_E$.

tion (2.1.16). One way is to read off the logarithmic contributions directly from the explicit calculation of the various coefficients. The other way is presented here, where we make use of the fact that the pressure as an observable is scale invariant and thus the scale violation has to be compensated by the running of the couplings.

The first thing to note is that the part $\hat{p}_G$ in eq. (2.1.4) only contributes at the order $\mathcal{O}(g^6)$ and can thus be neglected for this part. Furthermore, the running of the couplings is of the form [68]

$$g^2(\bar{\mu}) = g^2(\bar{\mu}_0) + \eta g^4(\bar{\mu}) \ln \frac{\bar{\mu}}{\bar{\mu}_0} + \mathcal{O}(g^6) \ , \qquad (2.2.1)$$

where η is a numerical constant and $\bar{\mu}_0$ some reference scale. Since we take the derivative of the pressure with respect to the renormalization scale $\bar{\mu}$ and derivatives of the runnings are of the order $\bar{\mu} dg^2/d\bar{\mu} \sim g^4$, we only need the pressure up to $\mathcal{O}(g^3)$. Up to this order the pressure reads

$$\hat{p}_E + \hat{p}_M =$$

$$= \alpha_{E1} + g_1^2 \alpha_{EB} + g_2^2 \alpha_{EA} + g_3^2 \alpha_{EC} + \lambda \alpha_{E\lambda} + h_t^2 \alpha_{EY} + \frac{\nu^2}{T^2} \alpha_{E\nu}$$

$$+ \frac{\nu^4}{(4\pi)^2 T^4} \left(\frac{1}{\epsilon} + \alpha_{E\nu\nu} \right) + \frac{1}{12\pi T^3} \left[\left(m_{E1}^{2(0)} \right)^{\frac{3}{2}} + 3 \left(m_{E2}^{2(0)} \right)^{\frac{3}{2}} + 8 \left(m_{E3}^{2(0)} \right)^{\frac{3}{2}} \right] .$$

$$(2.2.2)$$

The leading order contributions of the Debye masses are

$$m_{E1}^{2(0)} = \left(\frac{1}{6} + \frac{5n_G}{9} \right) g_1^2 T^2 \ , \quad m_{E2}^{2(0)} = \left(\frac{5}{6} + \frac{n_G}{3} \right) g_2^2 T^2 \ , \quad m_{E3}^{2(0)} = \left(1 + \frac{n_G}{3} \right) g_3^2 T^2 \ .$$

$$(2.2.3)$$

With the exception of $\alpha_{E\nu\nu}$, all coefficients in eq. (2.2.2) are scale independent. Our coefficient $\alpha_{E\nu\nu}$ differs from [68], where they chose to renormalize the pressure such that it vanishes in the symmetric phase at zero temperature. Our renormalization condition requires the pressure to vanish at zero temperature in the broken phase. In terms of the group theory factor $d_F = 2$ of $SU(2)$ and the number of scalars $n_S = 1$ this coefficient reads

$$\alpha_{E\nu\nu} = d_F n_S \left(\ln \frac{\bar{\mu}}{4\pi T} + \gamma_E \right) \ . \qquad (2.2.4)$$

Using now that explicit logarithms must cancel against the running of the couplings we write

$$\frac{[\partial \hat{p}_E + \hat{p}_M]_R}{\partial \ln[\bar{\mu}/T]} = -\alpha_{EB} \bar{\mu} \frac{dg_1^2}{d\bar{\mu}} - \alpha_{EA} \bar{\mu} \frac{dg_s^2}{d\bar{\mu}} - \alpha_{EC} \bar{\mu} \frac{dg_3^2}{d\bar{\mu}} - \alpha_{E\lambda} \bar{\mu} \frac{d\lambda}{d\bar{\mu}}$$

$$- \alpha_{EY} \bar{\mu} \frac{dh_t^2}{d\bar{\mu}} - \frac{\alpha_{E\nu}}{T^2} \bar{\mu} \frac{d\nu^2}{d\bar{\mu}} + \frac{\nu^4}{(4\pi)^2 T^4} \bar{\mu} \frac{d\alpha_{E\nu\nu}}{d\bar{\mu}}$$

$$- \sum_{i=1}^{3} \frac{d_i m_{Ei}^{(0)}}{8\pi T^3} \bar{\mu} \frac{dm_{Ei}^{2(0)}}{d\bar{\mu}} + \mathcal{O}(g^6) \ , \qquad (2.2.5)$$

where d_i are the degrees of freedom of the gauge bosons $d_1 = 1$, $d_2 = 3$ and $d_3 = 8$. Inserting the running of the couplings we arrive at

$$- \frac{[\partial \hat{p}_E + \hat{p}_M]_R}{\partial \ln[\bar{\mu}/T]} = \Delta_1(T) \ , \qquad (2.2.6)$$

with

$$
\begin{aligned}
\Delta_1(T) = \frac{1}{(4\pi)^2} & \left[\frac{198 + 141 n_G - 20 n_G^2}{54} g_3^4 + \frac{266 + 163 n_G - 40 n_G^2}{288} g_2^4 \right. \\
& - \frac{144 + 375 n_G + 1000 n_G^2}{7776} g_1^4 - \frac{g_1^2 g_2^2}{32} - h_t^2 \left(\frac{7 h_t^2}{32} - \frac{5 g_3^2}{6} - \frac{15 g_2^2}{64} - \frac{85 g_1^2}{576} \right) \\
& \left. - \lambda \left(\lambda + \frac{h_t^2}{2} - \frac{g_1^2 + 3 g_2^2}{8} \right) + \frac{\nu^2}{T^2} \left(h_t^2 + 2\lambda - \frac{g_1^2 + 3 g_2^2}{4} \right) - \frac{2\nu^2}{T^4} \right] \\
& - \frac{1}{(4\pi)^3} \left[32 g_3^5 \left(1 + \frac{n_G}{3} \right)^{\frac{3}{2}} \left(\frac{11}{4} - \frac{n_G}{3} \right) + 12 g_2^5 \left(\frac{5}{6} + \frac{n_G}{3} \right)^{\frac{3}{2}} \left(\frac{43}{24} - \frac{n_G}{3} \right) \right. \\
& \left. - 4 g_1^5 \left(\frac{1}{6} + \frac{5 n_G}{9} \right)^{\frac{3}{2}} \left(\frac{1}{24} + \frac{5 n_G}{9} \right) \right] + \mathcal{O}(g^6) \ .
\end{aligned}
\tag{2.2.7}
$$

2.3 Higgs Condensate

As in eq. (2.1.4), we split the pressure into contributions from different momentum scales and express the Higgs condensate as

$$
\mathcal{Z}_m \langle \phi^\dagger \phi \rangle = \frac{\partial p_E}{\partial \nu^2} + \frac{\partial p_M}{\partial \nu^2} + \frac{\partial p_G}{\partial \nu^2} \ .
\tag{2.3.1}
$$

Since $\mathcal{Z}_m \langle \phi^\dagger \phi \rangle$ is multiplied by ν^2 in our master equation (2.1.16) and since we assume $\nu^2 \sim g^2 T^2$ we only need to determine $\mathcal{Z}_m \langle \phi^\dagger \phi \rangle$ up to order $\mathcal{O}(g^3)$.

The first term, collecting the contributions from the hard scales, can be extracted directly from the perturbative expression for p_E in ref. [68]. It reads

$$
\begin{aligned}
\frac{\partial p_E}{\partial \nu^2} = T^2 & \left(\alpha_{E\nu} + \frac{g_1^2 \alpha_{EB\nu} + g_2^2 \alpha_{EA\nu} + \lambda \alpha_{E\lambda\nu} + h_t^2 \alpha_{EY\nu}}{(4\pi)^2} \right) \\
& + \frac{2\nu^2}{(4\pi)^2} \left(\frac{1}{\epsilon} + \alpha_{E\nu\nu} \right) + \mathcal{O}(g^4) \ .
\end{aligned}
\tag{2.3.2}
$$

Inserting the coefficients, some $1/\epsilon$ divergences still remain and we have

$$
\begin{aligned}
\frac{\partial p_E}{\partial \nu^2} = \frac{T^2}{6} & - \frac{T^2}{6(4\pi)^2} \left[\frac{3}{2} (g_1^2 + 3 g_2^2) \left(\frac{1}{\epsilon} + 3 \ln \frac{\bar{\mu}}{4\pi T} + \gamma_E + \frac{5}{3} + \frac{2\zeta'(-1)}{\zeta(-1)} \right) \right. \\
& \left. + 6 h_t^2 \left(\ln \frac{\bar{\mu}}{4\pi T} + \gamma_E \right) + 12\lambda \left(\ln \frac{\bar{\mu}}{4\pi T} + \gamma_E \right) \right] \\
& + \frac{4\nu^2}{(4\pi)^2} \left(\frac{1}{2\epsilon} + \ln \frac{\bar{\mu}}{4\pi T} + \gamma_E \right) + \mathcal{O}(g^4) \ .
\end{aligned}
\tag{2.3.3}
$$

The contributions from the soft scales originate from the dependence of the effective mass parameters on ν^2:

$$
\frac{\partial p_M}{\partial \nu^2} = \sum_{i=1,2} \frac{\partial m_{Ei}^2}{\partial \nu^2} \frac{\partial p_M}{\partial m_{Ei}^2} + \frac{\partial m_3^2}{\partial \nu^2} \frac{\partial p_M}{\partial m_3^2} + \mathcal{O}(g^6) \ .
\tag{2.3.4}
$$

The first two terms can be calculated from the Debye mass parameters

$$m_{E1}^2 = g_1^2 \left(T^2 \beta_{E1}' - \frac{\nu^2}{(4\pi)^2} \beta_{E\nu}' \right) + \dots \; , \quad m_{E2}^2 = g_2^2 \left(T^2 \beta_{E1} - \frac{\nu^2}{(4\pi)^2} \beta_{E\nu} \right) + \dots \; ,$$

(2.3.5)

where the coefficients β_{E1}' and β_{E1} are the coefficients given in eq. (2.2.3). The contribution of these two terms is then

$$\sum_{i=1,2} \frac{\partial m_{Ei}^2}{\partial \nu^2} \frac{\partial p_M}{\partial m_{Ei}^2} = -\frac{T^2}{(4\pi)^3} \left[3g_2^3 \left(\frac{5}{6} + \frac{n_G}{3} \right)^{\frac{1}{2}} + g_1^3 \left(\frac{1}{6} + \frac{5n_G}{9} \right)^{\frac{1}{2}} \right] + \mathcal{O}(g^4) \; . \quad (2.3.6)$$

The contribution of the last term in eq. (2.3.4) is a bit more cumbersome because there is a peculiarity in the parameter range under consideration. Since $|m_3^2| \sim |-\nu^2 + g^2 T^2| \lesssim g^3 T^2/\pi$, the derivative of m_3^2 is parametrically larger than m_3^2 itself:

$$\nu^2 \frac{\partial m_3^2}{\partial \nu^2} \sim \nu^2 \sim g^2 T^2 \; . \quad (2.3.7)$$

We thus have to take terms in p_M that are of higher order than $\mathcal{O}(g^3)$ into account. However, the computation is simplified, since p_G collects contributions from the ultrasoft scales. Therefore, we can treat the Higgs and gauge fields as massless for our computation of the matching coefficients and most diagrams vanish in dimensional regularization. What remains are diagrams with at least one adjoint scalar propagator and one mass insertion $m_3^2 \phi^\dagger \phi$, denoted by a blob in the diagrams below. The only two diagrams contributing at the relevant order are

$$\frac{\partial p_M}{\partial m_3^2} = \; \raisebox{-0.5em}{\includegraphics{diagram1}} \; + \; \raisebox{-0.5em}{\includegraphics{diagram2}} \quad , \quad (2.3.8)$$

where dashed lines are scalar propagators, solid lines are adjoint scalar propagators and wiggly lines are gauge fields.

To solve these kind of topologies we first calculate the propagator in coordinate space, i.e. Fourier transform to get

$$V(r) = \int_k e^{i\vec{k}\cdot\vec{r}} \frac{1}{k^2 + m^2} \; . \quad (2.3.9)$$

This Fourier transformed propagator can be expressed in terms of the modified Bessel function of the second kind $K_\alpha(z)$ [70] as

$$V(r) = \left(\frac{e^{\gamma_E} \bar{\mu}^2}{4\pi} \right)^\epsilon \frac{1}{(2\pi)^{\frac{3}{2}-\epsilon}} \left(\frac{m}{r} \right)^{\frac{1}{2}-\epsilon} K_{\frac{1}{2}-\epsilon}(mr) \; . \quad (2.3.10)$$

In the limit where $\epsilon \to 0$ this expression reduces to

$$V_0(r) = \frac{e^{-mr}}{4\pi r} \; . \quad (2.3.11)$$

In the end we want to take the limit where $r \to 0$. Therefore we expand $V(r)$ in a Laurent series for small r. For the Bessel function we use

$$K_\alpha(z) = \frac{\pi}{2} \frac{I_{-\alpha}(z) - I_\alpha(z)}{\sin \alpha\pi} \; , \quad I_\alpha(z) = \sum_{n=0}^\infty \frac{1}{n!\Gamma(n+\alpha+1)} \left(\frac{z}{2} \right)^{2n+\alpha} \; , \quad (2.3.12)$$

where $I_\alpha(z)$ is the modified Bessel function of the first kind. The expansion of the Bessel function is then written as

$$
K_{1/2-\epsilon}(mr) = \frac{\pi}{2} \frac{1}{\sin\left[\left(\frac{1}{2} - \epsilon\right)\pi\right]} \sum_{n=0}^{\infty} \left[\frac{\left(\frac{mr}{2}\right)^{2n-\frac{1}{2}+\epsilon}}{\Gamma\left(n + \frac{1}{2} + \epsilon\right)} - \frac{\left(\frac{mr}{2}\right)^{2n+\frac{1}{2}-\epsilon}}{\Gamma\left(n + \frac{3}{2} - \epsilon\right)} \right]
$$

$$
= \frac{1}{2}\Gamma\left(\frac{1}{2} - \epsilon\right)\left(\frac{mr}{2}\right)^{-\frac{1}{2}+\epsilon}\left[1 + \frac{2}{1+2\epsilon}\left(\frac{mr}{2}\right)^2 + \mathcal{O}(m^4 R^4)\right]
$$

$$
+ \frac{1}{2}\Gamma\left(-\frac{1}{2} + \epsilon\right)\left(\frac{mr}{2}\right)^{\frac{1}{2}-\epsilon}\left[1 + \frac{2}{3-2\epsilon}\left(\frac{mr}{2}\right)^2 + \mathcal{O}(m^4 r^4)\right],
$$

$$(2.3.13)$$

where in the second equality we have used the Euler reflection formula

$$
\frac{\pi}{\sin\left[\left(\frac{1}{2} - \epsilon\right)\pi\right]} = \Gamma\left(\frac{1}{2} - \epsilon\right)\Gamma\left(\frac{1}{2} + \epsilon\right). \tag{2.3.14}
$$

Inserting eq. (2.3.13) back into eq. (2.3.10) we get

$$
V(r) = \left(\frac{e^{\gamma_E}\bar{\mu}^2}{4}\right)^\epsilon \frac{\Gamma\left(\frac{1}{2} - \epsilon\right)}{4\pi\Gamma\left(\frac{1}{2}\right)} r^{-1+2\epsilon}\left[1 + \frac{(mr)^2}{2(1+2\epsilon)} + \mathcal{O}(m^4 r^4)\right]
$$

$$
- \left(e^{\gamma_E}\bar{\mu}^2\right)^\epsilon \frac{\Gamma\left(-\frac{1}{2} + \epsilon\right)}{4\pi\Gamma\left(-\frac{1}{2}\right)} m^{1-2\epsilon}\left[1 + \frac{(mr)^2}{2(3-2\epsilon)} + \mathcal{O}(m^4 r^4)\right]. \tag{2.3.15}
$$

The so called basketball diagram, corresponding to the topology of the first diagram in eq. (2.3.8), is written as

$$
\int_{kpq} \frac{1}{k^2 + m_1^2}\frac{1}{p^2 + m_2^2}\frac{1}{q^2 + m_3^2}\frac{1}{(\vec{k} + \vec{p} + \vec{q})^2 + m_4^2} = \int_r V^4(r), \tag{2.3.16}
$$

where $\int_r = [e^{\gamma_e}\bar{\mu}^2/(4\pi)]^{-\epsilon}\int d^{3-2\epsilon}r$ as defined in the notations and V^4 is to be understood as a product $\Pi_{i=1}^4 V(r, m_i)$. The masses m_i correspond to the four lines in the diagram. There are ultraviolet divergences coming from the region where $r \to 0$, therefore we split the integral into

$$
\int_r V^4(r) = \left(\frac{e^{\gamma_E}\bar{\mu}^2}{4}\right)^{-\epsilon}\frac{4\pi\Gamma\left(\frac{3}{2}\right)}{\Gamma\left(\frac{3}{2} - \epsilon\right)}\int_0^R dr\, r^{2-2\epsilon}V^4(r) + 4\pi\int_R^\infty dr\, r^2 V_0^4(r), \tag{2.3.17}
$$

where in the second term we have set $\epsilon = 0$. We choose $R \ll 1/m_i$ such that we can use the expansion (2.3.15) and dropping all terms that vanish as $R \to 0$, we get

$$
\left(\frac{e^{\gamma_E}\bar{\mu}^2}{4}\right)^{-\epsilon}\frac{4\pi\Gamma\left(\frac{3}{2}\right)}{\Gamma\left(\frac{3}{2} - \epsilon\right)}\int_0^R dr\, r^{2-2\epsilon}V^4(r)
$$

$$
= \left(\frac{e^{\gamma_E}\bar{\mu}^2}{4}\right)^{-\epsilon}\frac{4\pi\Gamma\left(\frac{3}{2}\right)}{\Gamma\left(\frac{3}{2} - \epsilon\right)}\int_0^R dr\left\{\left[\left(\frac{e^{\gamma_E}\bar{\mu}^2}{4}\right)^\epsilon \frac{\Gamma\left(\frac{1}{2} - \epsilon\right)}{4\pi\Gamma\left(\frac{1}{2}\right)}\right]^4 r^{-2+6\epsilon}\right.
$$

$$
\left. + 4\left[\left(\frac{e^{\gamma_E}\bar{\mu}^2}{4}\right)^\epsilon \frac{\Gamma\left(\frac{1}{2} - \epsilon\right)}{4\pi\Gamma\left(\frac{1}{2}\right)}\right]^3 \left(e^{\gamma_E}\bar{\mu}^2\right)^\epsilon \frac{\Gamma\left(-\frac{1}{2} + \epsilon\right)}{4\pi\Gamma\left(-\frac{1}{2}\right)} m^{1-2\epsilon} r^{-1+4\epsilon}\right\}
$$

$$= -\frac{1}{(4\pi)^3}\left[\frac{1}{R} + \sum_{i=1}^{4}\frac{m_i}{4}\left(\frac{1}{\epsilon} - 2\ln\frac{2m_i}{R^2\bar{\mu}^3} + 4\gamma_E + 4\right)\right] + \mathcal{O}(\epsilon) . \quad (2.3.18)$$

To evaluate the second integral in eq. (2.3.17) we use integration by parts and the exponential integral

$$\text{Ei}(x) = -\int_{-x}^{\infty} dt\frac{e^{-t}}{t} = \gamma_E + \ln|x| + \mathcal{O}(x) , \quad x \in \mathbb{R} , \quad x \neq 0 . \quad (2.3.19)$$

Dropping terms that vanish as $R \to 0$, we get

$$4\pi\int_{R}^{\infty} dr\ r^2 V_0^4(r) = \frac{1}{(4\pi)^3}\int_{R}^{\infty} dr\frac{e^{-Mr}}{r^2} = \frac{1}{(4\pi)^3}\left[-\frac{e^{-Mr}}{r}\Big|_{R}^{\infty} + M\int_{R}^{\infty} dr\frac{e^{-Mr}}{r}\right]$$

$$= \frac{1}{(4\pi)^3}\left[\frac{1}{R} + M\left(\ln MR + \gamma_E - 1\right)\right] , \quad (2.3.20)$$

where $M = \sum_{i=1}^{4} m_i$. We see that the terms $\sim 1/R$ and $\sim \ln R$ cancel between (2.3.18) and (2.3.20). The resulting expression for the basketball diagram in eq. (2.3.16) is then

$$\int_{kpq}\frac{1}{k^2+m_1^2}\frac{1}{p^2+m_2^2}\frac{1}{q^2+m_3^2}\frac{1}{(\vec{k}+\vec{p}+\vec{q})^2+m_4^2}$$

$$= \frac{1}{(4\pi)^3}\sum_{i=1}^{4} m_i\left[-\frac{1}{4\epsilon} - 2 + \frac{1}{2}\ln\frac{2m_i}{\bar{\mu}} + \ln\frac{\sum_{j=1}^{4}m_j}{\bar{\mu}}\right] + \mathcal{O}(\epsilon) . \quad (2.3.21)$$

The second diagram in eq. (2.3.8) is of the type

$$\mathcal{I}_6 = \int_{k,p,q}\frac{1}{k^2+m_1^2}\frac{1}{(\vec{k}+\vec{p})^2+m_2^2}\frac{1}{q^2+m_3^2}\frac{1}{(\vec{q}+\vec{p})^2+m_4^2}\frac{1}{p^2+m_5^2}\frac{1}{p^2+m_6^2} , \quad (2.3.22)$$

which can be reduced using the partial fraction decomposition

$$\frac{1}{p^2+m_5^2}\frac{1}{p^2+m_6^2} = \frac{1}{m_6^2-m_5^2}\left(\frac{1}{p^2+m_5^2} - \frac{1}{p^2+m_6^2}\right) . \quad (2.3.23)$$

The resulting integral correspond to the topology in the top right corner of figure 2.1. The Fourier transform of this integral is then [71]

$$\mathcal{I}_5 = \int_{k,p,q}\frac{1}{k^2+m_1^2}\frac{1}{(\vec{k}+\vec{p})^2+m_2^2}\frac{1}{q^2+m_3^2}\frac{1}{(\vec{q}+\vec{p})^2+m_4^2}\frac{1}{p^2+m_5^2}$$

$$= \frac{1}{(4\pi)^5}\int d^3x\frac{e^{-(m_1+m_2)x}}{x^2}\int d^3y\frac{e^{-(m_3+m_4)y}}{y^2}\frac{e^{-m_5|\vec{x}+\vec{y}|}}{|\vec{x}+\vec{y}|} , \quad (2.3.24)$$

where $x = |\vec{x}|$ and $y = |\vec{y}|$. For the second integration we use the law of cosines to write

$$|\vec{x}+\vec{y}| = \sqrt{x^2+y^2-2xy\cos\theta} , \quad (2.3.25)$$

and change the angular integration variable to

$$t = \sqrt{x^2+y^2+2xy\cos\theta} \quad \Rightarrow \quad d\theta\ \sin\theta = -dt\frac{t}{xy} . \quad (2.3.26)$$

We can then write the second integration in eq. (2.3.24) as

$$\int d^3y \frac{e^{-(m_3+m_4)y}}{y^2} \frac{e^{-m_5|\vec{x}+\vec{y}|}}{|\vec{x}+\vec{y}|} = 2\pi \int_0^\infty dy \frac{e^{-(m_3+m_4)y}}{xy} \int_{x-y}^{x+y} dt \, e^{-m_5 t}$$

$$= 2\pi \int_0^\infty dy \frac{e^{-(m_3+m_4)y}}{xy} \frac{1}{m_5} \left(e^{-m_5(x-y)} - e^{-m_5(x+y)} \right)$$

$$= \frac{2\pi}{m_5 x} \left[e^{-m_5 x} \int_0^x \frac{dy}{y} \left(e^{-(m_3+m_4-m_5)y} - e^{-(m_3+m_4+m_5)y} \right) \right.$$

$$\left. + \left(e^{m_5 x} - e^{-m_5 x} \right) \int_x^\infty \frac{dy}{y} e^{-(m_3+m_4+m_5)y} \right] , \tag{2.3.27}$$

where in the last equation we distinguished the two cases $y < x$ and $y > x$. Using the definition of the Euler integrals (see e.g. eq. (2.3.19)) this evaluates to

$$\int d^3y \frac{e^{-(m_3+m_4)y}}{y^2} \frac{e^{-m_5|\vec{x}+\vec{y}|}}{|\vec{x}+\vec{y}|}$$

$$= \frac{2\pi e^{-m_5 x}}{m_5 x} \left\{ \ln \frac{m_3 + m_4 + m_5}{m_3 + m_4 - m_5} + \text{Ei} \left[(m_3 + m_4 - m_5)x \right] \right\}$$

$$- \frac{2\pi e^{m_5 x}}{m_5 x} \text{Ei} \left[(m_3 + m_4 + m_5)x \right] . \tag{2.3.28}$$

Inserting this result into eq. (2.3.24) we can perform the remaining x integration. We use the expansion for small arguments of the Euler integral as given in eq. (2.3.19) and we get

$$\mathcal{I}_5 = \lim_{z \to 0} \frac{1}{(4\pi)^3 2m_5} \left\{ \ln \frac{m_3 + m_4 + m_5}{m_3 + m_4 - m_5} \left[-\gamma_E - \ln(m_1 + m_2 + m_5)z \right] \right.$$

$$- \frac{\zeta(2) + [\gamma_E + \ln(m_3 + m_4 - m_5)z]^2}{2} - \text{Li}_2 \left(-\frac{m_1 + m_2 + m_5}{m_1 + m_2 - m_5} \right)$$

$$\left. + \frac{\zeta(2) + [\gamma_E + \ln(m_3 + m_4 + m_5)z]^2}{2} + \text{Li}_2 \left(-\frac{m_1 + m_2 - m_5}{m_3 + m_4 + m_5} \right) \right\}$$

$$= \frac{1}{(4\pi)^3 2m_5} \left\{ \frac{1}{2} \ln \frac{m_3 + m_4 + m_5}{m_3 + m_4 - m_5} \ln \frac{(m_3 + m_4 + m_5)(m_3 + m_4 - m_5)}{(m_1 + m_2 + m_5)^2} \right.$$

$$\left. + \text{Li}_2 \left(-\frac{m_1 + m_2 - m_5}{m_3 + m_4 + m_5} \right) - \text{Li}_2 \left(-\frac{m_1 + m_2 + m_5}{m_3 + m_4 - m_5} \right) \right\} , \tag{2.3.29}$$

where $\text{Li}_2(u)$ is the dilogarithm function and $\zeta(s)$ is the Riemann zeta function. From this reduced integral where we have used the partial fraction decomposition given in eq. (2.3.23), we go back to the integral we started with in eq. (2.3.22) which is then

$$\mathcal{I}_6 = \frac{1}{(4\pi)^3 (m_6^2 - m_5^2)m_5} \left[\frac{\pi^2}{12} + \frac{1}{4} \left(\ln \frac{m_1 + m_2 + m_5}{m_3 + m_4 + m_5} \right)^2 \right.$$

$$\left. + \frac{1}{2} \text{Li}_2 \left(\frac{m_5 - m_1 - m_2}{m_5 + m_3 + m_4} \right) + \frac{1}{2} \text{Li}_2 \left(\frac{m_5 - m_3 - m_4}{m_5 + m_1 + m_2} \right) \right]$$

$$- \frac{1}{(4\pi)^3(m_6^2 - m_5^2)m_6}\left[\frac{\pi^2}{12} + \frac{1}{4}\left(\ln\frac{m_1 + m_2 + m_6}{m_3 + m_4 + m_6}\right)^2\right.$$
$$\left. + \frac{1}{2}\mathrm{Li}_2\left(\frac{m_6 - m_1 - m_2}{m_6 + m_3 + m_4}\right) + \frac{1}{2}\mathrm{Li}_2\left(\frac{m_6 - m_3 - m_4}{m_6 + m_1 + m_2}\right)\right], \qquad (2.3.30)$$

where we have used the following identity of the dilogarithm

$$\mathrm{Li}_2(z) + \mathrm{Li}_2\left(\frac{1}{z}\right) = -\frac{\pi^2}{6} - \frac{1}{2}\left[\ln(-z)\right]^2 . \qquad (2.3.31)$$

Using the Feynman rules and expressions for the couplings of the dimensionally reduced theory [68] as well as the results in eqs. (2.3.21) and (2.3.30) we obtain from eq. (2.3.8)

$$\frac{\partial m_3^2}{\partial \nu^2}\frac{\partial p_M}{\partial m_3^2} = -\frac{T^3}{16(4\pi)^3}\left[\frac{g_2^4}{m_{E2}}\left(-\frac{2}{\epsilon} - 12\ln\frac{\bar{\mu}}{2m_{E2}} + \frac{35}{3}\right) + \frac{g_1^4}{m_{E1}} + \frac{12g_1^2 g_2^2}{m_{E1} + m_{E2}}\right] . \qquad (2.3.32)$$

The last term in eq. (2.3.1) captures the contributions from the ultrasoft scales, i.e. the dependence of the MSM effective Higgs mass parameter $\bar{m}_3$ on ν^2. It can be expressed as

$$\frac{\partial p_G}{\partial \nu^2} = \frac{\partial \bar{m}_3^2}{\partial \nu^2}\frac{\partial p_G}{\partial \bar{m}_3^2} + \mathcal{O}(g^8) . \qquad (2.3.33)$$

The error comes from partial derivatives with respect to other effective couplings of the MSM. Only the leading term [62]

$$\frac{\partial \bar{m}_3^2}{\partial \nu^2} = -1 \qquad (2.3.34)$$

is needed and we get

$$\frac{\partial \bar{m}_3^2}{\partial \nu}\frac{\partial p_G}{\partial \bar{m}_3^2} = \left[1 + \frac{3}{2(4\pi)^2}\left((g_1^2 + 3g_2^2 - 8\lambda)\ln\frac{\bar{\mu}e^{\gamma_E}}{4\pi T} - 4h_t^2\ln\frac{\bar{\mu}e^{\gamma_E}}{\pi T}\right)\right]\langle\phi^\dagger\phi\rangle_{3d}(g_{M2}^2)$$
$$+ \frac{(g_1^2 + 3g_2^2)T^2}{(4\pi)^2}\left(\frac{1}{4\epsilon} + \ln\frac{\bar{\mu}}{g_{M2}^2}\right)$$
$$- \frac{g_2^4 T^3}{2(4\pi)^3 m_{E2}}\left(\frac{1}{4\epsilon} + \ln\frac{\bar{\mu}}{g_{M2}^2} + \frac{1}{2}\ln\frac{\bar{\mu}}{2m_{E2}}\right) + \mathcal{O}(g^4) . \qquad (2.3.35)$$

where the renormalization scale $\bar{\mu} = g_{M2}^2$ is used within the MSM. The condensate $\langle\phi^\dagger\phi\rangle_{3d}(g_{M2}^2)$ can be measured non-perturbatively. Thereby lattice measurements are extrapolated to the infinite-volume limit and proper counterterms are subtracted [72]. An extrapolation to the continuum limit has only been carried out for a small Higgs mass [60], but cutoff effects are modest as long as we are not in the broken phase. Therefore we use lattice results with the physical Higgs mass [59] only for the region $-0.1 \lesssim \bar{m}_3^2(g_{M2}^2)/g_{M2}^4 \lesssim 0.2$ and employ perturbative expressions for the extrapolations to high and low temperature.

At low temperature, i.e. for $\bar{m}_3 \gg 0$, the three-loop perturbative expression for $\langle\phi^\dagger\phi\rangle_{3d}$ can be extracted from ref. [68] (cf. Appendix B in ref. [1] for corrections). The expression reads

$$\frac{\langle\phi^\dagger\phi\rangle_{3d}(g_{M2}^2)}{(g_{M2}^2)T} = -\frac{\sqrt{y}}{2\pi} + \frac{1}{(4\pi)^2}\left[6x - (3 + z)\left(\frac{\ln y}{2} + \ln 2 - \frac{1}{4}\right)\right]$$

$$+ \frac{1}{(4\pi)^3\sqrt{y}}\left[\frac{51\ln y}{32} + \frac{61\ln 2}{16} + \frac{3\pi^2}{16} + \frac{485}{64} + x\left(\frac{9\ln y}{2} + 3\ln 2 + \frac{39}{4}\right)\right.$$

$$- x^2\left(6\ln y + 24\ln 2 - \frac{3}{2}\right) - z\left(\frac{9\ln y}{16} + \frac{27\ln 2}{8} - \frac{\pi^2}{8} - \frac{51}{32}\right)$$

$$\left. - z^2\left(\frac{5\ln y}{32} + \frac{41\ln 2}{48} - \frac{\pi^2}{48} + \frac{47}{192}\right) + xz\left(\frac{3\ln y}{2} - 3\ln 2 + \frac{21}{4}\right)\right] + \mathcal{O}\left(\frac{1}{y}\right) ,$$

$$(2.3.36)$$

where we have used the dimensionless variables for the MSM couplings λ_M, g_{M1}^2 and g_{M2}^2:

$$x = \frac{\lambda_M}{g_{M2}^2} , \quad y = \frac{\bar{m}_3^2(g_{M2}^2)}{g_{M2}^4} , \quad z = \frac{g_{M1}^2}{g_{M2}^2} . \quad (2.3.37)$$

In the broken phase, i.e. $\bar{m}_3 \ll 0$, the available two-loop results show poor convergence [51]. Therefore we employ the "Coleman-Weinberg (CW) method" which makes use of a numerically determined value of the location of the minimum of the potential in the broken phase from which the condensate is then computed. This has been tested against lattice simulations [51, 60]. The result in ref. [60] is derived in the approximation $g_{M1} = 0$, however, corrections originating from g_{M1} are expected to be small.

In figure 2.2 we compare the different methods. The result of the perturbative computation agrees very well with lattice data. The deviation of the CW method from lattice data is expected to be reduced by a continuum extrapolation [60]. The Higgs condensate becomes negative in the symmetric phase due to the renormalization of this effective parameter.

Summing together all contributions from (2.3.3), (2.3.6), (2.3.32) and (2.3.35) most of the $1/\epsilon$ divergences cancel and we get for the second term in our master equation (2.1.16)

$$-\frac{2\nu^2 \mathcal{Z}_m\langle\phi^\dagger\phi\rangle}{T^4} = \Delta_2(T;\bar{\mu}) - \frac{4\nu^4}{(4\pi)^2 T^4 \epsilon} + \mathcal{O}(g^6) , \quad (2.3.38)$$

where the finite part is

$$\Delta_2(T;\bar{\mu}) = -\frac{2\nu^2}{T^4}\left[1 + \frac{3}{2(4\pi)^2}\left((g_1^2 + 3g_2^2 - 8\lambda)\ln\frac{\bar{\mu}e^{\gamma_E}}{4\pi T} - 4h_t^2\ln\frac{\bar{\mu}e^{\gamma_E}}{\pi T}\right)\right]\langle\phi^\dagger\phi\rangle_{3d}(g_{M2}^2)$$

$$- \frac{\nu^2}{3T^2}\left[1 - \frac{3}{2(4\pi)^2}\left((g_1^2 + 3g_2^2)\left(4\ln\frac{g_{M2}^2}{\bar{\mu}} + 3\ln\frac{\bar{\mu}}{4\pi T} + \gamma_E + \frac{5}{3} + \frac{2\zeta'(-1)}{\zeta(-1)}\right)\right.\right.$$

$$\left.\left. + 4h_t^2\ln\frac{\bar{\mu}e^{\gamma_E}}{8\pi T} + 8\lambda\ln\frac{\bar{\mu}e^{\gamma_e}}{4\pi T}\right)\right]$$

$$+ \frac{2\nu^2}{(4\pi)^3 T^2}\left[\frac{g_1^2 m_{E1} + 3g_2^2 m_{E2}}{T} + \frac{g_1^4 T}{16m_{E1}} + \frac{3g_1^2 g_2^2 T}{4(m_{E1} + m_{E2})}\right.$$

$$\left. + \frac{g_2^4 T}{2m_{E2}}\left(\frac{35}{24} + \ln\frac{2m_{E2}}{g_{M2}^2}\right)\right] - \frac{8\nu^4}{(4\pi)^2 T^4}\ln\frac{\bar{\mu}e^{\gamma_E}}{4\pi T} . \quad (2.3.39)$$
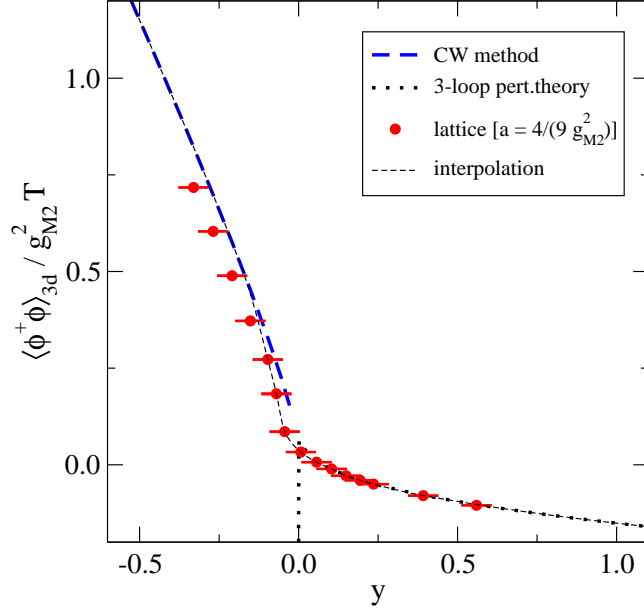
Figure 2.2:   The renormalized Higgs condensate as a function of $y = \bar{m}_3^2(g_{M2}^2)/g_{M2}^4$: Coleman-Weinberg (CW) method in the broken phase; three-loop perturbative expression; lattice data with fixed lattice spacing a [59, 60]; interpolation of the results.

2.4   Vacuum Subtraction

The vacuum subtraction part of the master equation (2.1.16) can be calculated by a direct diagrammatical computation. The tree-level vacuum expectation value of the Higgs field is $v^2 = \nu^2/\lambda$ and with this the one-loop expression for the bare pressure reads

$$
\begin{aligned}
p_{0B}\big|_{v^2=\frac{\nu^2}{\lambda}} = &\frac{1}{2}(\nu^2 + \delta\nu^2)v^2 - \frac{1}{4}(\lambda + \delta\lambda)v^4 \\
&+ \frac{3m_W^4}{32\pi^2}\left(\frac{1}{\epsilon} - \ln\frac{m_W^2}{\bar{\mu}^2} + \frac{5}{6}\right) + \frac{3m_Z^4}{64\pi^2}\left(\frac{1}{\epsilon} - \ln\frac{m_Z^2}{\bar{\mu}^2} + \frac{5}{6}\right) \\
&+ \frac{m_h^4}{64\pi^2}\left(\frac{1}{\epsilon} - \ln\frac{m_h^2}{\bar{\mu}^2} + \frac{3}{2}\right) - \frac{3m_t^4}{16\pi^2}\left(\frac{1}{\epsilon} - \ln\frac{m_t^2}{\bar{\mu}^2} + \frac{3}{2}\right) + \mathcal{O}(g^6) \ . \quad (2.4.1)
\end{aligned}
$$

The counterterms of the Higgs mass parameter and self-coupling are

$$
\delta\nu^2 = \frac{3\nu^2}{(4\pi)^2\epsilon}\left[-\frac{g_1^2 + 3g_2^2}{4} + h_t^2 + 2\lambda\right] \ , \qquad\qquad\qquad (2.4.2)
$$

$$
\delta\lambda = \frac{3}{(4\pi)^2\epsilon}\left[\frac{g_1^4 + 2g_1^2 g_2^2 + 3g_2^2}{16} - h_t^2(h_t^2 - 2\lambda) + \lambda\left(4\lambda - \frac{g_1^2 + 3g_2^2}{2}\right)\right] \ , \quad (2.4.3)
$$

and at the minimum the tree-level masses take the values

$$
m_W^2 = \frac{g_2^2\nu^2}{4\lambda} \ , \qquad m_Z^2 = \frac{(g_1^2 + g_2^2)\nu^2}{4\lambda} \ , \qquad m_h^2 = 2\nu^2 \ , \qquad m_t^2 = \frac{h_t^2\nu^2}{2\lambda} \ . \qquad (2.4.4)
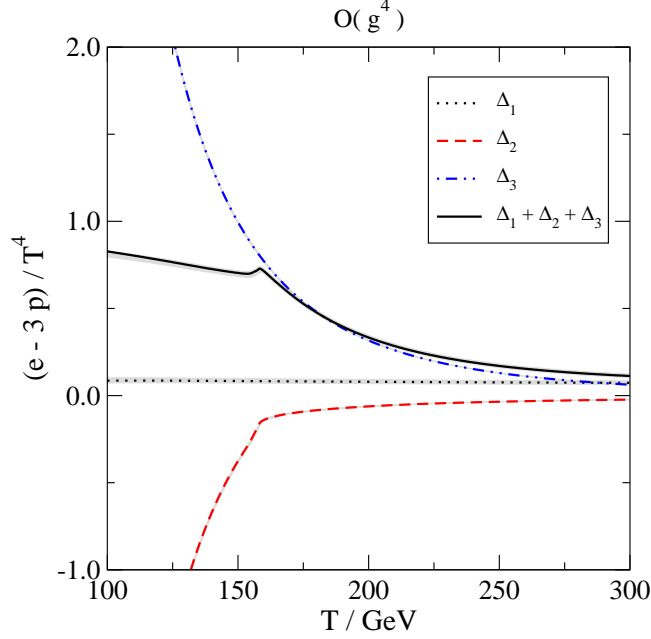$$

Figure 2.3: The trace anomaly and its different contributions. Gray bands reflect variations of the renormalization scale as described in the text.

Inserting these expressions, most divergences cancel in eq. (2.4.1) and the result is

$$\frac{4p_{0B}}{T^4} = \Delta_3(T;\bar{\mu}) + \frac{4\nu^4}{(4\pi)^2 T^4 \epsilon} \ , \tag{2.4.5}$$

where

$$\begin{aligned}
\Delta_3(T;\bar{\mu}) = &\ \frac{\nu^4}{\lambda T^4} + \frac{4\nu^4}{(4\pi)^2 T^4}\left(\ln\frac{\bar{\mu}^2}{\nu^2} + \frac{3}{2}\right) \\
&+ \frac{3\nu^4}{16\lambda^2(4\pi)^2 T^4}\left[2g_2^4\left(\ln\frac{4\lambda\bar{\mu}^2}{g_2^2\nu^2} + \frac{5}{6}\right) + (g_1^2 + g_2^2)^2\left(\ln\frac{4\lambda\bar{\mu}^2}{(g_1^2+g_2^2)\nu^2} + \frac{5}{6}\right)\right] \\
&- \frac{3\nu^4 h_t^4}{\lambda^2(4\pi)^2 T^4}\left(\ln\frac{2\lambda\bar{\mu}^2}{h_t^2\nu^2} + \frac{3}{2}\right) + \mathcal{O}(g^6) \ . \tag{2.4.6}
\end{aligned}$$

Since we choose the renormalization scale $\bar{\mu} \sim \pi T$, large logarithms are introduced if we evaluate Δ_3 directly. Therefore we evaluate the vacuum parameters first at a scale $\bar{\mu}_0 = m_Z$ and then run to the thermal scale using renormalization group equations. From the running of the couplings we get $\Delta_3(T;\bar{\mu}) = 4p_{0R}/T^4$. At the scale $\bar{\mu}_0$ we express the couplings in terms of physical parameters. How this is done is shown in [62] and we will describe the procedure in detail in the next chapter in section 3.3. We restrict ourselves to the one-loop expressions even though higher order computations exist for many parameters. This simplification is justified through the fact that thermal uncertainties outweigh these corrections.
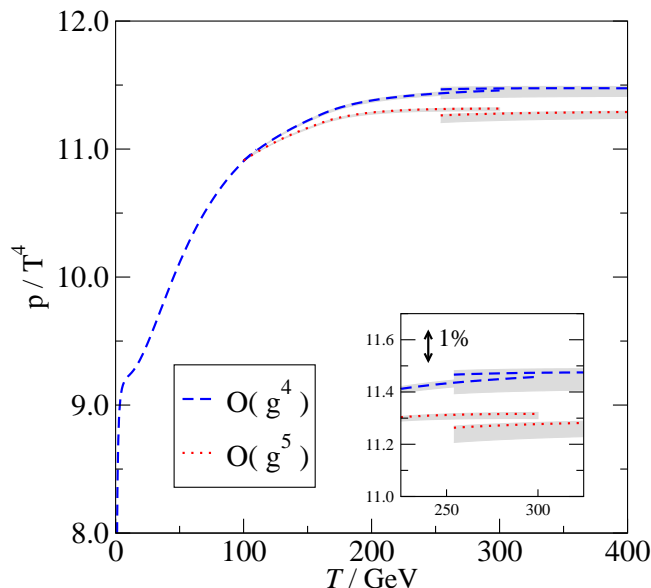
Figure 2.4: The Standard Model pressure.

2.5 Results

We now have all three parts of the master equation (2.1.16), namely (2.2.7), (2.3.39) and (2.4.6), and indeed all $1/\epsilon$ divergences cancel. Even though the trace anomaly

$$T\frac{d}{dT}\left[\frac{p(T)}{T^4}\right] = \Delta_1(T) + \Delta_2(T;\bar{\mu}) + \Delta_2(T;\bar{\mu}) + \mathcal{O}(g^6) \qquad (2.5.1)$$

is formally independent of the renormalization scale $\bar{\mu}$, since corresponding terms cancel between Δ_2 and Δ_3, a residual $\bar{\mu}$-dependence remains. It is an indication of not included higher-order corrections. We write $\bar{\mu} = \alpha\pi T$ and vary $\alpha \in (0.5\ldots 2.0)$ to get an estimate of these uncertainties.

Our study includes corrections up to order $\mathcal{O}(g^5)$. However, studies of the QCD pressure have shown that certain odd orders in the coupling constant show poor convergence. The order $\mathcal{O}(g^4)$ is related to corrections to the order $\mathcal{O}(g^2)$ and, likewise, the order $\mathcal{O}(g^5)$ to order $\mathcal{O}(g^3)$ corrections. Numerically, the most significant contributions are those from the terms proportional to g_3^2 in Δ_1. Therefore, we assume the order $\mathcal{O}(g^4)$, shown in figure 2.3, numerically to be the most accurate estimate for Δ and thus the following plots show the result up to this order. QCD contributions up to $\mathcal{O}(g^6)$ from [73] lead to results lying in between the $\mathcal{O}(g^4)$ and $\mathcal{O}(g^5)$ contributions implying that the latter is most probably on the low side.

As mentioned before, we match the pressure to already existing perturbative results on both the low- and the high-temperature side of the crossover. These results are taken from [73] for the low side and from [68] for high temperatures. The result can be seen in figure 2.4 where both $\mathcal{O}(g^4)$ and $\mathcal{O}(g^5)$ of the dimensionless ratio of the pressure are shown as functions of the temperature. The matching on the high-temperature side lies within an error of 1% and the gray
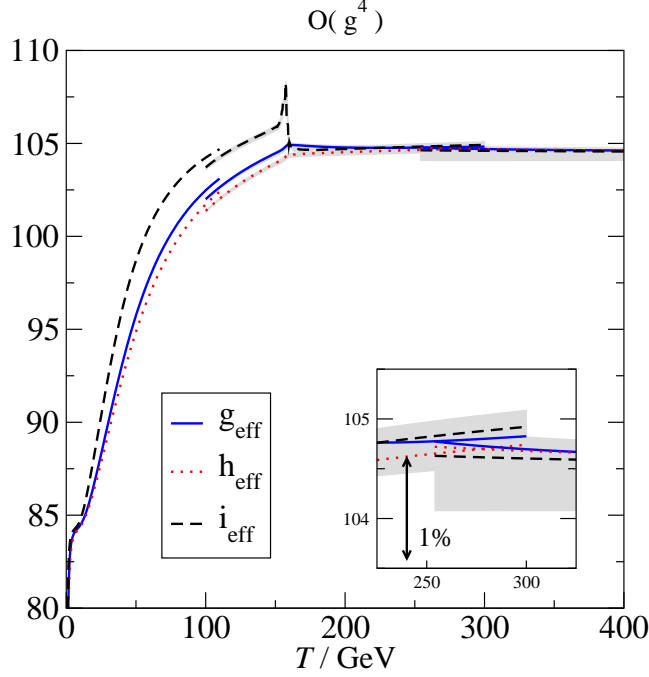
Figure 2.5: The dimensionless functions g_{eff}, h_{eff} and i_{eff} are defined in eq. (2.5.7). The errors in the matching are mostly due to electroweak corrections proportional to g_2^2 and h_t^2 which were omitted in [73] and corrections compared to ref. [68] as mentioned in the text.

bands show the variation of the renormalization scale in the range $\bar{\mu} = \alpha\pi T$ with $\alpha \in (0.5\ldots 2.0)$.

From the pressure and its logarithmic temperature derivative Δ we can now obtain other thermodynamic functions as follows:

energy density: $\qquad\qquad\qquad \dfrac{e}{T^4} = \Delta + \dfrac{3p}{T^4}$, $\qquad\qquad$ (2.5.2)

entropy density $s = p'$: $\qquad\qquad \dfrac{s}{T^3} = \Delta + \dfrac{4p}{T^4}$, $\qquad\qquad$ (2.5.3)

heat capacity $c = e'$: $\qquad\qquad \dfrac{c}{T^3} = T\Delta' + 7\Delta + \dfrac{12p}{T^4}$, $\qquad$ (2.5.4)

equation-of-state parameter: $\quad w = \dfrac{p}{e} = \left(3 + \dfrac{\Delta T^4}{p}\right)^{-1}$, $\qquad$ (2.5.5)

speed of sound squared: $\qquad c_s^2 = \dfrac{p'}{e'} = \dfrac{s}{c}$. $\qquad\qquad$ (2.5.6)

Derivatives are understood to be with respect to the temperature. Some of these functions are parametrized through

$$g_{\text{eff}}(T) = \frac{e(T)}{\left[\frac{\pi^2 T^4}{30}\right]} \ , \quad h_{\text{eff}}(T) = \frac{s(T)}{\left[\frac{2\pi^2 T^3}{45}\right]} \ , \quad i_{\text{eff}}(T) = \frac{c(T)}{\left[\frac{2\pi^2 T^3}{15}\right]} \ . \qquad (2.5.7)$$

The values of these functions across the crossover at the order $\mathcal{O}(g^4)$ are shown in figures 2.5 and 2.6. As can be seen, the most interesting quantities
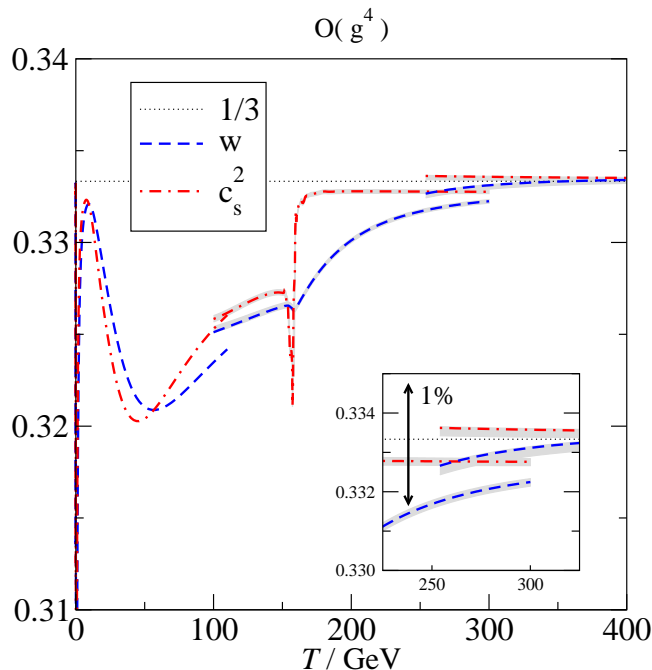
Figure 2.6: The equation-of-state parameter w and speed of sound squared c_s^2.

are the heat capacity and the speed of sound squared which show a peak or a minimum respectively. Again the gray error band correspond to variations of the renormalization scale.

For the non-perturbative contributions we have made use of already existing results in the literature [59, 60]. There has been made progress lately and new results, including the Abelian $U(1)$ contributions, exist [57]. However, the plots shown here (figures 2.3, 2.4, 2.5 and 2.6) were not updated with these new results since they only have a minor numerical effect.

2.6   Implications

Even though there is no phase transition in the Standard Model, Standard Model thermodynamics around the electroweak scale can still be important to other phenomena taking place in this temperature range, i.e. at that time in the early universe. Assuming a flat geometry we can express the temperature evolution of the early universe using the thermodynamic functions of the last section as

$$\frac{3}{2}\sqrt{\frac{5}{\pi^3}}\frac{m_{\mathrm{Pl}}}{T^3}\frac{dT}{dt} = -\frac{\sqrt{g_{\mathrm{eff}}(T)}h_{\mathrm{eff}}(T)}{i_{\mathrm{eff}}(T)} \ , \qquad (2.6.1)$$

where m_{Pl} is the Planck mass. A peak in the heat capacity i_{eff} thus leads to a short period of slower change in temperature. This in turn can lead to an increased abundance of particles produced at this time or inversely to a reduced density of weakly interacting relics of the early universe annihilating through co-annihilation processes that are taking place.

Regardless of the impact of the Standard Model background, new physics Beyond the Standard Model (BSM) is needed for addressing e.g. baryogenesis or dark matter. The effects studied in this chapter are usually not taken into account in models for new physics. The reason is that the parameter space for models is not as strongly constrained as one would hope. However, the ever increasing amount of data from the LHC is published on a regular basis and thus more and more regions of the allowed parameter spaces in BSM models are excluded.

New physics in beyond the Standard Model theories can be introduced in many different ways and with a variety of new particles. One possibility is to consider the Standard Model as a low-energy effective theory. One can then introduce higher-dimensional operators which in principle could render the phase transition strongly first order [74, 75]. However, we will not consider this, but instead use a simple renormalizable extension of the Standard Model.

Chapter 3

Phase Transition in the Inert Doublet Model

The Standard Model of particle physics works very well and with the discovery of the Higgs boson at the LHC in 2012 [46, 47] it has again proven to be a predictive theory. However, we have known for a long time now that it is not the final answer. There are a lot of phenomena which remain unexplained by the Standard Model. Amongst them are dark matter, dark energy, neutrino oscillations, the enormous hierarchy between the electroweak scale ($\mathcal{O}(10^2)$ GeV) and the Planck scale ($\mathcal{O}(10^{19})$ GeV), the reason for the number of families to be three and the origin of the baryon asymmetry of the universe.

In order to address some of these phenomena, many different models have been built. Unfortunately, experiments have not yet shown significant hints of the nature of this new, beyond the Standard Model physics. Thus, most of these models remain yet to be disproved and for now we are stuck with this plethora of models.

There are a number of models with extended Higgs sectors with new scalars in the singlet, doublet, triplet or even higher representations. These simple extensions have small numbers of new parameters and are thus the most constrained ones, although not excluded. Depending on the new physics these models aim to explain, conflicting ranges of couplings are required. To account for an allowed dark matter relic density, co-annihilation of dark matter to Standard Model particles cannot be too strong and thus their interactions, i.e. the couplings, have to be small. On the other hand large couplings are needed to strengthen a first order phase transition for baryogenesis. However, large couplings can compromise or even spoil a perturbative analysis as well as the high-temperature expansion used for dimensionally reduced lattice studies.

This chapter focuses on one such model where a new scalar doublet is introduced and a further simplification in terms of an unbroken $\mathbb{Z}_2$ is imposed. This theory is called the Inert Doublet Model (IDM) [76–78]. The IDM is interesting because it combines the two aforementioned regimes of small couplings for dark matter [79–95] and large ones for a strong electroweak phase transition [96–103].

To create a strong first order phase transition, new large couplings are needed. If new massive degrees of freedom were to be weakly coupled, they could just be integrated out, leaving us with the same effective theory as before,

i.e. the Standard Model. However, in this effective theory one could include higher-order operators which in principle could render the phase transition first order [75]. Nevertheless, we restrict ourselves to the renormalizable case and do not consider higher-order operators. One way to prevent the new fields from being integrated out, is to make these degrees of freedom light. They can then have a phase transition of their own which can then have a substantial effect on the dynamics of the electroweak phase transition [104, 105]. In our study, however, we focus on the case of large couplings which change the effective couplings of the low-energy theory significantly.

In this chapter we want to calculate the full two-loop effective potential to estimate the strength of a possible phase transition in the IDM. Besides the estimation of the convergence of the perturbative series, we want to compare our results to the high-temperature expansion. One goal is then to justify or set limits to the use of the high-temperature expansion used in dimensionally reduced lattice simulations. Furthermore, we provide the techniques to calculate a thermal two-loop effective potential in a model independent way. All relevant diagrams in any model can be reduced to a handful of master integral functions which are presented in Appendix A.2.

For simplicity we neglect the gauge group $U(1)$ in our calculations, i.e. setting $g_1 = 0$. This is justified because the loop-expansion parameter α is small $(\alpha = g_1^2/(4\pi) \sim 10^{-2})$ and the resulting corrections are much smaller than thermal uncertainties originating from the variation of our thermal scale as described below.

In section 3.1 we introduce the Inert Doublet Model, its particle content and degrees of freedom as well as all the tree-level masses and their thermal mass contributions. In section 3.2 we then describes the procedure for the computation of the one- and two-loop potential and derive the master integrals. The potential is then numerically evaluated and the results are presented in section 3.3. Finally, a number of theoretical and experimental constraints for the IDM are then given in section 3.4.

3.1 The Inert Doublet Model

We consider the Inert Doublet Model with the Lagrangian of the scalar sector

$$\mathcal{L}_{\text{scalar}} = (D_\mu \phi)^\dagger (D^\mu \phi) + (D_\mu \chi)^\dagger (D^\mu \chi) - V(\phi, \chi) \ , \qquad (3.1.1)$$

where the tree-level potential takes the form

$$V(\phi, \chi) = V_0 = \mu_1^2 \phi^\dagger \phi + \mu_2^2 \chi^\dagger \chi + \lambda_1 (\phi^\dagger \phi)^2 + \lambda_2 (\chi^\dagger \chi)^2 + \lambda_3 (\phi^\dagger \phi)(\chi^\dagger \chi)$$
$$+ \lambda_4 (\phi^\dagger \chi)(\chi^\dagger \phi) + \frac{\lambda_5}{2} \left[(\phi^\dagger \chi)^2 + (\chi^\dagger \phi)^2 \right] \ . \qquad (3.1.2)$$

All coefficients $\{\mu_1, \mu_2, \lambda_1, \lambda_2, \lambda_3, \lambda_4, \lambda_5\}$ are real. This is not the case in general, since λ_5 could be complex, in which case the last term in the potential would read

$$\delta V_{\lambda_5}(\phi, \chi) = \frac{\lambda_5}{2} (\phi^\dagger \chi)^2 + \frac{\lambda_5^*}{2} (\chi^\dagger \phi)^2 = \frac{|\lambda_5|}{2} \left[e^{i\alpha} (\phi^\dagger \chi)^2 + e^{-i\alpha} (\chi^\dagger \phi)^2 \right] \ . \quad (3.1.3)$$

However, the phase α can be absorbed into a field redefinition of ϕ and χ. Considering a transformation $\phi \to \phi e^{i\theta_\phi}$, $\chi \to \chi e^{i\theta_\chi}$, eq. (3.1.3) transforms into

$$\delta V_{\lambda_5}(\phi, \chi) \to \frac{|\lambda_5|}{2} \left[e^{i(\alpha - 2\theta_\phi + 2\theta_\chi)} (\phi^\dagger \chi)^2 + e^{-i(\alpha - 2\theta_\phi + 2\theta_\chi)} (\chi^\dagger \phi)^2 \right] . \qquad (3.1.4)$$

The phase α is then eliminated by choosing θ_ϕ and θ_χ such that for $n \in \mathbb{Z}$ they obey the relation

$$\alpha - 2\theta_\phi + 2\theta_\chi = n \cdot 2\pi \quad \Rightarrow \quad \theta_\phi - \theta_\chi = \frac{\alpha}{2} + n \cdot \pi . \qquad (3.1.5)$$

We want to study the effective potential as a tool for physical quantities like the critical temperature T_c of the phase transition, the latent heat L or the discontinuity of the Higgs condensate v_{phys}. The effective potential is defined through a shift of the neutral Higgs component, such that the two scalar doublets can be written as

$$\phi = \frac{1}{\sqrt{2}} \begin{pmatrix} G_2 + iG_1 \\ v + h - iG_3 \end{pmatrix} , \quad \chi = \frac{1}{\sqrt{2}} \begin{pmatrix} H_2 + iH_1 \\ H_0 - iH_3 \end{pmatrix} , \qquad (3.1.6)$$

where h is the physical Standard Model Higgs boson. The new, inert, scalars are the CP even $H = H_0$, CP odd $A = H_3$ and the charged ones $H^\pm = (H_1 \pm iH_2)/\sqrt{2}$. The G's are the Goldstone bosons and we use the usual definitions, e.g. $G^\pm = (G_1 \pm iG_2)/\sqrt{2}$.

The Lagrangian of the IDM is invariant under a $\mathbb{Z}_2$ transformation under which the inert doublet is odd while all the Standard Model fields are even

$$\phi \to \phi , \quad \chi \to -\chi , \quad f_{\mathrm{SM}} \to f_{\mathrm{SM}} . \qquad (3.1.7)$$

This means that there are no Yukawa interactions between the inert doublet and the SM fermions, hence the name of the model. Moreover, the $\mathbb{Z}_2$ symmetry implies that the inert particles cannot decay into SM particles only, such that the lightest new scalar is stable. If it is one of the electrically neutral ones, i.e. H or A, it is a dark matter candidate.

From the potential (3.1.2) we can derive the tree-level masses of the inert scalars

$$m_H^2 = \mu_2^2 + \frac{\lambda_L}{2} v^2 , \quad m_A^2 = \mu_2^2 + \frac{\lambda_S}{2} v^2 , \quad m_{H^\pm}^2 = \mu_2^2 + \frac{\lambda_3}{2} v^2 , \qquad (3.1.8)$$

with $\lambda_L = (\lambda_3 + \lambda_4 + \lambda_5)$ and $\lambda_S = (\lambda_3 + \lambda_4 - \lambda_5)$. We choose H to be the lightest new scalar, i.e. the dark matter candidate, thus rendering λ_5 negative.[1]

We consider the case where only ϕ acquires a vacuum expectation value $\langle h \rangle = v$ as in the Standard Model. This means that μ_2^2 is positive while μ_1^2 is negative. In principle $\langle \chi \rangle$ could be non-zero at some high temperature where $\langle \phi \rangle = 0$ before going to the electroweak minimum where $\langle \chi \rangle = 0$ and $\langle \phi \rangle \neq 0$. The scenario of this two step phase transition has also been studied for the IDM [101] and could in general lead to an even stronger first order transition [106]. In our computation, however, we want the $\mathbb{Z}_2$ symmetry to be unbroken.

---

[1]This leads to a misleading notation with $\lambda_{\mathrm{L(arge)}}$ to be smaller than $\lambda_{\mathrm{S(mall)}}$. However, we stay with this convention used in the literature.

Our computations are performed using the $\overline{\text{MS}}$ renormalization scheme in Feynman R_ξ gauge. The gauge fixing and $SU(2)$ Faddeev-Popov ghost $(c_A^a, \bar{c}_A^a)$ terms coupling to the scalar degrees of freedom are

$$\mathcal{L}_{\text{gauge fixing}} = \frac{1}{2\xi} \sum_{a=1}^{3} \left(\partial_\mu A_\mu^a - \frac{\xi g v}{2} G_a^2 \right) + \frac{\xi g^2 v}{4} \left(\bar{c}_A^a h c_A^a + \epsilon^{abc} \bar{c}_A^a G_b c_A^c \right) . \quad (3.1.9)$$

In R_ξ gauges the parameter v appears here as a background field and is in general different from the shift of the Higgs field in eq. (3.1.6). For a proper renormalization of gauge-dependent quantities they need to be renormalized separately (cf. refs. [107, 108]).

There is a contribution from the gauge fixing term to the masses of the Goldstone bosons $\delta m_G^2 = \xi m_W^2$. In Feynman gauge ($\xi = 1$) the tree-level masses of the Higgs and Goldstones are then

$$m_h^2 = \mu_1^2 + 3\lambda_1 v^2 , \quad m_G^2 = \mu_1^2 + \lambda_1 v^2 + m_W^2 . \quad (3.1.10)$$

In this model we have introduced five additional parameters to the ones from the Standard Model: $\mu_2, \lambda_2, \lambda_3, \lambda_4, \lambda_5$. We express these in a different basis with a more convenient set of variables

$$\{m_H, m_A, m_{H^\pm}, \lambda_2, \lambda_L\} . \quad (3.1.11)$$

In our numerical study of various benchmark points we will use different values for these five parameters as input parameters. However, we also want to relate them, together with the other couplings, to physical parameters using one-loop self-energies for physical pole mass expressions. How this is done is explained in section 3.3.

The next step is to determine the thermal mass contributions. As described in the introduction we have to consider the one-loop corrections to the propagator at high-temperature in the symmetric phase and with vanishing external momenta. We thus omit higher-order corrections of order $\mathcal{O}(g^4 T^2)$ and $\mathcal{O}(g^2 m^2)$. We remember the high-temperature expansions which in the massless case are

$$I(0_b) = \frac{T^2}{12} , \quad I(0_f) = -\frac{T^2}{24} , \quad (3.1.12)$$

where we denote by a subscript b or f whether it corresponds to a massless boson or fermion respectively. It is then straightforward to calculate the thermal mass corrections. However, we do this in D dimensions. Since $I(0)$ can be multiplied by factors of $1/\epsilon$ in loop diagrams, the terms of $\mathcal{O}(\epsilon)$ from using dimensional regularization where $D = 4 - 2\epsilon$ have to be kept.

Within the high-temperature expansion (see Appendix A.2) these so called linear terms $\sim g^2 I(0) I_{n=0}(m)$, where the contribution from the Matsubara zero-modes is $I_{n=0}(m) = -mT/(4\pi)[1 + \mathcal{O}(\epsilon)]$ (cf. eq. (1.3.15)), cancel. This cancellation is also a crosscheck for the consistency of our resummation. However, within the Inert Doublet Model with large couplings, the corrections omitted by using (3.1.12) can be large. Thus beyond the high-temperature expansion the cancellation is incomplete. However, such terms only become visible at small v/T, i.e. for weak transitions, and thus we will not go into more detail.

The full expressions for the masses squared including the thermal mass corrections are summarized in table 3.1. The thermal masses in D dimensions

field	vacuum mass	thermal mass	degeneracy
h	$m_h^2 = \mu_1^2 + 3\lambda_1 v^2$	$\widetilde{m}_h^2 = m_h^2 + \delta m_{\phi T}^2$	1
G	$m_G^2 = \mu_1^2 + \lambda_1 v^2 + m_W^2$	$\widetilde{m}_G^2 = m_G^2 + \delta m_{\phi T}^2$	3
H	$m_H^2 = \mu_2^2 + \frac{1}{2}\lambda_L v^2$	$\widetilde{m}_H^2 = m_H^2 + \delta m_{\chi T}^2$	1
A	$m_A^2 = \mu_2^2 + \frac{1}{2}\lambda_S v^2$	$\widetilde{m}_A^2 = m_A^2 + \delta m_{\chi T}^2$	1
$H^\pm$	$m_{H^\pm}^2 = \mu_2^2 + \frac{1}{2}\lambda_3 v^2$	$\widetilde{m}_{H^\pm}^2 = m_{H^\pm}^2 + \delta m_{\chi T}^2$	2
A_i	$m_W^2 = \frac{1}{4}g_2^2 v^2$	m_W	$3(D-1)$
A_0	m_W^2	$\widetilde{m}_W^2 = m_W^2 + m_{\mathrm{E}2}^2$	3
$c_A, \bar{c}_A$	m_W^2	m_W^2	-6
C_i	0	0	$8(D-1)$
C_0	0	$m_{\mathrm{E}3}^2$	8
$c_C, \bar{c}_C$	0	0	-16
t	$m_t^2 = \frac{1}{2}h_t^2 v^2$	m_t^2	12

Table 3.1: Tree-level masses squared in Feynman R_ξ gauge with thermal masses given in eqs. (3.1.13) - (3.1.16). The gauge fields A_μ and C_μ correspond to the gauge groups $SU(2)$ and $SU(3)$ and $c_A, \bar{c}_A, c_C, \bar{c}_C$ are the Faddeev-Popov ghosts. The top quark is denoted by t.

are

$$\delta m_{\phi T}^2 = \frac{1}{2}\left[6\lambda_1 + 3 \cdot 2\lambda_1 + \lambda_L + \lambda_S + 2\lambda_3 + \frac{3(D-1)}{2}g_2^2\right]I(0_b) - \frac{12}{2}h_t^2 I(0_f)$$

$$= \left[\frac{6\lambda_1 + 2\lambda_3 + \lambda_4}{12} + \frac{3g_2^2}{16} + \frac{h_t^2}{4}\right]T^2 + \mathcal{O}(\epsilon T) , \tag{3.1.13}$$

$$\delta m_{\chi T}^2 = \frac{1}{2}\left[6\lambda_2 + 3 \cdot 2\lambda_2 + \lambda_L + \lambda_S + 2\lambda_3 + \frac{3(D-1)}{2}g_2^2\right]I(0_b)$$

$$= \left[\frac{6\lambda_2 + 2\lambda_3 + \lambda_4}{12} + \frac{3g_2^2}{16}\right]T^2 + \mathcal{O}(\epsilon T) , \tag{3.1.14}$$

$$m_{\mathrm{E}2}^2 = (D-2)g_2^2\left[2(D-1)I(0_b) - 4n_G I(0_f)\right]$$

$$= \left[1 + \frac{n_G}{3}\right]g_2^2 T^2 + \mathcal{O}(\epsilon T) , \tag{3.1.15}$$

$$m_{\mathrm{E}3}^2 = (D-2)g_3^2\left[3(D-2)I(0_b) - 4n_G I(0_f)\right]$$

$$= \left[1 + \frac{n_G}{3}\right]g_3^2 T^2 + \mathcal{O}(\epsilon T) . \tag{3.1.16}$$

With these tree-level expressions we can now begin our computation of the scalar potential.

3.2 The Two-Loop Potential

With the masses and degeneracies given in table 3.1 as well as the already introduced J-function (cf. eq. (2.1.5) and section 3.2.1) we can now easily write down the one-loop contribution of the potential. Including counterterms, the

tree-level and one-loop potential is then

$$
\begin{aligned}
V_0 + V_1 = {} & \frac{\mu_1^2 v^2}{2} + \frac{\lambda_1 v^4}{2} + \frac{\delta\mu_1^2 v^2}{2} + \frac{\delta\lambda_1 v^4}{2} \\
& + J(\widetilde{m}_h) + 3J(\widetilde{m}_G) + J(\widetilde{m}_H) + J(\widetilde{m}_A) + 2J(\widetilde{m}_{H^\pm}) \\
& + 3\big[(D-3)J(m_W) + J(\widetilde{m}_W)\big] + 8\big[(D-3)J(0_b) + J(m_{E3})\big] \\
& - 12J(m_t) - (30n_G - 12)J(0_f) \, ,
\end{aligned}
\tag{3.2.1}
$$

where the masses are listed in table 3.1, the counterterms are given in Appendix C.1 and $n_G = 3$ is the number of fermion generations. The last term includes five massless quarks and nine massless leptons.

We now introduce a notation where we keep track of the $1/\epsilon$ expansion in a superscript index. This notation is used for the potential and similarly for all the master integral functions, e.g. the J-function below. We expand the potential as

$$
V = \frac{1}{\epsilon} V^{(-1)} + V^{(0)} + \epsilon V^{(1)} + \mathcal{O}(\epsilon^2) \, .
\tag{3.2.2}
$$

We are using dimensional regularization in all our calculations, i.e. setting $D = 4 - 2\epsilon$. Therefore, the numbers of degrees of freedom of the spatial components of the gauge fields are ϵ-dependent. To some extent vacuum counterterms cancel divergences and some of the temperature dependent divergences cancel in the sum of all terms. The remaining divergences, however, which are proportional to thermal masses and thus formally of higher order are removed by hand. Since these divergences cancel at higher order we do not expand thermal masses in ϵ.

Using the notation of eq. (3.2.2) in eq. (3.2.1) and proceed as described, the finite part of the one-loop potential becomes

$$
\begin{aligned}
V_1^{(0)} = {} & J^{(0)}(\widetilde{m}_h) + 3J^{(0)}(\widetilde{m}_G) + J^{(0)}(\widetilde{m}_H) + J^{(0)}(\widetilde{m}_A) + 2J^{(0)}(\widetilde{m}_{H^\pm}) \\
& + 3\big[J^{(0)}(m_W) - 2J^{(-1)}(m_W) + J^{(0)}(\widetilde{m}_W)\big] \\
& + 8\big[J^{(0)}(0_b) - 2J^{(-1)}(0_b) + J^{(0)}(m_{E3})\big] \\
& - 12J^{(0)}(m_t) - (30n_G - 12)J^{(0)}(0_f) \, .
\end{aligned}
\tag{3.2.3}
$$

We now turn to the two-loop potential. The topologies of the Feynman diagrams for its calculation are of course the same as in chapter 2. We include the counterterm and denote them by

$$
\bigcirc\!\!\!\bullet = (\mathrm{x}) \, , \qquad \bigcirc\!\!\bigcirc = (\mathrm{xx}) \, , \qquad \ominus = (\mathrm{xxx}) \, .
\tag{3.2.4}
$$

The fields inside the brackets are either scalars (s), vector bosons (v), ghosts (g) or fermions (f). All the contributions are expressed in terms of the master sum-integrals derived in sections 3.2.1 and 3.2.2.

In perturbation theory we do a weak-coupling expansion, i.e. a Taylor series in the coupling constant. We can write the action as $S = S_0 + S_I$, where S_0 captures the kinetic and the mass terms and S_I the interaction terms proportional to the coupling constants. We can then write the partition function as

$$
\mathcal{Z} = \int \mathcal{D}[\ldots] e^{-S_0 - S_I} \, ,
\tag{3.2.5}
$$

where $\mathcal{D}[\ldots]$ is the path integration measure for all the fields. Introducing the free partition function $\mathcal{Z}_0 = \int \mathcal{D}[\ldots]e^{-S_0}$ we expand eq. (3.2.5) in terms of the coupling constants and write

$$\mathcal{Z} = \mathcal{Z}_0 \left[1 - \langle S_I \rangle_0 + \frac{1}{2}\langle S_I^2 \rangle_0 + \mathcal{O}(\langle S_I^3 \rangle_0)\right] , \qquad (3.2.6)$$

where the expectation value is defined as $\langle A \rangle_0 = \mathcal{Z}_0^{-1} \int \mathcal{D}[\ldots]Ae^{-S_0}$. The free energy density can be expressed with the partition function as

$$f = -\frac{T}{V} \ln \mathcal{Z} = f_0 - \frac{T}{V}\left[-\langle S_I \rangle_0 + \frac{1}{2}\left(\langle S_I^2 \rangle_0 - \langle S_I \rangle_0^2\right) + \mathcal{O}(\langle S_I^3 \rangle_0)\right] , \qquad (3.2.7)$$

where f_0 contains contributions from S_0 and the thermodynamical limit $V \to \infty$ is implied. We denote the second term in eq. (3.2.7) with f_I, such that $f = f_0 + f_I$, and rewrite it as

$$f_I = -\frac{T}{V}\langle e^{-S_I} - 1 \rangle_0 = \langle S_I - \frac{1}{2}S_I^2 + \mathcal{O}(S_I^3) \rangle_0 . \qquad (3.2.8)$$

In the last step we have dropped an overall integration $\int_X$ because it cancels against the factor T/V. Inserting the interaction part of the action into eq. (3.2.8) and using Wick's theorem [109] we can write the expectation value in terms of two-point functions.

The diagrams of eq. (3.2.4) are then constructed by contracting the fields in the corresponding terms. The first two types, (x) and (xx), originate from the first term of the expansion in eq. (3.2.8), whereas the last one comes from the second term. Therefore, diagrams with the sunset topology (xxx) have to be multiplied by a factor of $-1/2$.

As an example of the computation of the two-loop potential we consider the diagrams with only scalar fields. The Feynman rules are derived by inserting the expressions for the scalar doublets (3.1.6) into the potential (3.1.2) and then taking explicit derivatives. The term $\sim \lambda_1$ for example reads

$$\delta V_{\lambda_1} = \lambda_1 \left[G^+ G^- + \frac{1}{2}\left(v^2 + 2hv + h^2 + G^0 G^0\right)\right]^2 \qquad (3.2.9)$$

and leads to the Feynman rules

$$\left. \frac{\delta^3 V_{\lambda_1}}{\partial h^3}\right|_{\langle f \rangle = 0} = 6v\lambda_1 , \qquad (3.2.10)$$

$$\left. \frac{\delta^3 V_{\lambda_1}}{\partial h \partial (G^0)^2}\right|_{\langle f \rangle = 0} = 2v\lambda_1 , \qquad (3.2.11)$$

$$\left. \frac{\delta^3 V_{\lambda_1}}{\partial h \partial G^+ \partial G^-}\right|_{\langle f \rangle = 0} = 2v\lambda_1 , \qquad (3.2.12)$$

where $\langle f \rangle = 0$ means that all the fields, here $f \in \{h, G^0, G^\pm\}$, are set to zero. The expression of the full scalar potential (3.1.2) leads to the rest of the scalar Feynman rules. We denote the Goldstone bosons as $G \in \{G^0, G^\pm\}$ and write down the scalar sunset diagrams with their appropriate symmetry factors:

$$-\frac{1}{12} \times \text{\small(sunset)} = -3v^2 \lambda_1^2 H(\widetilde{m}_h, \widetilde{m}_h, \widetilde{m}_h) \ , \tag{3.2.13}$$

$$-\frac{3}{4} \times \text{\small(sunset)} = -3v^2 \lambda_1^2 H(\widetilde{m}_h, \widetilde{m}_G, \widetilde{m}_G) \ , \tag{3.2.14}$$

$$-\frac{1}{4} \times \text{\small(sunset)} = -\frac{v^2}{4} \lambda_L^2 H(\widetilde{m}_h, \widetilde{m}_H, \widetilde{m}_H) \ , \tag{3.2.15}$$

$$-\frac{1}{4} \times \text{\small(sunset)} = -\frac{v^2}{4} \lambda_S^2 H(\widetilde{m}_h, \widetilde{m}_A, \widetilde{m}_A) \ , \tag{3.2.16}$$

$$-\frac{1}{2} \times \text{\small(sunset)} = -\frac{v^2}{2} \lambda_3^2 H(\widetilde{m}_h, \widetilde{m}_{H^\pm}, \widetilde{m}_{H^\pm}) \ , \tag{3.2.17}$$

$$-\frac{1}{2} \times \text{\small(sunset)} = -\frac{v^2}{2} \lambda_5^2 H(\widetilde{m}_G, \widetilde{m}_H, \widetilde{m}_A) \ , \tag{3.2.18}$$

$$-\frac{1}{2} \times \text{\small(sunset)} = -\frac{v^2}{4} (\lambda_4 + \lambda_5)^2 H(\widetilde{m}_G, \widetilde{m}_H, \widetilde{m}_{H^\pm}) \ , \tag{3.2.19}$$

$$-\frac{1}{2} \times \text{\small(sunset)} = -\frac{v^2}{4} (\lambda_4 - \lambda_5)^2 H(\widetilde{m}_G, \widetilde{m}_A, \widetilde{m}_{H^\pm}) \ , \tag{3.2.20}$$

The Feynman rules for the quartic vertices are derived by taking four derivatives of the potential. For the part given in eq. (3.2.9) these are for example

$$\text{\small(vertex)} = \frac{\delta^4 V_{\lambda_1}}{\partial h^4} = 6\lambda_1 \ , \tag{3.2.21}$$

$$\frac{\delta^4 V_{\lambda_1}}{\partial h^2 \partial G^{0\,2}} = 2\lambda_1 \ , \tag{3.2.22}$$

$$\frac{\delta^4 V_{\lambda_1}}{\partial h^2 \partial G^+ \partial G^-} = 2\lambda_1 \ , \tag{3.2.23}$$

which lead to the diagrams

$$\frac{1}{8} \times \quad = \frac{3}{4}\lambda_1 I^2(\widetilde{m}_h) \ , \tag{3.2.24}$$

$$\frac{3}{4} \times \quad = \frac{3}{2}\lambda_1 I(\widetilde{m}_h) I(\widetilde{m}_G) \ . \tag{3.2.25}$$

The Feynman rules for all the other vertices are derived in a similar way. The results for all the diagrams contributing to the two-loop potential are listed in Appendix B.

To express diagrams with fermion lines in terms of the master integrals, we need to rewrite traces as

$$\mathrm{Tr}\left[(\slashed{K} + m_1)(\slashed{P} + m_2)\right] = 4(K \cdot P + m_1 m_2)$$
$$= 2\left[(K+P)^2 + m_3^2 - (K^2 + m_1^2) - (P^2 + m_2^2) + (m_1 + m_2)^2 - m_3^2\right] \ . \tag{3.2.26}$$

Using this we can simply read off the contributions from the different master integrals as shown in the following example:

$$-\frac{1}{2} \times \quad = \frac{3h_t^2}{4} \oint_{K,P} \frac{\mathrm{Tr}\left[(\slashed{K} + m_1)(\slashed{P} + m_2)\right]}{(K^2 + m_t^2)(P^2 + m_t^2)\left[(K+P)^2 + \widetilde{m}_h^2\right]}$$
$$= \frac{3h_t^2}{2} \oint_{K,P} \frac{\left[(K+P)^2 + \widetilde{m}_h^2\right] - (K^2 + m_t^2) - (P^2 + m_t^2) + 4m_t^2 - \widetilde{m}_h^2}{(K^2 + m_t^2)(P^2 + m_t^2)\left[(K+P)^2 + \widetilde{m}_h^2\right]}$$
$$= -\frac{3h_t^2}{2}\left[(\widetilde{m}_h^2 - 4m_t^2)H(\widetilde{m}_h, m_t, m_t) + 2I(\widetilde{m}_h)I(m_t) - I^2(m_t)\right] \ . \tag{3.2.27}$$

In the following two sections we derive the master integral functions for one- and two-loop finite temperature integrals. An overview as well as their high-temperature expansions can be found in Appendix A.2. The derivation follows a similar path in each case. We rewrite the integrals in a convenient

way such that the Matsubara sums can be performed. The remaining integrals are then evaluated if possible or otherwise left to be evaluated numerically. These numerical integrals are usually rapidly converging, although there are some difficulties in the two-loop integral functions concerning poles. These technicalities are discussed below.

3.2.1 One-Loop Finite Temperature Integrals

The integral function $I(m)$, also called the tadpole integral, is

$$I(m) = \oint_K \frac{1}{K^2 + m^2} = T \sum_{k_0} \int_k \frac{1}{k_0^2 + k^2 + m^2} \; . \tag{3.2.28}$$

For the moment we want to keep the bosonic and fermionic cases separated. Which modes k_0 stands for is implicitly given by the argument of the I-function. The Matsubara sums can be evaluated as

$$T \sum_{n=-\infty}^{\infty} \frac{1}{(2\pi n T)^2 + \omega^2} = \frac{1}{2\omega} \coth\left[\frac{\omega}{2T}\right] \; ,$$

$$T \sum_{n=-\infty}^{\infty} \frac{1}{\left((2n+1)\pi T\right)^2 + \omega^2} = \frac{1}{2\omega} \tanh\left[\frac{\omega}{2T}\right] \; . \tag{3.2.29}$$

We can rewrite the hyperbolic functions as

$$\coth x = \frac{e^x + e^{-x}}{e^x - e^{-x}} = 1 + \frac{2e^{-x}}{e^x - e^{-x}} = 1 + \frac{2}{e^{2x} - 1} = 1 + 2n_b(\omega) \; ,$$

$$\tanh x = \frac{e^x - e^{-x}}{e^x + e^{-x}} = 1 - \frac{2e^{-x}}{e^x + e^{-x}} = 1 - \frac{2}{e^{2x} + 1} = 1 - 2n_f(\omega) \; , \tag{3.2.30}$$

where in the last step we have set $x = \omega/(2T)$, where $\omega = \sqrt{k^2 + m^2}$. The tadpole integral now splits into a zero-temperature and a finite-temperature part

$$I_b(m) = I_{\text{vac}}(m) + I_{T,b}(m) = \int_k \frac{1}{2\omega} + \int_k \frac{n_b(\omega)}{\omega} \; ,$$

$$I_f(m) = I_{\text{vac}}(m) + I_{T,f}(m) = \int_k \frac{1}{2\omega} - \int_k \frac{n_f(\omega)}{\omega} \; , \tag{3.2.31}$$

where the minus sign in the fermionic integrals stems from the fermionic loop. We now introduce the distribution function $n(\omega)$ which is understood to be either the Bose-Einstein distribution $n(\omega) = n_b(\omega)$ for bosonic arguments or minus the Fermi-Dirac distribution $n(\omega) = -n_f(\omega)$ for fermionic arguments. The zero-temperature integral $I_{\text{vac}}(m)$ is the same as the integral $A(m)$ given in Appendix A.1, since

$$\int_K \frac{1}{K^2 + m^2} = \int_k \int_{-\infty}^{\infty} \frac{dk_0}{2\pi} \frac{1}{k_0^2 + \omega^2} = \int_k \frac{1}{2\omega} \; . \tag{3.2.32}$$

We thus write

$$I(m) = A(m) + \int_k \frac{n(\omega)}{\omega} \; . \tag{3.2.33}$$

Since we need the integral function at hand for our two-loop potential computation where there are terms $\sim I(m)/\epsilon$ we need the terms up to order $\mathcal{O}(\epsilon)$

in the ϵ-expansion. For the $A(m)$ function this is easily evaluated using the general function for such integrals given in eq. (A.0.5). The expansion reads

$$
\begin{aligned}
A(m) &= \frac{1}{2} \int_k \frac{1}{\sqrt{k^2 + m^2}} = \frac{1}{2} \left(\frac{\bar{\mu}^2 e^{\gamma_E}}{4\pi} \right)^e \frac{1}{(4\pi)^{\frac{3}{2}-\epsilon}} \frac{\Gamma(\epsilon-1)}{\Gamma\left(\frac{1}{2}\right)} \left(m^2\right)^{1-\epsilon} \\
&= \frac{m^2}{(4\pi)^2} \left[-\frac{1}{\epsilon} + \ln \frac{m^2}{\bar{\mu}^2} - 1 - \epsilon \left(1 + \frac{\pi^2}{12} + \frac{1}{2} \ln^2 \frac{m^2}{\bar{\mu}^2} - \ln \frac{m^2}{\bar{\mu}^2} \right) \right] + \mathcal{O}(\epsilon^2) \ .
\end{aligned}
$$
(3.2.34)

The finite temperature integrals only depend on the absolute value of the momentum and thus the angular integrals can be performed leaving

$$
I_T(m) = \frac{1}{2\pi^2} \int_0^\infty dk \ k^2 \frac{n(\omega)}{\omega} + \frac{\epsilon}{2\pi} \int_0^\infty dk \ k^2 \left(2 - 2\ln 2 - \ln \frac{k^2}{\bar{\mu}^2} \right) \frac{n(\omega)}{\omega} \ . \quad (3.2.35)
$$

In our calculations we also need a modified expression of the tadpole integral function which is

$$
I(\underline{m}) \equiv \oint_K \frac{k^2}{K^2 + m^2} = \int_k \frac{k^2}{2\omega} + \int_k \frac{k^2 n(\omega)}{\omega} \ . \quad (3.2.36)
$$

For the first term, which is independent of the temperature, we use [110]

$$
\int d^d p \frac{(p^2)^\alpha}{(p^2 + m^2)^\beta} = \pi^{\frac{d}{2}} m^{d+2\alpha-2\beta} \frac{\Gamma\left(\alpha + \frac{d}{2}\right) \Gamma\left(\beta - \alpha - \frac{d}{2}\right)}{\Gamma\left(\frac{d}{2}\right) \Gamma(\beta)} \ . \quad (3.2.37)
$$

We set $\alpha = 1$, $\beta = 1/2$ and $d = 3 - 2\epsilon$ and we expand to $\mathcal{O}(\epsilon)$ and get

$$
\int_k \frac{k^2}{2\omega} = \frac{m^4}{4(4\pi)^2} \left[\frac{3}{\epsilon} + \frac{5}{2} - \ln \frac{m^2}{\bar{\mu}^2} + \epsilon \left(\frac{9}{4} + \frac{\pi}{4} + \frac{3}{2} \ln^2 \frac{m^2}{\bar{\mu}^2} - \frac{5}{2} \ln \frac{m^2}{\bar{\mu}^2} \right) \right] \ . \quad (3.2.38)
$$

In the finite temperature part of eq. (3.2.36) where the integration over k remains to be evaluated numerically, this modification just changes the exponent $k^2 \to k^4$ with respect to the I-function in eq. (3.2.35). For the counterterms we need the following relation which is true for both bosonic and fermionic modes,

$$
\oint_K \frac{K^2}{K^2 + m^2} = -m^2 \oint_K \frac{1}{K^2 + m^2} = -m^2 I(m) \ , \quad (3.2.39)
$$

where the first equality is true in this context since a power law divergence vanishes in dimensional regularization $\oint_K 1 \to 0$.

The $J(m)$ function needed in the one-loop potential is related to the $I(m)$ function through

$$
I(m) = \frac{1}{m} \frac{d}{dm} J(m) \quad \Rightarrow \quad J(m) = \int dm \ m I(m) \ , \quad (3.2.40)
$$

where we have set the additive constant to zero. Using this relation the J-function reads

$$
J(m) = \frac{1}{2} \oint_K \ln\left(K^2 + m^2\right) = \frac{m^2 A(m)}{D} - \frac{1}{D-1} \int_k \frac{k^2 n(\omega)}{\omega}
$$

$$= -\frac{m^4}{4(4\pi)^2}\left[\frac{1}{\epsilon}+\frac{3}{2}-\ln\frac{m^2}{\bar{\mu}^2}\right]-\frac{I_T^{(0)}(m)}{3}+\mathcal{O}(\epsilon)\ . \tag{3.2.41}$$

3.2.2   Two-Loop Finite Temperature Integrals

The calculation of the two-loop integral function has already been done in ref. [111]. The relevant integral for the sunset diagram is

$$H(m_1,m_2,m_3)=\oiint_{K,P}\frac{1}{(K^2+m_1^2)(P^2+m_2^2)\left[(K+P)^2+m_3^2\right]}\ . \tag{3.2.42}$$

To solve this integral for arbitrary masses m_i we first have to evaluate the Matsubara sums. We introduce a third momentum $Q=(q_0,\vec{q})$ which comes with a delta function. We can then rewrite one of delta functions as an integral $\delta(a)=T\int_0^\beta dx\ e^{iax}$, where $\beta=T^{-1}$, such that

$$H(m_1,m_2,m_3)=\frac{1}{T}\oiiint_{K,P,Q}\frac{\delta(k_0+p_0+q_0)(2\pi)^3\delta^{(3)}\left(\vec{k}+\vec{p}+\vec{q}\right)}{(K^2+m_1^2)(P^2+m_2^2)(Q^2+m_3^2)}$$

$$=\oiiint_{K,P,Q}\int_0^\beta dx\ (2\pi)^3\delta^{(3)}\left(\vec{k}+\vec{p}+\vec{q}\right)\frac{e^{ik_0x}}{K^2+m_1^2}\frac{e^{ip_0x}}{P^2+m_2^2}\frac{e^{iq_0x}}{Q^2+m_3^2}$$

$$=\oiiint_{K,P,Q}\int_0^\beta dx\ (2\pi)^3\delta^{(3)}\left(\vec{k}+\vec{p}+\vec{q}\right)\frac{e^{ik_0x}}{k_0^2+\omega_1^2}\frac{e^{ip_0x}}{p_0^2+\omega_2^2}\frac{e^{iq_0x}}{q_0^2+\omega_3^2}\ , \tag{3.2.43}$$

where in the last step we have introduced $\omega_i^2=k_i^2+m_i^2$. We can now perform the Matsubara sums using

$$T\sum_{k_0}\frac{e^{ik_0x}}{k_0^2+\omega^2}=\frac{n(\omega)}{2\omega}\left[e^{(\beta-x)\omega}+e^{x\omega}\right]=\frac{1}{2\omega}\frac{\cosh\left[\left(\frac{\beta}{2}-x\right)\omega\right]}{\sinh\left[\frac{\beta\omega}{2}\right]}\ . \tag{3.2.44}$$

Using this identity we can then perform the integration over x to get

$$H(m_1,m_2,m_3)=\frac{1}{4}\int_{k,p,q}(2\pi)^3\delta^{(3)}\left(\vec{k}+\vec{p}+\vec{q}\right)D(\omega_1,\omega_2,\omega_3)\ ,$$

$$D(\omega_1,\omega_2,\omega_3)=\frac{n_1n_2n_3}{\omega_1\omega_2\omega_3}\left[\frac{e^{\beta(\omega_1+\omega_2+\omega_3)}-1}{\omega_1+\omega_2+\omega_3}+\frac{e^{\beta(\omega_1+\omega_2)}-e^{\beta\omega_3}}{\omega_1+\omega_2-\omega_3}\right.$$

$$\left.+\frac{e^{\beta(\omega_1+\omega_3)}-e^{\beta\omega_2}}{\omega_1-\omega_2+\omega_3}+\frac{e^{\beta(\omega_2+\omega_3)}-e^{\beta\omega_1}}{-\omega_1+\omega_2+\omega_3}\right], \tag{3.2.45}$$

where we have introduced the notation $n_i=n(\omega_i)$. The exponential functions can be rewritten in terms of the distribution functions which for either of them reads

$$e^{\beta\omega}=\frac{e^{\beta\omega}}{e^{\beta\omega}-1}(e^{\beta\omega}-1)=\left(1+\frac{1}{e^{\beta\omega}-1}\right)(e^{\beta\omega}-1)=\frac{1+n_b(\omega)}{n_b(\omega)}\ , \tag{3.2.46}$$

$$e^{\beta\omega} = \frac{e^{\beta\omega}}{e^{\beta\omega}+1}\left(e^{\beta\omega}+1\right) = \left(1 - \frac{1}{e^{\beta\omega}+1}\right)\left(e^{\beta\omega}+1\right) = \frac{1-n_f(\omega)}{n_f(\omega)} \ . \qquad (3.2.47)$$

Writing these expressions using the definition of $n(\omega)$ as given below eq. (3.2.31) there arises a minus sign in the fermionic expression. We will keep this in mind, however, for simplicity we will continue with the case of only bosonic particles. We then get

$$
\begin{aligned}
D(\omega_1,\omega_2,\omega_3) &= \frac{1}{\omega_1\omega_2\omega_3}\Bigg[\frac{(1+n_1)(1+n_2)(1+n_3) - n_1 n_2 n_3}{\omega_1+\omega_2+\omega_3} \\
&\quad + \frac{(1+n_1)(1+n_2)n_3 - n_1 n_2(1+n_3)}{\omega_1+\omega_2-\omega_3} \\
&\quad + \frac{(1+n_1)n_2(1+n_3) - n_1(1+n_2)n_3}{\omega_1-\omega_2+\omega_3} \\
&\quad + \frac{n_1(1+n_2)(1+n_3) - (1+n_1)n_2 n_3}{-\omega_1+\omega_2+\omega_3} \Bigg] \\
&= \frac{1}{\omega_1\omega_2\omega_3}\Bigg[\frac{1 + n_1 n_2 + n_1 n_3 + n_2 n_3 + n_1 + n_2 + n_3}{\omega_1+\omega_2+\omega_3} \\
&\quad + \frac{-n_1 n_2 + n_1 n_3 + n_2 n_3 + n_3}{\omega_1+\omega_2-\omega_3} \\
&\quad + \frac{n_1 n_2 - n_1 n_3 + n_2 n_3 + n_2}{\omega_1-\omega_2+\omega_3} + \frac{n_1 n_2 + n_1 n_3 - n_2 n_3 + n_1}{-\omega_1+\omega_2+\omega_3} \Bigg] . \qquad (3.2.48)
\end{aligned}
$$

The terms proportional to $n_1 n_2 n_3$ have vanished and only terms with one, two or no n_i remain. We first take the terms inside the square brackets with two n_i and collect those with the same numerator which are of the form

$$
\begin{aligned}
\tilde{D} &= n_1 n_2 \left(\frac{1}{\omega_1+\omega_2+\omega_3} - \frac{1}{\omega_1+\omega_2-\omega_3} + \frac{1}{\omega_1-\omega_2+\omega_3} + \frac{1}{-\omega_1+\omega_2+\omega_3} \right) \\
&= \frac{4\omega_3(\omega_1^2 + \omega_2^2 - \omega_3^2)n_1 n_2}{(\omega_1+\omega_2+\omega_3)(\omega_1+\omega_2-\omega_3)(\omega_1-\omega_2+\omega_3)(-\omega_1+\omega_2+\omega_3)} \\
&= -\frac{4\omega_3(\omega_1^2 + \omega_2^2 - \omega_3^2)n_1 n_2}{\left[(\omega_1+\omega_2)^2 - \omega_3^2\right]\left[(\omega_1-\omega_2)^2 - \omega_3^2\right]} \ . \qquad (3.2.49)
\end{aligned}
$$

At this point we use the delta function to rewrite e.g. $\vec{q} = -\left(\vec{k}+\vec{p}\right)$.[2] Thus we can write

$$\omega_3^2 = q^2 + m_3^2 = (\vec{k}+\vec{p})^2 + m_3^2 = \omega_1^2 + \omega_2^2 + m_3^2 - m_1^2 - m_2^2 + 2zkp \ , \qquad (3.2.50)$$

where e.g. $k = |\vec{k}|$ and $z = \vec{k}\cdot\vec{p}/(kp)$. The newly introduced parameter z takes values $-1 \le z \le 1$. Eq. (3.2.49) is then

$$
\begin{aligned}
\tilde{D} &= -\frac{4\omega_3(m_1^2 + m_2^2 - m_3^2 - 2zkp)n_1 n_2}{\left[2\omega_1\omega_2 + m_1^2 + m_2^2 - m_3^2 - 2zkp\right]\left[-2\omega_1\omega_2 + m_1^2 + m_2^2 - m_3^2 - 2zkp\right]} \\
&= \frac{4\omega_3(m_1^2 + m_2^2 - m_3^2 - 2zkp)n_1 n_2}{4\omega_1^2\omega_2^2 - (m_1^2 + m_2^2 - m_3^2 - 2zkp)^2} \ . \qquad (3.2.51)
\end{aligned}
$$

---

[2]The integral evaluated using the delta function is always the one over the momentum where there is no corresponding n_i factor.

Of the nine integrations in eq. (3.2.45) three are evaluated using the delta function and three angular integrations can be performed, since the expression $D(\omega_1, \omega_2, \omega_3)$ now only depends on k, p and z:

$$H(m_1, m_2, m_3) = \frac{1}{4} \int\limits_{k,p,q} (2\pi)^3 \delta^{(3)}\left(\vec{k} + \vec{p} + \vec{q}\right) D(\omega_1, \omega_2, \omega_3)$$

$$= \sum_{i \neq j} \frac{1}{4 \cdot 8\pi^4} \int\limits_0^\infty dk \int\limits_0^\infty dp \int\limits_{-1}^1 dz \frac{k^2 p^2}{\omega_1 \omega_2 \omega_3} \tilde{D}(\omega_i, \omega_j, z) + H' + H_{\text{vac}} \ . \tag{3.2.52}$$

Here H' captures the contribution from the terms proportional to one n_i in eq. (3.2.48) and H_{vac} is the zero-temperature contribution. In the first term of eq. (3.2.52) the integration over z can be performed. It is of the form

$$\int\limits_{-1}^1 dz \frac{A - 2Bz}{C^2 - (A - 2Bz)^2} = \frac{1}{4B} \ln\left[\frac{(A - 2B)^2 - C^2}{(A + 2B)^2 - C^2}\right] \ . \tag{3.2.53}$$

We then get

$$\int\limits_{-1}^1 dz \frac{k^2 p^2}{\omega_1 \omega_2 \omega_3} \tilde{D}(\omega_1, \omega_2, z) = \frac{kp}{\omega_1 \omega_2} \ln\left[\frac{(m_1^2 + m_2^2 - m_3^2 - 2kp)^2 - 4\omega_1 \omega_2}{(m_1^2 + m_2^2 - m_3^2 + 2kp)^2 - 4\omega_1^2 \omega_2^2}\right] \ . \tag{3.2.54}$$

The argument of the logarithm could be negative, so we are going to take the absolute value which is equivalent of taking the real part of the logarithm. The imaginary part anyway cancels against the imaginary part of other terms in the final expression as stated in ref. [111].

For the terms with only one n_i in eq. (3.2.48) we need the Passarino-Veltman integral $B(P; m_1, m_2)$ given in Appendix A in eq. (A.1.3). We can perform the integration over k_0 and then set the external particle on-shell, i.e. $p_0 = i\omega_3$, yielding

$$\frac{1}{2\pi} \int\limits_{-\infty}^\infty dk_0 \frac{1}{(k_0^2 + \omega_1^2)\left[(k_0 + p_0)^2 + \omega_2^2\right]} = \frac{1}{2\omega_2} \frac{\omega_3^2 - \omega_1^2 - \omega_2^2}{\omega_1^4 + (\omega_2^2 - \omega_3^2)^2 - 2\omega_1^2(\omega_2^2 + \omega_3^2)}$$

$$= \frac{1}{2\omega_2} \frac{\omega_1^2 - \omega_2^2 - \omega_3^2}{\left[(\omega_1 + \omega_2)^2 - \omega_3^2\right]\left[(\omega_1 - \omega_2)^2 - \omega_3^2\right]}$$

$$= \frac{1}{\left[(\omega_1 + \omega_2)^2 - \omega_3^2\right]\left[(\omega_1 - \omega_2)^2 - \omega_3^2\right]} \left[\frac{\omega_1^2 - \omega_2^2 - \omega_3^2}{4\omega_2} + \frac{-\omega_1^2 + \omega_2^2 - \omega_3^2}{4\omega_1}\right] \ , \tag{3.2.55}$$

where the symmetrization in the last equation was carried out since $B(P; m_1, m_2)$ is symmetric under the simultaneous exchange of the masses and the momentum $m_1 \leftrightarrow m_2$, $K \rightarrow -K - P$. The integrand, however, only depends on $|p_0|$ and $\vec{p}$ will be integrated over anyway, so our last step is justified. The last term can then be rewritten as

$$\frac{\omega_1^2 - \omega_2^2 - \omega_3^2}{4\omega_2} + \frac{-\omega_1^2 + \omega_2^2 - \omega_3^2}{4\omega_1} = \frac{(\omega_2 - \omega_1)(\omega_1^2 - \omega_2^2) - \omega_3^2(\omega_1 + \omega_2)}{4\omega_1 \omega_2}$$

$$= \frac{\left[(\omega_1 - \omega_2)^2 - \omega_3^3\right](\omega_1 + \omega_2)}{4\omega_1\omega_2} . \qquad (3.2.56)$$

The integral in eq. (3.2.55) is then

$$\frac{1}{2\pi} \int_{-\infty}^{\infty} dk_0 \frac{1}{(k_0^2 + \omega_1^2)\left[(k_0 + i\omega_3)^2 + \omega_2^2\right]} = \frac{1}{2\omega_1\omega_2} \frac{\omega_1 + \omega_2}{(\omega_1 + \omega_2)^2 - \omega_3^2} . \qquad (3.2.57)$$

The terms with only one n_i in eq. (3.2.48) have a similar structure. We reinsert the factor of $1/4$ we have taken out of the integral and rewrite the terms with one n_i as

$$\frac{1}{4} \int_{k,p,q} (2\pi)^3 \delta^{(3)}\left(\vec{k} + \vec{p} + \vec{q}\right) \frac{2n_3}{\omega_1\omega_2\omega_3} \frac{\omega_1 + \omega_2}{(\omega_1 + \omega_2)^2 - \omega_3^2} = 2I_{T,b}(m_3)B(-im_3; m_1, m_2) .$$
$$(3.2.58)$$

Since the B-function is symmetric in its second and third argument, in the above expression we can use the symmetrization

$$2B(-im_3; m_1, m_2) = B(-im_3; m_1, m_2) + B(-im_3; m_2, m_1) . \qquad (3.2.59)$$

The last remaining term of eq. (3.2.48), i.e. the one without n_i's in the numerator, is equal to the vacuum sunset diagram

$$\int_{-\infty}^{\infty} \frac{dp_0}{2\pi} \frac{1}{p_0^2 + \omega_2^2} \int_{-\infty}^{\infty} \frac{dk_0}{2\pi} \frac{1}{(k_0^2 + \omega_1^2)\left[(k_0 + p_0)^2 + \omega_3^2\right]} = \frac{1}{4\omega_1\omega_2\omega_3(\omega_1 + \omega_2 + \omega_3)} .$$
$$(3.2.60)$$

Finally we can put everything together and write

$$H(m_1, m_2, m_3) = H_{\text{vac}}(m_1, m_2, m_3) + \sum_{i \neq j \neq \ell} I_{T,b}(m_i)\text{Re } B(-im_i, m_j, m_\ell)$$

$$+ \frac{1}{32\pi^4} \sum_{i \neq j \neq \ell} \int_0^{\infty} dk \int_0^{\infty} dp \, kp \frac{n_b(\omega_{k,i})}{\omega_{k,i}} \frac{n_b(\omega_{p,j})}{\omega_{p,j}} f_{k,p}(m_i, m_j, m_\ell) ,$$

$$f_{k,p}(m_1, m_2, m_3) = \ln\left|\frac{(m_1^2 + m_2^2 - m_3^2 - 2kp)^2 - 4(k^2 + m_1^2)(p^2 + m_2^2)}{(m_1^2 + m_2^2 - m_3^2 + 2kp)^2 - 4(k^2 + m_1^2)(p^2 + m_2^2)}\right| .$$
$$(3.2.61)$$

The vacuum contribution of the sunset integral has been extensively studies in the literature, e.g. in refs. [112–114]. We take the results from ref. [114], however, we need to adjust them to our conventions by first multiplying by a factor of $1/(2\pi)^4$. Furthermore, in dimensional regularization they use $n - 4$ dimensions while we use $4 - 2\epsilon$ leading to a different expansion by a factor of 2 and we have to take the factor $\bar{\mu}^{4\epsilon}$ into our expansion. Our result H_{vac} is expressed through the results V from ref. [114] as

$$H_{\text{vac}}^{(-2)} = \frac{1}{4\epsilon^2}V^{(-2)} ,$$

$$H_{\text{vac}}^{(-1)} = \frac{1}{2\epsilon}\left(V^{(-2)}\ln\bar{\mu}^2 - V^{(-1)}\right) ,$$

$$H_{\text{vac}}^{(0)} = \left(\frac{\pi^2}{24} + \frac{1}{2} \ln^2 \bar{\mu}^2 \right) V^{(-2)} - V^{(-1)} \ln \bar{\mu}^2 + V^{(0)} \ . \tag{3.2.62}$$

For the computation of the two-loop potential we also need a modified version of the H-function with one line weighted by a spatial momentum. It is defined as

$$H(\underline{m_1}, m_2, m_3) = \oiint_{K,P} \frac{k^2}{(K^2 + m_1^2)(P^2 + m_2^2)\left[(K+P)^2 + m_3^2\right]} \ . \tag{3.2.63}$$

The Matsubara sums can be carried out as in the H-function and similar to the function D, defined in (A.1.9) in the Appendix, we use Lorentz symmetry to write the vacuum part as

$$H_{\text{vac}}(\underline{m_1}, m_2, m_3) = \frac{D-1}{D}\left[-m_1^2 H_{\text{vac}}(m_1, m_2, m_3) + I_{\text{vac}}(m_2) I_{\text{vac}}(m_3) \right] \ , \tag{3.2.64}$$

where $I_{\text{vac}}(m) = A(m)$ is given in eq. (3.2.34). This modified H-function is needed for contributions of an odd number of vectors in a sunset diagram. The reason this structure appears is that only the temporal components of the gauge fields have a thermal mass term and we have to use

$$\frac{K_0 K_0}{K^2 + \widetilde{m}^2} + \frac{K_i K_i}{K^2 + m^2} = \frac{K^2}{K^2 + \widetilde{m}^2} + \frac{k^2}{K^2 + m^2} - \frac{k^2}{K^2 + \widetilde{m}^2} \ . \tag{3.2.65}$$

The following example, where W stands for an $SU(2)$ gauge boson, shows how this is implemented in practice:

$$\tag{3.2.66}$$

$$= \frac{3g_2^2}{8} \oiint_{K,P} \frac{(K-P)_0 (P-K)_0}{(K^2 + \widetilde{m}_h^2)(P^2 + \widetilde{m}_G^2)\left[(K+P)^2 + \widetilde{m}_W^2\right]}$$

$$+ \frac{3g_2^2}{8} \oiint_{K,P} \frac{(K-P)_i (P-K)_i}{(K^2 + \widetilde{m}_h^2)(P^2 + \widetilde{m}_G^2)\left[(K+P)^2 + m_W^2\right]}$$

$$= -\frac{3g_2^2}{8} \oiint_{K,P} \frac{2K^2 + 2P^2 - (K+P)^2}{(K^2 + \widetilde{m}_h^2)(P^2 + \widetilde{m}_G^2)\left[(K+P)^2 + \widetilde{m}_W^2\right]}$$

$$+ \frac{3g_2^2}{8} \oiint_{K,P} \frac{2k^2 + 2p^2 - (k+p)^2}{(K^2 + \widetilde{m}_h^2)(P^2 + \widetilde{m}_G^2)\left[(K+P)^2 + \widetilde{m}_W^2\right]}$$

$$- \frac{3g_2^2}{8} \oiint_{K,P} \frac{2k^2 + 2p^2 - (k+p)^2}{(K^2 + \widetilde{m}_h^2)(P^2 + \widetilde{m}_G^2)\left[(K+P)^2 + m_W^2\right]}$$

$$= -\frac{3g_2^2}{8}\Bigg[2\left[I(\widetilde{m}_h) + I(\widetilde{m}_G)\right] I(\widetilde{m}_W) - I(\widetilde{m}_h) I(\widetilde{m}_G)$$

$$+ (\widetilde{m}_W^2 - 2\widetilde{m}_h^2 - 2\widetilde{m}_W^2) H(\widetilde{m}_h, \widetilde{m}_G, \widetilde{m}_W)$$

$$+ 2H(\underline{\widetilde{m}_h}, \widetilde{m}_G, \widetilde{m}_W) + 2H(\widetilde{m}_h, \underline{\widetilde{m}_G}, \widetilde{m}_W) - H(\widetilde{m}_h, \widetilde{m}_G, \underline{\widetilde{m}_W})$$

	m_H/GeV	m_A/GeV	$m_{H^\pm}/\text{GeV}$	$\lambda_L(m_Z)/2$	$\lambda_2(m_z)$
BM1	66	300	300	$1.07{\times}10^{-2}$	0.01
BM2	200	400	400	$1.00{\times}10^{-2}$	0.01
BM3	5	265	265	$-0.60{\times}10^{-2}$	0.01

Table 3.2: The three benchmark points from ref. [102]. The coupling λ_L is chosen to be small to comply with dark matter relic abundance, whereas λ_2 is small because of dark matter self-interaction constraints.

$$- 2H(\underline{\widetilde{m}_h}, \widetilde{m}_G, m_W) - 2H(\widetilde{m}_h, \underline{\widetilde{m}_G}, m_W) + H(\widetilde{m}_h, \widetilde{m}_G, \underline{m_W}) \Bigg].$$
$$(3.2.67)$$

3.3 Numerical Evaluation

We want to consider the three benchmark points that were introduced in ref. [102] for our numerical evaluation. For our purpose to compare the full two-loop result with the high-temperature expansion, these points are sufficient.

The input parameters for these three benchmark points are listed in table 3.2. All three points share some common features like the degeneracy of the two heavy scalars A and $H^\pm$ and, although the mass of the lightest one varies significantly in the three cases, the splitting between the heavy masses and m_H is large ($m_{A,H^\pm} - m_H \gg m_Z$). This implies that some of the new couplings are large. Moreover, the coupling λ_L is chosen to be small to obey dark matter relic abundance limits [89].

Due to the fact that some of the couplings are large, the one-loop corrections to e.g. pole masses are also large and of order $\mathcal{O}(100\%)$. Since we want to express the couplings in terms of physical pole masses (see Appendix C.2), we need to solve the corresponding system of equations iteratively in a self-consistent way. The numerical values of the couplings are listed in table 3.3.

Instead of using the expressions for the couplings in terms of the self-energies, we use a different procedure to determine the Higgs couplings μ_1^2 and λ_1. This procedure uses the effective potential, and we call it the Coleman-Weinberg (CW) method (inspired by ref. [115]). The two conditions are

$$\frac{\partial V(\phi)}{\partial \phi} = 0 \quad \text{and} \quad \frac{\partial^2 V(\phi)}{\partial \phi^2} = m_h^2 \ , \qquad (3.3.1)$$

where the derivatives are evaluated at the minimum of the potential. We can now first solve these two equations keeping all the other couplings at their initial value and then using them as input values to solve the other equations. This leads to one more step in each iteration, however, it also allows us to include higher-order corrections by using the two-loop potential without having to calculate higher-order corrections to the self-energies. The results of this method are denoted by "2-loop" in table 3.3, where the quotation marks hint at an incomplete two-loop computation.

As can be seen from table 3.3, the reference scale is $\bar{\mu} = m_Z$ from where we run the couplings to the thermal scale using renormalization group equations.

	BM1		BM2		BM3	
	1-loop	"2-loop"	1-loop	"2-loop"	1-loop	"2-loop"
$\mu_1^2(m_Z)/\mathrm{GeV}^2$	-6669	-6568	-8463	-8127	-7392	-7251
$\mu_2^2(m_Z)/\mathrm{GeV}^2$	842	842	36620	36620	-1243	-1243
$\lambda_1(m_Z)$	0.0670	0.0634	0.0671	0.0579	0.1021	0.0979
$\lambda_2(m_Z)$	0.010	0.010	0.010	0.010	0.010	0.010
$\lambda_3(m_Z)$	2.757	2.757	2.618	2.618	2.243	2.243
$\lambda_4(m_Z)$	-1.368	-1.368	-1.299	-1.299	-1.127	-1.127
$\lambda_5(m_Z)$	-1.368	-1.368	-1.299	-1.299	-1.127	-1.127
$g_2^2(m_Z)$	0.425	0.425	0.425	0.425	0.425	0.425
$g_3^2(m_Z)$	1.489	1.489	1.489	1.489	1.489	1.489
$h_t^2(m_Z)$	0.971	0.971	0.973	0.973	0.969	0.969

Table 3.3: Values of the couplings at $\bar{\mu} = m_Z$. The "two-loop" column indicates that μ_1^2 and λ_1 were obtained by the CW-method for the two-loop potential as described in the text.

As usual, the scale is chosen to cancel large logarithms which in our case originate from thermal fluctuations and give rise to terms $\sim \ln[\bar{\mu}/(\pi T)]$. Therefore, the thermal scale we choose is

$$\bar{\mu} = \alpha \pi T \;, \quad \alpha \in (0.5 \ldots 2.0) \;. \tag{3.3.2}$$

The variation of the scale, introduced through α allows us to estimate errors of our perturbative expansion. Furthermore, we settle for our considerations for the one-loop beta-functions derived from counterterms listed in Appendix C.1 since we believe these uncertainties to be not so important for our qualitative statements.

Looking at table 3.3 we see that λ_1 is smaller than in the Standard Model, where $\lambda_1(m_Z) \sim 0.13$. The shape of the Higgs potential for values of ϕ larger than the vacuum expectation value (the part $\sim \phi^4$ in figure 1.2) is mostly given by the Higgs self-coupling. Therefore, a small quartic coupling, in addition to the new bosonic degrees of freedom, also favors a strong phase transition.

Even though different techniques in deriving the couplings, i.e. iterative solutions using one-loop self energies and a combination of the iterative procedure and CW method, lead to large variations of $\mathcal{O}(20\%)$ for BM2, our conclusions concerning thermal effects remain the same.

Everything is now set for the numerical evaluation of the two-loop potential and its high-temperature expansion. Nevertheless, caution has to be taken when using the two-loop master integral functions. For one thing, the function L, appearing in the H-function (A.2.25) and its modified version (A.2.32) is singular in certain limits, e.g.

$$L(m^2, \epsilon^2, \epsilon^2) = -\frac{\pi^2}{6} - 2\ln^2 \frac{m}{\epsilon} \;, \quad \text{as} \quad \epsilon \to 0^+ \;. \tag{3.3.3}$$

This limit is relevant for the computation of diagrams involving massless fermions. However, divergences from such terms are canceled from other infrared divergent terms.

Moreover, if the masses are not all of the same order, the finite part of the modified H-function has divergent terms as some masses tend to zero. In eq.
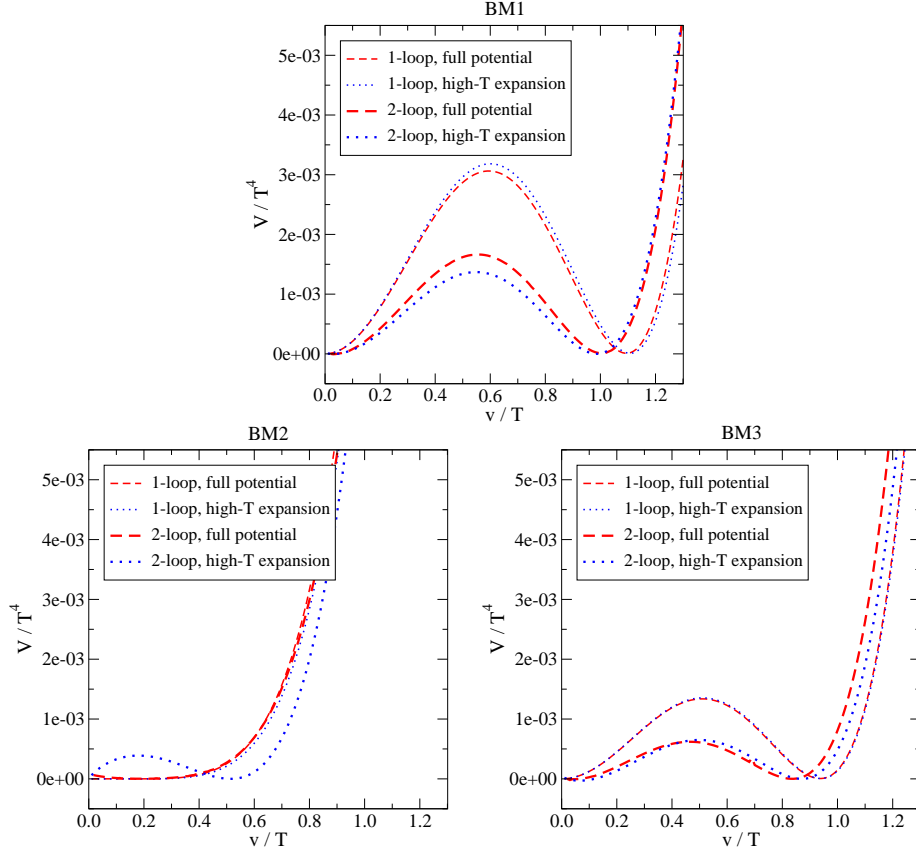
Figure 3.1: One- and two-loop effective potentials and their high-temperature expansions taken at their respective critical temperatures for the three benchmark points given in table 3.2.

(A.2.32) the term multiplying $I_T^{(0)}(\underline{m_2})$ has divergent terms $\sim 1/m_2^4$ as $m_2 \to 0$, however in the sum the limit is finite. The same is true for the term multiplying $I_T^{(0)}(m_2)$, with divergences $\sim 1/m_2^2$. In these terms, there are also cusps at $m_2 = m_1 + m_3$ from the functions $B^{(0)}$. However, equal and opposite terms appear in the numerical integrations, i.e. the last four lines of eq. (A.2.32).

For the high-temperature expansions in eqs. (A.2.33) - (A.2.35) we want to note that the function $H^{(0)}(\underline{m_1}, m_2, m_3)$ always appears in a difference, containing various masses. Therefore, the leading term $\sim T^4$ drops out completely. Moreover, at the next order ($\sim m^2$) there are only the contributions from the Matsubara zero-modes kept, since the other contributions lead to v-independent terms $\sim g^2(\widetilde{m}_W^2 - m_W^2)T^2 \sim g^4T^4$ which do not effect the physical parameters shown in table 3.4.

Considering all these issues, the effective potential can then be computed. Figure 3.1 shows both the one-loop and the two-loop full potential as well as the corresponding high-temperature expansion for the three benchmark points respectively. The critical temperatures T_c differ between the effective potential approach and the high-temperature expansion, especially for the two-loop re-

full effective potential

	T_c/GeV		L/T_c^4		v_{phys}/T_c		v_{min}/T_c	
	1-loop	2-loop	1-loop	2-loop	1-loop	2-loop	1-loop	2-loop
BM1	139(14)	155(21)	0.44(1)	0.34(1)	1.14(12)	0.98(4)	1.15(12)	0.98(3)
BM2	159(13)	181(22)	0.07(7)	0.03(3)	0.39(28)	0.16(16)	0.39(28)	0.17(17)
BM3	138(8)	167(19)	0.35(3)	0.20(1)	0.96(10)	0.84(6)	0.98(10)	0.81(2)

high-temperature expansion

	T_c/GeV		L/T_c^4		v_{phys}/T_c		v_{min}/T_c	
	1-loop	2-loop	1-loop	2-loop	1-loop	2-loop	1-loop	2-loop
BM1	140(14)	124(8)	0.45(1)	0.49(22)	1.15(13)	1.04(31)	1.16(13)	1.05(32)
BM2	159(14)	140(9)	0.08(8)	0.16(8)	0.42(30)	0.60(19)	0.42(30)	0.60(19)
BM3	138(8)	125(3)	0.35(3)	0.37(16)	0.97(10)	0.89(23)	0.98(10)	0.91(23)

Table 3.4: Results from the full effective potential and the high-temperature expansion for the physical quantities T_c, L and v_{phys} as well as for v_{min} for the benchmark points listed in table 3.2. Uncertainties are obtained by varying the thermal scale $\bar{\mu} = (0.5\ldots2.0)\pi T$.

sults, as can be read off from table 3.4. Therefore, the curves in the figures are plotted at their respective critical temperatures, which allows us to compare the strength of the phase transition.

Table 3.4 shows the physical parameters we want to study, i.e. the critical temperature T_c, the latent heat L and the discontinuity of the Higgs condensate v_{phys}, defined by $v_{\mathrm{phys}}/2 = Z_{\mu_1^2}\Delta\langle\phi^\dagger\phi\rangle$, where $Z_{\mu_1^2}$ is the renormalization factor related to the bare mass parameter μ_1^2. The value of v at which the potential reaches its minimum depends on our gauge choice. It is listed as v_{min} in table 3.4. Taking the difference of v_{phys} and v_{min} allows us to estimate our error due to our choice of the Feynman R_ξ gauge. It is in fact much smaller than the thermal uncertainties originating from the variation of the thermal scale.

Both figure 3.1 and table 3.4 show that the two-loop corrections are large. They do not, however, change the physical interpretation of these points. Even though the phase transition is weakened, at least for BM1 a first order transition remains viable. Although such a transition is strengthened in the high-temperature expansion of BM2, the large value of μ_2^2 questions the reliability of this result. Therefore, besides BM2 the high-temperature expansions seems to work very well and leads to the same qualitative conclusions.

For one observable, i.e. the critical temperature T_c, the high-temperature expansion does not work well. This can be read off from the first two columns in table 3.4 where we see that T_c slightly increases by adding the two-loop corrections to the full effective one-loop potential, whereas in the high-temperature expansion the two-loop contributions decrease T_c. But since we are dealing with some scalars that do have large masses this should not come as a surprise. They do contribute to large corrections to the effective Higgs mass parameter. However, their effect on the phase transition is marginal. This can be seen by comparing the rows of v_{phys}/T_c in table 3.4 for the full effective potential and the high-temperature expansion for the benchmark point BM1 where a first order phase transition is feasible. This is also true for BM3 where v_{phys}/T_c is only slightly below 1.

The cosmological interpretation concerning a first order electroweak phase

transition is that such a transition remains a possibility. This is true at least for BM1 and could be true for a whole region of parameter space that is not yet excluded.

We want to emphasize that the effective potential as a tool to e.g. study the phase transition is only theoretically consistent at stable points. These points are the high-temperature symmetric phase as well as the low-temperature Higgs phase. Away from these local minima the potential is not gauge-independent and contains uncanceled divergences and furthermore, masses can become tachyonic. In our numerical evaluation we replace the masses squared by their absolute values while removing ultraviolet divergences proportional to thermal masses introduced by resummation (cf. discussion below (1.3.32)) by hand. However, this procedure leaves terms dependent on the renormalization scale $\bar{\mu}$.

3.4 Constraints

The parameters of every new model are to some extent constrained. Even in the most generic case one wants a model to satisfy some theoretical aspects and obviously it should agree with experimental data. If we want to perform a perturbative analysis, we better make sure we are in fact in a perturbative regime. Furthermore, to be able to describe nature and have a predictive model we impose the conditions of vacuum (meta-)stability and unitarity.

Electroweak precision tests, i.e. measuring the Peskin-Takeuchi parameters [116, 117], set bounds on Beyond the Standard Model models as do various experiments measuring the dark matter relic density for models with a dark matter candidate. Since most extensions of the Standard Model interact via the Higgs boson with the SM sector, Higgs physics like the di-photon decay $H \to \gamma\gamma$ constrains the parameter space.

Although many theoretical [118–122] and collider [124–139] constraints for the Inert Doublet Model have already and extensively been considered in the literature, we want to look at some of these more closely. Techniques for theoretical constraints, such as unitarity bounds, can be adapted to other extensions of the Standard Model.

3.4.1 Theoretical Constraints

Although we explicitly have large couplings in the IDM, we still want our theory to remain in the perturbative regime. Therefore, all couplings have to satisfy

$$|\lambda_{1,2,3,4,5}| \ll 4\pi \ . \tag{3.4.1}$$

The couplings can a priori be negative and indeed we choose $\lambda_5 < 0$. These constraints are easily satisfied by our benchmark points and even the large coupling $\lambda_3 \sim 3$ is well inside the allowed region.

The world we want to describe lies at the electroweak broken minimum of the potential. To guarantee vacuum stability, we want to make sure that this minimum is a global one.[3] At tree-level this translates into the inequalities

$$\lambda_{1,2} \geq 0 \ , \quad \lambda_{3,L,S} \geq -2\sqrt{\lambda_1\lambda_2} \ . \tag{3.4.2}$$

---

[3]If it were only a local minimum we would live in an unstable vacuum. However, if the global minimum is very far away and our vacuum thus very long lived, i.e. of the order of the age of the universe, we speak of a meta-stable vacuum.

The first two constraints concerning λ_1 and λ_2 are obvious, the other ones are an implication of the reparametrization invariance of the scalar potential [140]. A short derivation is given below.

Calculating scattering amplitudes, in particular scalar-scalar, scalar-gauge boson and gauge boson-gauge boson scatterings [141], there arise constraints from the eigenvalues of the corresponding S-matrix [127]:

$$|\lambda_3 + 2\lambda_4 \pm 3\lambda_5| \leq 8\pi \; ,$$

$$\left| -\lambda_1 - \lambda_2 \pm \sqrt{(\lambda_1 - \lambda_2)^2 + \lambda_4^2} \right| \leq 8\pi \; ,$$

$$\left| -3\lambda_1 - 3\lambda_2 \pm \sqrt{9(\lambda_1 - \lambda_2)^2 + (2\lambda_3 + \lambda_4)^2} \right| \leq 8\pi \; ,$$

$$\left| -\lambda_1 - \lambda_2 \pm \sqrt{(\lambda_1 - \lambda_2)^2 + \lambda_5^2} \right| \leq 8\pi \; . \tag{3.4.3}$$

In the rest of this section we want to derive the constraints given in eqs. (3.4.2) and (3.4.3). We first note that the scalar potential of the Inert Doublet Model, given in eq. (3.1.2), has a freedom of reparametrization. Changing the coefficients m_i^2 and λ_i into $m_i'^2$ and λ_i' the potential can be brought back to its original form via a field transformation

$$\phi_i \;\to\; \phi_i' = R\phi_i \; , \tag{3.4.4}$$

where R is an element of the general linear group $GL(2, \mathbb{C})$. For simplicity we choose here to write the two doublets as $\phi_1 = \phi$ and $\phi_2 = \chi$. The physics of the potentials V and V' has to be the same. The common way to introduce this reparametrization freedom is to consider the two scalar doublets ϕ_1 and ϕ_2 as components of a hyperspinor Φ with the transformation $\Phi \to U\Phi$, $U \in U(2)$.

It is convenient to switch from the fundamental representations of $SU(2)$ to the adjoint [140]. Since $2 \otimes \bar{2} = 1 \oplus 3$ we write

$$r_0 = \Phi^\dagger \Phi = \phi_1^\dagger \phi_1 + \phi_2^\dagger \phi_2 \; , \tag{3.4.5}$$

$$r_i = \Phi^\dagger \sigma_i \Phi = \begin{pmatrix} \phi_2^\dagger \phi_1 + \phi_1^\dagger \phi_2 \\ -i \left(\phi_1^\dagger \phi_2 - \phi_2^\dagger \phi_1 \right) \\ \phi_1^\dagger \phi_1 - \phi_2^\dagger \phi_2 \end{pmatrix} \; , \tag{3.4.6}$$

where σ_i are the Pauli matrices, as the components of $r^\mu = (r_0, r_i)$. These quantities are gauge invariant and thus r^μ parametrize gauge orbits of the Higgs fields [142].

The quartic part of the scalar potential of a general two Higgs doublet model contains all possible forth-order terms and is thus invariant not only under a $U(2)$ transformation but under $GL(2, \mathbb{C})$. However, multiplication by an arbitrary complex number does not change the potential since the couplings can be rescaled by the absolute value of that number and an overall phase leaves the potential invariant. Therefore, the interesting symmetries are in the subgroup $SL(2, \mathbb{C})$, which induces the proper Lorentz group $SO(1, 3)$ on our adjoint representation.

The four-vector r^μ is an irreducible representation of $SO(1, 3)$, thus there is a Minkowski space structure in the orbit space of the Higgs potential. The

potential takes the simple form

$$V_0 = -M_\mu r^\mu + \frac{1}{2}\Lambda_{\mu\nu}r^\mu r^\nu \ , \tag{3.4.7}$$

where M_μ is a mass four-vector, i.e. its entries are combinations of the masses of the two doublets. This vector, however, is not important here. The matrix Λ is given by

$$\Lambda^{\mu\nu} = \begin{pmatrix} \lambda_+ + \lambda_3 & 0 & 0 & \lambda_- \\ 0 & \lambda_4 + \lambda_5 & 0 & 0 \\ 0 & 0 & \lambda_4 - \lambda_5 & 0 \\ \lambda_- & 0 & 0 & \lambda_+ - \lambda_3 \end{pmatrix} \ , \tag{3.4.8}$$

with $\lambda_\pm = \lambda_1 \pm \lambda_2$. In order for the potential to be bounded from below, the matrix $\Lambda^{\mu\nu}$ must be positive-definite. This is true if (and only if) the following three properties are fulfilled (see Appendix A of ref. [140] for a proof of this equivalence):

(i) $\Lambda^{\mu\nu}$ has to be diagonalizable by an $SO(1,3)$ transformation,

(ii)   the time-like eigenvalue Λ^0 has to be non-negative and

(iii) all space-like eigenvalues are smaller or equal to Λ^0.

With the metric $g_{\mu\nu}$ we construct the in general not symmetric mixed tensor

$$\Lambda^\mu_\nu = g_{\nu\sigma}\Lambda^{\mu\sigma} = \begin{pmatrix} \lambda_+ + \lambda_3 & 0 & 0 & \lambda_- \\ 0 & -(\lambda_4 + \lambda_5) & 0 & 0 \\ 0 & 0 & \lambda_5 - \lambda_4 & 0 \\ -\lambda_- & 0 & 0 & -(\lambda_+ - \lambda_3) \end{pmatrix} \ . \tag{3.4.9}$$

Diagonalizing this matrix as $\Lambda^\mu_\nu = (T\Lambda T^{-1})^\mu_\nu$ we get

$$\Lambda = \begin{pmatrix} \lambda_3 + 2\sqrt{\lambda_1\lambda_2} & 0 & 0 & 0 \\ 0 & -\lambda_4 - \lambda_5 & 0 & 0 \\ 0 & 0 & \lambda_5 - \lambda_4 & 0 \\ 0 & 0 & 0 & \lambda_3 - 2\sqrt{\lambda_1\lambda_2} \end{pmatrix} \ . \tag{3.4.10}$$

According to property (ii), the time-like eigenvalue $\Lambda^0 = \lambda_3 + 2\sqrt{\lambda_1\lambda_2}$ has to be non-negative. This leads to the constraint

$$\lambda_3 \geq -2\sqrt{\lambda_1\lambda_2} \ , \tag{3.4.11}$$

whereas property (iii) leads to

$$\lambda_L = \lambda_3 + \lambda_4 + \lambda_5 \geq -2\sqrt{\lambda_1\lambda_2} \ ,$$
$$\lambda_S = \lambda_3 + \lambda_4 - \lambda_5 \geq -2\sqrt{\lambda_1\lambda_2} \ . \tag{3.4.12}$$

Thus there are three additional constraints from imposing vacuum stability, summarized in eq. (3.4.2).

We now turn to the issue of unitarity. We start with the partial wave decomposition of the amplitude $\mathcal{M}$ of the scattering $S_1 S_2 \to S_3 S_4$, which is [143]

$$\mathcal{M}(s,t,u) = 16\pi \sum_{\ell=0}^\infty (2\ell + 1)P_\ell(\cos\theta)a_\ell(s) \ , \tag{3.4.13}$$

where s, t, u are the Mandelstam variables and P_ℓ are the Legendre polynomials. These polynomials are orthogonal and thus the total cross section σ becomes

$$\sigma = \frac{16\pi}{s} \sum_{\ell=0}^{\infty} |a_\ell|^2 \ . \tag{3.4.14}$$

Using the optical theorem we can derive the unitarity constraint

$$|a_\ell|^2 = (\mathrm{Re}\ a_\ell)^2 + (\mathrm{Im}\ a_\ell)^2 = \mathrm{Im}\ a_\ell \ , \quad \forall \ell \ , \tag{3.4.15}$$

which describes a circle in the complex plane with the center for the extreme value $|a_\ell| = 1$ lying at $i/2$ and with radius $1/2$. Thus

$$|\mathrm{Re}\ a_\ell| \le \frac{1}{2} \ , \quad \forall \ell \ . \tag{3.4.16}$$

Inverting the decomposition in eq. (3.4.13), the partial wave $a_\ell(s)$ can be expressed as

$$a_\ell(s) = \frac{1}{32\pi} \int_{-1}^{1} d\cos\theta \ P_\ell(\cos\theta) \mathcal{M}(s, t, u) \ . \tag{3.4.17}$$

We now consider the $J = \ell = 0$ s-wave $a_0(s)$ for vanishing external masses which corresponds to the high energy limit $s \gg m$. The Legendre polynomial is $P_0(x) = 1$ and the Mandelstam variables t and u are rewritten as

$$t = -\frac{s}{2}(1 - \cos\theta) \ , \quad u = -\frac{s}{2}(1 + \cos\theta) \ . \tag{3.4.18}$$

This leads to

$$a_0(s) = \frac{1}{16\pi} \left\{ Q + \left[\frac{T_h^{12} T_h^{34}}{s - m_h^2} - \frac{1}{s} \left(c_t T_h^{13} T_h^{24} + c_u T_h^{14} T_h^{23} \right) \ln\left(1 + \frac{s}{m_h^2} \right) \right] \right\} \ , \tag{3.4.19}$$

where Q is the four point vertex and T_h^{ij} are the trilinear vertices hS_iS_j. We have introduced c_t and c_u which take values 1 or 0 depending on whether or not t- and u-channels are open in the considered process. In high energy collisions the contributions of the trilinear couplings are suppressed and the quartic interaction dominates. Eq. (3.4.16) then takes the form $|Q(S_1, S_2, S_3, S_4)| \le 8\pi$.

Going back to our two Higgs doublet model and again denoting $\phi_1 = \phi$ and $\phi_2 = \chi$ we rewrite the products $(\phi_a^\dagger \phi_b)(\phi_c^\dagger \phi_d) = (\phi_{a\alpha}^* \phi_{b\alpha})(\phi_{c\beta}^* \phi_{d\beta})$ by introducing the decomposition [144]

$$(\phi_{a\alpha}^* \phi_{b\alpha})(\phi_{c\beta}^* \phi_{d\beta}) = \frac{1}{2} \left[(\phi_{a\alpha}^* \phi_{d\alpha})(\phi_{c\beta}^* \phi_{b\beta}) + \sum_r (\phi_{a\alpha}^* \sigma_{\alpha\beta}^r \phi_{d\beta})(\phi_{c\gamma}^* \sigma_{\gamma\delta}^r \phi_{b\delta}) \right] \ , \tag{3.4.20}$$

where σ^i are the Pauli matrices. This decomposition can easily be derived by an explicit calculation

$$(\phi_{a\alpha}^* \phi_{d\alpha})(\phi_{c\beta}^* \phi_{b\beta}) + \sum_r (\phi_{a\alpha}^* \sigma_{\alpha\beta}^r \phi_{d\beta})(\phi_{c\gamma}^* \sigma_{\gamma\delta}^r \phi_{b\delta}) =$$

$$= \phi_{a1}^* \phi_{d1} \phi_{c1}^* \phi_{b1} + \phi_{a1}^* \phi_{d1} \phi_{c2}^* \phi_{b2} + \phi_{a2}^* \phi_{d2} \phi_{c1}^* \phi_{b1} + \phi_{a2}^* \phi_{d2} \phi_{c2}^* \phi_{b2}$$

$$+ \phi_{a1}^* \phi_{d2} \phi_{c1}^* \phi_{b2} + \phi_{a1}^* \phi_{d2} \phi_{c2}^* \phi_{b1} + \phi_{a2}^* \phi_{d1} \phi_{c1}^* \phi_{b2} + \phi_{a2}^* \phi_{d1} \phi_{c2}^* \phi_{b1}$$

$$-\phi_{a2}^*\phi_{d1}\phi_{c2}^*\phi_{b1} + \phi_{a2}^*\phi_{d1}\phi_{c1}^*\phi_{b2} + \phi_{a1}^*\phi_{d2}\phi_{c2}^*\phi_{b1} - \phi_{a1}^*\phi_{d2}\phi_{c1}^*\phi_{b2}$$
$$+ \phi_{a1}^*\phi_{d1}\phi_{c1}^*\phi_{b1} - \phi_{a1}^*\phi_{d1}\phi_{c2}^*\phi_{b2} - \phi_{a2}^*\phi_{d2}\phi_{c1}^*\phi_{b1} + \phi_{a2}^*\phi_{d2}\phi_{c2}^*\phi_{b2}$$
$$= 2\left[\phi_{a1}^*\phi_{d1}\phi_{c1}^*\phi_{b1} + \phi_{a1}^*\phi_{d2}\phi_{c2}^*\phi_{b1} + \phi_{a2}^*\phi_{d1}\phi_{c1}^*\phi_{b2} + \phi_{a2}^*\phi_{d2}\phi_{c2}^*\phi_{b2}\right]$$
$$= 2(\phi_{a\alpha}^*\phi_{b\alpha})(\phi_{c\beta}^*\phi_{d\beta}) . \tag{3.4.21}$$

The weak hypercharge is the generator of the $U(1)$ subgroup of the electroweak gauge group $SU(2) \times U(1)$ [145]. The weak hypercharge of the scalar fields are both $Y = +1$ such that in a scalar-scalar scattering the three states $Y = \{0, 2, -2\}$ are possible. For states with hypercharge $Y = 2$ we introduce $\tilde{\phi}_a = (i\sigma_2\phi_a)^T$ where the isoscalar $\tilde{\phi}_a\phi_b = -\tilde{\phi}_b\phi_a$ is antisymmetric under $a \leftrightarrow b$. The decomposition is then

$$(\phi_{a\alpha}^*\phi_{b\alpha})(\phi_{c\beta}^*\phi_{d\beta}) = \frac{1}{2}\left[(\phi_{a\alpha}^*\tilde{\phi}_{c\alpha}^*)(\tilde{\phi}_{d\beta}\phi_{b\beta}) + \sum_r(\phi_{a\alpha}^*\sigma_{\alpha\beta}^r\tilde{\phi}_{c\beta}^*)(\tilde{\phi}_{d\gamma}\sigma_{\gamma\delta}^r\phi_{b\delta})\right] . \tag{3.4.22}$$

From the potential

$$V_0 = \lambda_1(\phi_1^\dagger\phi_1)^2 + \lambda_2(\phi_2^\dagger\phi_2)^2 + \lambda_3(\phi_1^\dagger\phi_1)(\phi_2^\dagger\phi_2)$$
$$+ \lambda_4(\phi_1^\dagger\phi_2)(\phi_2^\dagger\phi_1) + \frac{\lambda_5}{2}\left[(\phi_1^\dagger\phi_2)^2 + (\phi_2^\dagger\phi_1)^2\right] \tag{3.4.23}$$

and the decompositions (3.4.20) and (3.4.22) we get the following contributions for the hypercharge Y:

- $Y = 0$

$$\lambda_1 : (\phi_1^\dagger\phi_1)(\phi_1^\dagger\phi_1) = \frac{1}{2}\left[(\phi_1^\dagger\phi_1)(\phi_1^\dagger\phi_1) + \sum_r(\phi_1^\dagger\sigma^r\phi_1)(\phi_1^\dagger\sigma^r\phi_1)\right]$$

$$\lambda_2 : (\phi_2^\dagger\phi_2)(\phi_2^\dagger\phi_2) = \frac{1}{2}\left[(\phi_2^\dagger\phi_2)(\phi_2^\dagger\phi_2) + \sum_r(\phi_2^\dagger\sigma^r\phi_2)(\phi_2^\dagger\sigma^r\phi_2)\right]$$

$$\lambda_3 : (\phi_1^\dagger\phi_1)(\phi_2^\dagger\phi_2) = \frac{1}{2}\left[(\phi_1^\dagger\phi_2)(\phi_2^\dagger\phi_1) + \sum_r(\phi_1^\dagger\sigma^r\phi_2)(\phi_2^\dagger\sigma^r\phi_1)\right]$$

$$\lambda_4 : (\phi_1^\dagger\phi_2)(\phi_2^\dagger\phi_1) = \frac{1}{2}\left[(\phi_1^\dagger\phi_1)(\phi_2^\dagger\phi_2) + \sum_r(\phi_1^\dagger\sigma^r\phi_1)(\phi_2^\dagger\sigma^r\phi_2)\right]$$

$$\lambda_5 : (\phi_1^\dagger\phi_2)(\phi_1^\dagger\phi_2) = \frac{1}{2}\left[(\phi_1^\dagger\phi_2)(\phi_1^\dagger\phi_2) + \sum_r(\phi_1^\dagger\sigma^r\phi_2)(\phi_1^\dagger\sigma^r\phi_2)\right]$$

$$(\phi_2^\dagger\phi_1)(\phi_2^\dagger\phi_1) = \frac{1}{2}\left[(\phi_2^\dagger\phi_1)(\phi_2^\dagger\phi_1) + \sum_r(\phi_2^\dagger\sigma^r\phi_1)(\phi_2^\dagger\sigma^r\phi_1)\right] \tag{3.4.24}$$

- $Y = 2$

$$\lambda_1 : (\phi_1^\dagger\phi_1)(\phi_1^\dagger\phi_1) = \frac{1}{2}\left[(\phi_1^\dagger\tilde{\phi}_1^\dagger)(\tilde{\phi}_1\phi_1) + \sum_r(\phi_1^\dagger\sigma^r\tilde{\phi}_1^\dagger)(\tilde{\phi}_1\sigma^r\phi_1)\right]$$

$$\lambda_2 : (\phi_2^\dagger\phi_2)(\phi_2^\dagger\phi_2) = \frac{1}{2}\left[(\phi_2^\dagger\tilde{\phi}_2^\dagger)(\tilde{\phi}_2\phi_2) + \sum_r(\phi_2^\dagger\sigma^r\tilde{\phi}_2^\dagger)(\tilde{\phi}_2\sigma^r\phi_2)\right]$$

$$\lambda_3 : (\phi_1^\dagger\phi_1)(\phi_2^\dagger\phi_2) = \frac{1}{2}\left[(\phi_1^\dagger\tilde{\phi}_2^\dagger)(\tilde{\phi}_2\phi_1) + \sum_r(\phi_1^\dagger\sigma^r\tilde{\phi}_2^\dagger)(\tilde{\phi}_2\sigma^r\phi_1)\right]$$

	$\mathbb{Z}_2$-even	$\mathbb{Z}_2$-odd
$Y=0\,,\ \sigma=0$	$\frac{1}{\sqrt{2}}(\phi_1^\dagger\phi_1)\,,\ \frac{1}{\sqrt{2}}(\phi_2^\dagger\phi_2)$	$\frac{1}{\sqrt{2}}(\phi_1^\dagger\phi_2)\,,\ \frac{1}{\sqrt{2}}(\phi_2^\dagger\phi_1)$
$Y=0\,,\ \sigma=1$	$\frac{1}{\sqrt{2}}(\phi_1^\dagger\sigma^i\phi_1)\,,\ \frac{1}{\sqrt{2}}(\phi_2^\dagger\sigma^i\phi_2)$	$\frac{1}{\sqrt{2}}(\phi_1^\dagger\sigma^i\phi_2)\,,\ \frac{1}{\sqrt{2}}(\phi_2^\dagger\sigma^i\phi_1)$
$Y=2\,,\ \sigma=0$	-	$\frac{1}{\sqrt{2}}(\tilde{\phi}_1\phi_2)=-\frac{1}{\sqrt{2}}(\tilde{\phi}_2\phi_1)$
$Y=2\,,\ \sigma=1$	$\frac{1}{2}(\tilde{\phi}_1\sigma^i\phi_1)\,,\ \frac{1}{2}(\tilde{\phi}_2\sigma^i\phi_2)$	$\frac{1}{\sqrt{2}}(\tilde{\phi}_1\sigma^i\phi_2)=-\frac{1}{\sqrt{2}}(\tilde{\phi}_2\sigma^i\phi_1)$

Table 3.5: All possible states with weak hypercharge Y and isospin σ.

$$\lambda_4\ :\ (\phi_1^\dagger\phi_2)(\phi_2^\dagger\phi_1)=\frac{1}{2}\left[(\phi_1^\dagger\tilde{\phi}_2^\dagger)(\tilde{\phi}_1\phi_2)+\sum_r(\phi_1^\dagger\sigma^r\tilde{\phi}_2^\dagger)(\tilde{\phi}_1\sigma^r\phi_2)\right]$$

$$\lambda_5\ :\ (\phi_1^\dagger\phi_2)(\phi_1^\dagger\phi_2)=\frac{1}{2}\left[(\phi_1^\dagger\tilde{\phi}_1^\dagger)(\tilde{\phi}_1\phi_1)+\sum_r(\phi_1^\dagger\sigma^r\tilde{\phi}_1^\dagger)(\tilde{\phi}_1\sigma^r\phi_1)\right]$$

$$(\phi_2^\dagger\phi_1)(\phi_2^\dagger\phi_1)=\frac{1}{2}\left[(\phi_2^\dagger\tilde{\phi}_2^\dagger)(\tilde{\phi}_1\phi_1)+\sum_r(\phi_2^\dagger\sigma^r\tilde{\phi}_2^\dagger)(\tilde{\phi}_1\sigma^r\phi_1)\right]\quad(3.4.25)$$

The weak isospin T_3 is a quantum number related to the weak interaction and obeys the relation $Q=T_3+Y/2$, where Q is the charge and Y the weak hypercharge. Thus a state with two scalars can have either $\sigma=0$ or $\sigma=1$, where σ is the absolute value of the isospin of the two-scalar state.

We can now construct the set of states with weak hypercharge $Y=\{0,2\}$ and isospin $\sigma=\{0,1\}$. They are summarized in table 3.5. The states with $Y=-2$ are obtained from the ones with $Y=2$ by charge conjugation.

Taking these states we can construct the S-matrices from the potential (3.1.2) with the decompositions (3.4.20) and (3.4.22). For given quantum numbers Y and σ they are

$$S_{Y=2,\sigma=1}=\frac{1}{8\pi}\begin{pmatrix}2\lambda_1 & \lambda_5 & 0\\ \lambda_5 & 2\lambda_2 & 0\\ 0 & 0 & \lambda_3+\lambda_4\end{pmatrix}\,,\qquad(3.4.26)$$

$$S_{Y=2,\sigma=0}=\frac{1}{8\pi}(\lambda_3-\lambda_4)\,,\qquad(3.4.27)$$

$$S_{Y=0,\sigma=1}=\frac{1}{8\pi}\begin{pmatrix}2\lambda_1 & \lambda_4 & 0 & 0\\ \lambda_4 & 2\lambda_2 & 0 & 0\\ 0 & 0 & \lambda_3 & \lambda_5\\ 0 & 0 & \lambda_5 & \lambda_3\end{pmatrix}\,,\qquad(3.4.28)$$

$$S_{Y=0,\sigma=0}=\frac{1}{8\pi}\begin{pmatrix}6\lambda_1 & 2\lambda_3+\lambda_4 & 0 & 0\\ 2\lambda_3+\lambda_4 & 6\lambda_2 & 0 & 0\\ 0 & 0 & \lambda_3+2\lambda_4 & 3\lambda_5\\ 0 & 0 & 3\lambda_5 & \lambda_3+2\lambda_4\end{pmatrix}\,.\qquad(3.4.29)$$

The matrices are block diagonal and the upper left corner corresponds to scattering of $\mathbb{Z}_2$-even states, the bottom right corner to $\mathbb{Z}_2$-odd states. In the $Y=0$, $\sigma=0$ matrix there is a factor of 3 which comes from the different possibilities of contracting the fields. For example the matrix element $S_{Y=0,\sigma=0}^{12}=(2\lambda_3+\lambda_4)/(8\pi)$ has contributions from λ_4 and $2\cdot\lambda_3/2$.

We impose unitarity on the scattering matrix which implies that the eigenvalues are ±1. However, since we only included the leading partial wave, i.e. the s-wave, in our derivation of the unitarity constraint (3.4.16), imposing unitarity on the matrices (3.4.26) - (3.4.29) translates into $S \leq \mathbb{I}$, which means that the eigenvalues Λ of the matrices $\hat{S} = 8\pi S$ satisfy $|\Lambda| \leq 8\pi$ [146]. The eigenvalues of the matrices $\hat{S}$ in eqs. (3.4.26) - (3.4.29) are

$$
\begin{aligned}
\Lambda_{21\pm}^{\text{even}} &= \lambda_1 + \lambda_2 \pm \sqrt{(\lambda_1 - \lambda_2)^2 + \lambda_5^2} \ , \\
\Lambda_{21}^{\text{odd}} &= \lambda_3 + \lambda_4 \ , \\
\Lambda_{20}^{\text{odd}} &= \lambda_3 - \lambda_4 \ , \\
\Lambda_{01\pm}^{\text{even}} &= \lambda_1 + \lambda_2 \pm \sqrt{(\lambda_1 - \lambda_2)^2 + \lambda_4^2} \ , \\
\Lambda_{01\pm}^{\text{odd}} &= \lambda_3 \pm \lambda_5 \ , \\
\Lambda_{00\pm}^{\text{even}} &= 3(\lambda_1 + \lambda_2) \pm \sqrt{9(\lambda_1 - \lambda_2)^2 + (2\lambda_3 + \lambda_4)^2} \ , \\
\Lambda_{00\pm}^{\text{odd}} &= \lambda_3 + 2\lambda_4 \pm 3\lambda_5 \ .
\end{aligned}
\tag{3.4.30}
$$

Since we have already imposed perturbativity, three of these inequalities are easily satisfied. The other relations are the given unitarity constraints in eq. (3.4.3).

3.4.2 Experimental Constraints

From LEP I data of the Z-boson decay [123], a decay $Z \to HA$ is in tension with measurements and thus for practical purposes we require that

$$
m_H + m_A > m_Z \ .
\tag{3.4.31}
$$

LEP II results, interpreted in ref. [124], exclude models that satisfy simultaneously

$$
m_H < 80 \text{ GeV} \ , \quad m_A < 100 \text{ GeV} \quad \text{and} \quad \Delta m_{AH} = m_A - m_H > 8 \text{ GeV} \ .
\tag{3.4.32}
$$

This means that in a low dark matter mass region where $m_H < 80$ GeV, either the mass of the other neutral scalar is large ($m_A > 100$ GeV) or the mass splitting is small ($\Delta m_{AH} < 8$ GeV).

Constraints from electroweak precision measurements [78, 127] are imposed, using the Peskin-Takeuchi parameters S and T. The additional contributions are given by

$$
\Delta T = \frac{1}{32\pi^2 \alpha v^2} \left[F(m_{H^\pm}^2, m_A^2) + F(m_{H^\pm}^2, m_H^2) - F(m_H^2, m_A^2) \right] \ ,
\tag{3.4.33}
$$

where

$$
F(m_1^2, m_2^2) = \frac{m_1^2 + m_2^2}{2} - \frac{m_1^2 m_2^2}{m_1^2 - m_2^2} \log \frac{m_1^2}{m_2^2} \ ,
\tag{3.4.34}
$$

and

$$
\Delta S = \frac{1}{6\pi} \left[\frac{1}{2} \log \frac{m_H^2}{m_{H^\pm}^2} - \frac{5}{12} + \frac{m_H^2 m_A^2}{(m_A^2 - m_H^2)^2} + \frac{m_A^4(m_A^2 - 3m_H^2)}{2(m_A^2 - m_H^2)^3} \log \frac{m_A^2}{m_H^2} \right] \ .
\tag{3.4.35}
$$

Electroweak precision measurements set an upper bound on the oblique parameters [147]. $|\Delta T| \leq 0.2$ is easily realized if either m_H or m_A is approximately degenerate with $m_{H^\pm}$. In the exact degenerate case, ΔT vanishes. However, the constraint is not very restrictive as long as the mass splittings do not become large. $|\Delta S| \leq 0.15$ does not much constrain our parameter space, since it is fulfilled for a wide range of masses and mass splittings. When the mass splittings are small, we can approximate

$$\frac{m_1^2 m_2^2}{m_1^2 - m_2^2} \log \frac{m_1^2}{m_2^2} \approx m_1 m_2 \tag{3.4.36}$$

and write

$$\Delta T \approx \frac{1}{32\pi^2 \alpha v^2} (m_{H^\pm} - m_A)(m_{H^\pm} - m_H) . \tag{3.4.37}$$

The particles of the inert scalar doublet could have interesting consequences in the Higgs di-photon decay $h \to \gamma\gamma$ [127], which does not occur at tree-level. In the Standard Model, this decay is dominantly mediated through a charged gauge boson and a top loop. This diagram is proportional to the mass of the particle in the loop and thus a heavy new charged scalar can give a significant contribution. If the decay channel $h \to HH$ is kinematically open, this decay has to be taken into account as well and thus we should not compare decay widths but rather branching ratios.

If BSM theories have a dark matter candidate they should be able to reproduce the correct DM relic abundance. If one assumes that there are further extensions of the model with new particles contributing to the dark matter content in the universe, the relic abundance does not necessarily have to be reproduced but rather acts as an upper bound.

The current value of the Cold Dark Matter (CDM) relic abundance by Planck [15] is $\Omega_{\text{CDM}} h^2 = 0.1199 \pm 0.0022$, which leads to the 3σ (99.7% confidence level) range of

$$0.1133 < \Omega_{\text{CDM}} h^2 < 0.1265 \quad \text{or} \quad \Omega_{\text{CDM}} h^2 < 0.1265 . \tag{3.4.38}$$

The calculation of the relic abundance can be done using different codes from the literature with SARAH, SPheno and micrOMEGAs [148–151] being the most commonly used. Nevertheless, we did not perform these calculations, relying rather on the benchmark points from ref. [102] where this has been done.

Chapter 4

Conclusions

To really understand the origin of the matter-antimatter asymmetry it is of course important to consider all of the three Sakharov conditions mentioned in the introduction. However, even the third one alone, non-equilibrium of the system, can have many different origins as the literature shows. The electroweak phase transition is but one possible mechanism and even so, the number of models to realize such a transition is huge. We constrained ourselves to one such model for the reasons stated in chapter 3. These are simplicity, falsifiability, and the combination of effects requiring a priori contradictory parameter ranges, i.e. small couplings for dark matter and large ones for a first order phase transition.

For one thing we have shown that the high-temperature expansion is still quite accurate for describing the strength of the electroweak phase transitions, even though some of the masses are large. The implication of these findings, that simple expressions from the high-temperature expansions can be used for calculations within the Inert Doublet Model and other simple extensions of the Standard Model simplifies numerical calculations significantly. This allows to scan parameter spaces more efficiently and especially facilitates dimensionally reduced lattice studies which are necessary for cases in which good precision is needed. Furthermore, it allows investigations of properties with inhomogeneous configurations like surface tension [152, 153], bubble nucleation rate [154] and sphaleron rate [57, 59, 60].

It should be noted that there is one observable for which the high-temperature expansion does not work well. As can be seen from table 3.4 in chapter 3 this is the critical temperature T_c. In the Inert Doublet Model the large masses of the inert scalars have little effect on the strength of the phase transition but they do contribute to the effective Higgs mass parameter by a large amount. However, in a dimensionally reduced computation, these effects can be implemented without having to make use of a high-temperature expansion [111]. Therefore, good precision can be expected even for T_c.

We have also presented general expressions for master integral functions which allow the evaluation of the full two-loop effective thermal potential in a model independent way without having to resort to a high-temperature expansion or to the introduction of a mass scale hierarchy. Furthermore, we have shown that a first order phase transition is in fact possible, at least for two of the three benchmark points given.

Whether or not the Standard Model background really is important in the

evolution of the early universe, e.g. dark matter production or annihilation, is unknown. What we have shown, however, is that the electroweak crossover does experience unexpected behavior around a soft point at $T \sim 160$ GeV.

As already mentioned, the electroweak phase transition only tackles one part of the full story of baryogenesis. We have neither discussed baryon number violation nor the breaking of C and CP symmetries. Many different theories and ideas are presented in the literature and all model builders and phenomenologists await eagerly the newest results from various experiments. Meanwhile, we are hoping that some evidence can and will be found, be it either in favor or against a certain model. While the hope for conclusive proof is dim or even absent, the possibility of exclusion, at least for models with a modest number of independent parameters, is there.

Experimentalists and engineers around the world are working on various experiments and instruments to gather new or better data. These projects are not only big and expensive but also very sophisticated and thus the timescales are rather large. For high energy particle collisions this means that for now we have to do with the 13 TeV Large Hadron Collider (LHC) at CERN. However, concerning the electroweak phase transition there is a new promising star on the horizon: gravitational waves.

4.1   Outlook

The hope for model builders and physicists in general is that new particles are found at the LHC or any other (future) collider. This would not only allow us to get rid of many models and constraining the remaining ones but we would also gain some direct insight into the regime of new physics beyond the Standard Model. Besides new interactions, scatterings and decay channels new degrees of freedom could also shed some light on a possible electroweak phase transition. But finding new particles is not the only way to learn more about the early universe.

The electroweak phase transition, or in the case of the Standard Model the crossover, occurred in the very early universe at $\sim 10^{-12}$ seconds after the big bang. Given that the oldest particles that we can actually see, the photons in the cosmic microwave background, were created 10^5 years later, it is hard to imagine that we can observe what actually happened at the electroweak symmetry breaking scale. However, besides neutrinos there is one other source that does not require a transparent universe to make itself seen and that source is gravity. Propagating gravitational waves could have survived since the very beginning of the universe and their perturbation of e.g. the CMB could in principle be measured today.

Every source of energy that is in motion produces gravitational waves through a change in their quadrupole moment [155]. The problem with gravity, however, is that it is very weak. So to be able to detect these waves, their source must have released an enormous amount of energy through gravitational waves and their origin must thus be a very violent process. Fortunately, a cosmological first order phase transition is indeed extremely violent.

There are three main sources for the creation of gravitational waves in a first order phase transition. First of all there are the collisions of expanding bubbles during the transition [156, 157], as well as the sound waves generated afterward

[158, 159]. The collision of many bubbles also creates magneto-hydrodynamical turbulence in the plasma [160] which produce gravitational waves for many Hubble times after the transition.

To calculate the spectrum of gravitational waves produced by a first order phase transition, an important ingredient is the latent heat [161]. The efficiency factor describing the conversion from the latent heat into bulk motion of the expanding and colliding bubbles of the broken symmetry phase also depends on the bubble-wall velocity. For the velocity v_w of the expanding bubble-wall, the runaway scenario where there is no bound on the acceleration and thus $v_w \to c$ is mostly ruled out [162]. Therefore, assuming the non-runaway case where v_w asymptotically approaches a constant value and using parameters of a first order transition as presented in this thesis, namely the latent heat, the gravitational wave spectrum can be calculated. However, another important parameter which in principle could be determined from the potential [37] but we did not calculate is the inverse time duration of the phase transition [161].

The frequency of cosmological gravitational waves lies in the range covered by LISA ($10^{-4} - 10^{-1}$Hz) [163]. The Laser Interferometer Space Antenna (LISA) is thus a promising experiment to probe the nature of the electroweak phase transition or of other phase transitions that took place in the early universe. For a full frequency classification of gravitational waves according to their detection method, see ref. [164].

While there exist many ground-based gravitational waves interferometers, e.g. LIGO, VIRGO, GEO, TAMA, we will only look briefly into one of them, namely LIGO for reasons explained below. However, there are also many space-based interferometer experiments proposed [165] or even planned which are far more relevant for the topic of this thesis. We will introduce the most promising next gravitational wave experiment, LISA, which consist of three spacecrafts and we will also look even further into the future.

The Laser Interferometer Gravitational Wave Observatory (LIGO or since the upgrade in 2014/15 Advanced LIGO) is a Michelson interferometer type experiment [166, 167]. Its two identical facilities are located in the US at Hanford and Livingston. With its 4 km long arms the LIGO detectors are most sensitive around 100 Hz with its total range being $10 - 10^3$ Hz. Events producing gravitational waves in this range are for example supernovae, neutron star inspirals and black hole mergers. LIGO is estimated to measure $\mathcal{O}(80)$ such events each year. However, it will not be able to measure gravitational waves from cosmological phase transitions. Nevertheless, LIGO deserves to be mentioned since it is responsible for the first direct measurements of gravitational waves ever [168–170].

The Laser Interferometer Space Antenna (LISA) is a collaboration of the European Space Agency (ESA) and the National Aeronautics and Space Administration (NASA). One of its main goals is to detect gravitational waves produced in the very early universe [171]. However, such gravitational waves from non-equilibrium phenomena, including (p)reheating, cosmic defects, cosmic strings and global phase transitions, are not all detectable by LISA. The frequency peak of gravitational waves from preheating lies well out of range for LISA, whereas cosmic defects, depending on the scenario, produce gravitational waves in a wide range and should therefore be detectable. The gravitational wave background from the electroweak phase transition, however, lies precisely in the frequency window where LISAs precision is highest. The whole range where LISA is to

detect gravitational waves is $10^{-5} - 0.1$ Hz. Not only the aforementioned primordial sources produce gravitational waves in this range. LISA is also expected to detect massive black hole binaries (MBHB) with $10^4 - 10^7 M_\odot$, black hole mergers as detected by LIGO and extreme mass ratio inspirals (EMRI).

An interesting point in the setup is that other than in ground-based experiments, the LISA spacecrafts rather than the test masses have to be stabilized. The test masses are in free fall and thus on very well behaved trajectories while the spacecraft itself is moving around the masses.

The Big Bang Observer (BBO) is a space-based experiment in its planning phase [172]. Its goal is to close the gap in the frequency spectrum between Advanced LIGO and LISA. In this range between $0.1 - 10$ Hz lies the expected primordial gravitational wave background created during inflation. However, BBO will also be able to detect gravitational waves from supernovae and compact body inspirals like white dwarfs, neutron stars and stellar mass black holes.

The arms of BBO will be shorter than those of LISA, however, the laser is more powerful to improve on the signal to noise ratio. In a first stage, three spacecrafts will be placed in a triangular shape much like LISA. In the second stage nine additional spacecrafts will be placed in a second triangle and a star of David shaped constellation on different points spaced 120° apart in solar orbit.

The departure from thermal equilibrium during a first order electroweak phase transition remains a viable possibility for the origin of the matter antimatter asymmetry of the universe. Future experiments at particle colliders and the ongoing search for gravitational waves will not only shed light on a possible phase transition at the electroweak scale but also provide us with new insights into the history and nature of our universe. Through these experiments and the theoretical studies of the gathered results, the scientific field of physics will keep up improving our understanding of nature and continue to fascinate us.

Appendix A

Master Integrals

In this Appendix we derive the one-loop zero temperature expressions for the calculation of the on-shell self-energies in Appendix C.2. Furthermore, we provide an overview of the one- and two-loop master integrals derived in chapter 3 as well as their high-temperature expansions.

Before we tackle the integrals needed there is a very general integral we want to compute, since we are going to use it on various occasions, namely

$$\Phi(m, d, A) = \int \frac{d^d k}{(2\pi)^d} \frac{1}{(k^2 + m^2)^A} \quad . \tag{A.0.1}$$

Since the integrand only depends on the absolute value of k all the angular integrations can be carried out. The momentum measure is then

$$d^d k = \frac{\pi^{\frac{d}{2}}}{\Gamma\left(\frac{d}{2}\right)} k^{d-2} d(k^2) \quad , \tag{A.0.2}$$

where $\Gamma(s)$ is the Euler gamma function. Performing the two consecutive substitutions $k^2 \to m^2 t$ and $t \to 1/s - 1$ we get

$$\begin{aligned}
\Phi(m, d, A) &= \frac{m^{d-2A}}{(4\pi)^{\frac{d}{2}} \Gamma\left(\frac{d}{2}\right)} \int_0^\infty dt \; t^{\frac{d}{2}-1} (1+t)^{-A} \\
&= \frac{m^{d-2A}}{(4\pi)^{\frac{d}{2}} \Gamma\left(\frac{d}{2}\right)} \int_0^1 ds \; s^{A-\frac{d}{2}-1} (1-s)^{\frac{d}{2}-1} \quad .
\end{aligned} \tag{A.0.3}$$

This last integral corresponds to the Euler beta function $B(x, y)$ which can be expressed in terms of Euler gamma functions as

$$B(x, y) = \frac{\Gamma(x)\Gamma(y)}{\Gamma(x+y)} \tag{A.0.4}$$

and we have thus arrived at the simple form

$$\Phi(d, m, A) = \int \frac{d^d k}{(2\pi)^d} \frac{1}{(k^2 + m^2)^A} = \frac{(m^2)^{\frac{d}{2}-A}}{(4\pi)^{\frac{d}{2}}} \frac{\Gamma\left(A - \frac{d}{2}\right)}{\Gamma(A)} \quad . \tag{A.0.5}$$

We can now turn to the derivation of the vacuum integrals.

A.1   Vacuum Integrals $A(m)$, $B(P; m_1, m_2)$, $C(P; m_1, m_2)$ and $D_{\mu\nu}(P; m_1, m_2)$
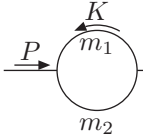
The integral $A(m)$ is

$$A(m) = \int_K \frac{1}{K^2 + m^2} \ . \tag{A.1.1}$$

We can directly use (A.0.5) in $d = 4 - 2\epsilon$ dimensions to get

$$A(m) = \frac{m^2}{(4\pi)^2} \left[-\frac{1}{\epsilon} - 1 + \ln \frac{m^2}{\bar{\mu}^2} \right] + \mathcal{O}(\epsilon) \ . \tag{A.1.2}$$

The integral $B(P; m_1, m_2)$ is

$$B(P; m_1, m_2) = \quad \text{} \quad = \int_K \frac{1}{\left(K^2 + m_1^2\right)\left[(P + K)^2 + m_2^2\right]} \ . \tag{A.1.3}$$

In the first step we use Feynman parametrization and then we change the integration variable as usual, i.e. $K \to K - (1 - x)P$. We can then apply (A.0.5) to get

$$\int_K \frac{1}{\left(K^2 + m_1^2\right)\left[(P + K)^2 + m_2^2\right]}$$

$$= \int_0^1 dx \int_K \frac{1}{\left[K^2 + x(1-x)P^2 + (1-x)m_1^2 + x m_2^2\right]^2}$$

$$= \int_0^1 \frac{dx}{(4\pi)^2} \left[\frac{1}{\epsilon} - \ln \left(\frac{x(1-x)P^2 + (1-x)m_1^2 + x m_2^2}{\bar{\mu}^2} \right) + \mathcal{O}(\epsilon) \right] \ . \tag{A.1.4}$$

Since the diagram in eq. (A.1.3) is symmetric under an exchange of $m_1 \leftrightarrow m_2$ we exchange the masses in half of the expression in eq. (A.1.4). We perform the integration over x such that the symmetrized result then reads

$$B(P; m_1, m_2) = \frac{1}{(4\pi)^2} \left[\frac{1}{\epsilon} + 2 - \ln \frac{m_1 m_2}{\bar{\mu}^2} + \frac{m_1^2 - m_2^2}{P^2} \ln \frac{m_1}{m_2} \right.$$

$$\left. - \frac{2\sqrt{(m_1 - m_2)^2 + P^2}\sqrt{(m_1 + m_2)^2 + P^2}}{P^2} \mathrm{atanh} \frac{\sqrt{(m_1 - m_2)^2 + P^2}}{\sqrt{(m_1 + m_2)^2 + P^2}} \right] \ . \tag{A.1.5}$$

The remaining two integrals can be expressed in terms of the masters A and B. We first consider the C function where

$$P_\mu C(P; m_1, m_2) = \int_K \frac{K_\mu}{\left(K^2 + m_1^2\right)\left[(P + K)^2 + m_2^2\right]} \ . \tag{A.1.6}$$

We multiply this by P^μ and use the decomposition

$$P^\mu K_\mu = \frac{1}{2}\left[(P+K)^2 - K^2 - P^2\right]$$
$$= \frac{1}{2}\left[(P+K)^2 + m_2^2 - (K^2 + m_1^2) - P^2 + m_1^2 - m_2^2\right] . \qquad (A.1.7)$$

We divide by P^2 and thus get

$$C(P; m_1, m_2) = \frac{1}{2P^2}\left[A(m_1) - A(m_2) - (P^2 - m_1^2 + m_2^2)B(P; m_1, m_2)\right] . \qquad (A.1.8)$$

The last function to compute here is

$$D_{\mu\nu}(P; m_1, m_2) = \int_K \frac{K_\mu K_\nu}{(K^2 + m_1^2)\left[(P+K)^2 + m_2^2\right]} . \qquad (A.1.9)$$

Lorentz invariance now implies that the resulting structure must be

$$D_{\mu\nu}(P; m_1, m_2) = \delta_{\mu\nu}D_0(P; m_1, m_2) + P_\mu P_\nu D_1(P; m_1, m_2) . \qquad (A.1.10)$$

Contracting this equation with the Euclidean metric $\delta_{\mu\nu}$ gives us one equation and multiplying it by P_μ a second one to build the system

$$\delta_{\mu\nu}D_{\mu\nu}(P; m_1, m_2) = DD_0(P; m_1, m_2) + P^2 D_1(P; m_1, m_2) ,$$
$$P_\mu D_{\mu\nu}(P; m_1, m_2) = P_\nu\left[D_0(P; m_1, m_2) + P^2 D_1(P; m_1, m_2)\right] . \qquad (A.1.11)$$

The first equation is easily solved to

$$\delta_{\mu\nu}D_{\mu\nu}(P; m_1, m_2) = \int_K \frac{K^2}{(K^2 + m_1^2)\left[(P+K)^2 + m_2^2\right]}$$
$$= A(m_2) - m_1^2 B(P; m_1, m_2) . \qquad (A.1.12)$$

For the second equation in the system in eq. (A.1.11) we again use the decomposition in eq. (A.1.7) to get

$$P_\mu D_{\mu\nu}(P; m_1, m_2) = \int_K \frac{(P \cdot K)K_\nu}{(K^2 + m_1^2)\left[(P+K)^2 + m_2^2\right]}$$
$$= \frac{1}{2}\left[\int_K \frac{K_\nu}{K^2 + m_1^2} - \int_K \frac{K_\nu}{(P+K)^2 + m_2^2} - P_\nu(P^2 - m_1^2 + m_2^2)C(P; m_1, m_2)\right] . \qquad (A.1.13)$$

Changing integration variables from $K \to K - P$ in the second term and using that the first term, being odd, vanishes, we get

$$P_\mu D_{\mu\nu}(P; m_1, m_2) = \frac{P_\nu}{2}\left[A(m_2) - (P^2 - m_1^2 + m_2^2)C(P; m_1, m_2)\right] . \qquad (A.1.14)$$

We can now solve the system in eq. (A.1.11) for D_0 and D_1 and finally get

$$D_{\mu\nu}(P; m_1, m_2) = \left(\frac{\delta_{\mu\nu}}{4(D-1)P^2} - \frac{DP_\mu P_\nu}{4(D-1)P^4}\right)\left\{(P^2 - m_1^2 + m_2^2)A(m_1)\right.$$

$$+ (P^2 + m_1^2 - m_2^2)A(m_2)$$

$$- \left[P^4 + 2P^2(m_1^2 + m_2^2) + (m_1^2 - m_2^2)^2 \right] B(P; m_1, m_2) \bigg\}$$

$$+ \frac{P_\mu P_\nu}{P^2} \left[A(m_2) - m_1^2 B(P; m_1, m_2) \right] . \qquad (A.1.15)$$

For our calculation of the vector boson self-energy we only need the transverse part $D^{(T)}$ which is defined through $D_{\mu\nu} = D^{(T)} \delta_{\mu\nu} + \mathcal{O}(P_\mu P_\nu)$.

A.2   Overview and High-Temperature Expansions

In this summary, all the different terms in the ϵ-expansion defined in eq. (3.2.2) of the functions computed in chapter 3 as well as their high-temperature limit are presented in a compact form.

The expressions for the J-function are

$$J^{(-1)}(m) = -\frac{m^4}{4(4\pi)^2} , \qquad (A.2.1)$$

$$J^{(0)}(m) = -\frac{m^4}{4(4\pi)^2} \left(\frac{3}{2} - \ln \frac{m^2}{\bar{\mu}^2} \right) - \frac{I_T^{(0)}(m)}{3} , \qquad (A.2.2)$$

with the high-temperature expansion for bosonic particles with mass m_b and fermionic particles with mass m_f

$$J^{(0)}(m_b) = -\frac{\pi^2 T^4}{90} + \frac{m_b^2 T^2}{24} - \frac{m_b^3 T}{12\pi} - \frac{m_b^4}{2(4\pi)^2} \ln \left(\frac{\bar{\mu} e^{\gamma_E}}{4\pi T} \right) + \mathcal{O}\left(\frac{m_b^6}{\pi^4 T^2} \right) , \quad (A.2.3)$$

$$J^{(0)}(m_f) = -\frac{7}{8} \frac{\pi^2 T^4}{90} + \frac{m_f^2 T^2}{48} - \frac{m_f^4}{2(4\pi)^2} \ln \left(\frac{\bar{\mu} e^{\gamma_E}}{\pi T} \right) + \mathcal{O}\left(\frac{m_f^6}{\pi^4 T^2} \right) . \qquad (A.2.4)$$

For the I-function we need one more term in the ϵ-expansion

$$I^{(-1)}(m) = -\frac{m^2}{(4\pi)^2} , \qquad (A.2.5)$$

$$I^{(0)}(m) = -\frac{m^2}{(4\pi)^2} \left(1 - \ln \frac{m^2}{\bar{\mu}^2} \right) + I_T^{(0)}(m) , \qquad (A.2.6)$$

$$I_T^{(0)}(m) = \int_0^\infty \frac{dp \, p^2 n(\omega)}{2\pi^2 \omega} , \qquad (A.2.7)$$

$$I^{(1)}(m) = -\frac{m^2}{(4\pi)^2} \left(\frac{1}{2} \ln^2 \frac{m^2}{\bar{\mu}^2} - \ln \frac{m^2}{\bar{\mu}^2} + 1 + \frac{\pi^2}{12} \right) + I_T^{(1)}(m) , \qquad (A.2.8)$$

$$I_T^{(1)}(m) = \int_0^\infty \frac{dp \, p^2 n(\omega)}{2\pi^2 \omega} \left(\ln \frac{\bar{\mu}^2}{4p^2} + 2 \right) . \qquad (A.2.9)$$

The high-temperature contributions read

$$I^{(0)}(m_b) = \frac{T^2}{12} - \frac{m_b T}{4\pi} - \frac{2m_b^2}{(4\pi)^2} \ln \left(\frac{\bar{\mu} e^{\gamma_E}}{4\pi T} \right) + \mathcal{O}\left(\frac{m_b^4}{\pi^4 T^2} \right) , \qquad (A.2.10)$$

$$I^{(1)}(m_b) = \frac{T^2}{6}\left[\ln\left(\frac{\bar{\mu}e^{\gamma_E}}{2T}\right) - \frac{\zeta'(2)}{\zeta(2)}\right] - \frac{m_b T}{2\pi}\left[1 - \ln\frac{2m_b}{\bar{\mu}}\right]$$
$$- \frac{2m_b^2}{(4\pi)^2}\left[\ln^2\left(\frac{\bar{\mu}e^{\gamma_E}}{4\pi T}\right) - \gamma_E^2 - 2\gamma_1 + \frac{\pi^2}{8}\right] + \mathcal{O}\left(\frac{m_b^4}{\pi^4 T^2}\right) , \quad \text{(A.2.11)}$$

$$I^{(0)}(m_f) = -\frac{T^2}{24} - \frac{2m_f^2}{(4\pi)^2}\ln\left(\frac{\bar{\mu}e^{\gamma_E}}{\pi T}\right) + \mathcal{O}\left(\frac{m_f^4}{\pi^4 T^2}\right) , \quad \text{(A.2.12)}$$

$$I^{(1)}(m_f) = -\frac{T^2}{12}\left[\ln\left(\frac{\bar{\mu}e^{\gamma_E}}{4T}\right) - \frac{\zeta'(2)}{\zeta(2)}\right]$$
$$- \frac{2m_f^2}{(4\pi)^2}\left[\ln^2\left(\frac{\bar{\mu}e^{\gamma_E}}{\pi T}\right) - \gamma_E^2 - 2\ln^2 2 - 2\gamma_1 + \frac{\pi^2}{8}\right] + \mathcal{O}\left(\frac{m_f^4}{\pi^4 T^2}\right) , $$
$$\text{(A.2.13)}$$

where γ_1 is the Stieltjes constant defined by the expansion of the ζ-function $\zeta(s) = 1/(s-1) + \sum_{n=0}^{\infty}\gamma_n(-1)^n(s-1)^n/n!$. The contributions to the modified I-function appearing in the two-loop potential are

$$I^{(-1)}(\underline{m}) = \frac{3m^4}{4(4\pi)^2} , \quad \text{(A.2.14)}$$

$$I^{(0)}(\underline{m}) = \frac{m^4}{(4\pi)^2}\left(\frac{5}{8} - \frac{3}{4}\ln\frac{m^2}{\bar{\mu}^2}\right) + I_T^{(0)}(\underline{m}) , \quad \text{(A.2.15)}$$

$$I_T^{(0)}(\underline{m}) = \int_0^{\infty}\frac{dp\ p^4 n(\omega)}{2\pi^2\omega} , \quad \text{(A.2.16)}$$

$$I^{(1)}(\underline{m}) = \frac{m^4}{(4\pi)^2}\left(\frac{3}{8}\ln^2\frac{m^2}{\bar{\mu}^2} + \frac{5}{8}\ln\frac{m^2}{\bar{\mu}^2} + \frac{9}{16} + \frac{\pi^2}{16}\right) + I_T^{(1)}(\underline{m}) , \quad \text{(A.2.17)}$$

$$I_T^{(1)}(\underline{m}) = \int_0^{\infty}\frac{dp\ p^4 n(\omega)}{2\pi^2\omega}\left(\ln\frac{\bar{\mu}^2}{4p^2} + 2\right) . \quad \text{(A.2.18)}$$

The high-temperature expansion thereof is

$$I^{(0)}(\underline{m_b}) = \frac{\pi^2 T^4}{30} - \frac{m_b^2 T^2}{8} + \mathcal{O}\left(\frac{m_b^3 T}{\pi}\right) , \quad \text{(A.2.19)}$$

$$I^{(1)}(\underline{m_b}) = \frac{\pi^2 T^4}{15}\left[\ln\left(\frac{\bar{\mu}e^{\gamma_E}}{2T}\right) - \frac{\zeta'(4)}{\zeta(4)} - \frac{5}{6}\right]$$
$$- \frac{m_b^2 T^2}{4}\left[\ln\left(\frac{\bar{\mu}e^{\gamma_E}}{2T}\right) - \frac{\zeta'(2)}{\zeta(2)} - \frac{1}{3}\right] + \mathcal{O}\left(\frac{m_b^3 T}{\pi}\right) , \quad \text{(A.2.20)}$$

$$I^{(0)}(\underline{m_f}) = -\frac{7}{8}\frac{\pi^2 T^4}{30} + \frac{m_f^2 T^2}{16} + \mathcal{O}\left(\frac{m_f^4}{\pi^4 T^2}\right) , \quad \text{(A.2.21)}$$

$$I^{(1)}(\underline{m_f}) = -\frac{7\pi^2 T^4}{120}\left[\ln\left(\frac{\bar{\mu}e^{\gamma_E}}{2T}\right) - \frac{\zeta'(4)}{\zeta(4)} - \frac{\ln 2}{7} - \frac{5}{6}\right]$$
$$- \frac{m_f^2 T^2}{8}\left[\ln\left(\frac{\bar{\mu}e^{\gamma_E}}{4T}\right) - \frac{\zeta'(2)}{\zeta(2)} - \frac{1}{3}\right] + \mathcal{O}\left(\frac{m_f^4}{\pi^2}\right) . \quad \text{(A.2.22)}$$

The expressions for the sunset H-function are

$$H^{(-2)}(m_1, m_2, m_3) = \frac{m_1^2 + m_2^2 + m_3^2}{2(4\pi)^4} , \quad \text{(A.2.23)}$$

$$H^{(-1)}(m_1, m_2, m_3) = -\frac{1}{(4\pi)^4} \sum_{i=1}^{3} m_i^2 \left(\frac{3}{2} - \ln \frac{m_i^2}{\bar{\mu}^2} \right) + \sum_{i=1}^{3} \frac{I_T^{(0)}(m_i)}{(4\pi)^2} \, , \qquad \text{(A.2.24)}$$

$$H^{(0)}(m_1, m_2, m_3)$$

$$= \frac{1}{(4\pi)^4} \left[-\frac{1}{2} \sum_{i=1}^{3} m_i^2 \ln^2 \left(\frac{m_i^2}{\bar{\mu}^2} \right) + 3 \sum_{i=1}^{3} m_i^2 \ln \left(\frac{m^2}{\bar{\mu}^2} \right) - \left(\frac{7}{2} + \frac{\pi^2}{12} \right) \sum_{i=1}^{3} m_i^2 \right.$$

$$- \frac{m_1^2 + m_2^2 - m_3^2}{2} \ln \left(\frac{m_1^2}{\bar{\mu}^2} \right) \ln \left(\frac{m_2}{\bar{\mu}^2} \right) - \frac{m_1^2 + m_3^2 - m_2^2}{2} \ln \left(\frac{m_1^2}{\bar{\mu}^2} \right) \ln \left(\frac{m_3}{\bar{\mu}^2} \right)$$

$$\left. - \frac{m_2^2 + m_3^2 - m_1^2}{2} \ln \left(\frac{m_2^2}{\bar{\mu}^2} \right) \ln \left(\frac{m_3}{\bar{\mu}^2} \right) - \frac{1}{2} R(m_1^2, m_2^2, m_3^2) L(m_1^2, m_2^2, m_3^2) \right]$$

$$+ I_T^{(0)}(m_1) \operatorname{Re} B^{(0)}(-im_1; m_2, m_3) + I_T^{(0)}(m_2) \operatorname{Re} B^{(0)}(-im_2; m_3, m_1)$$

$$+ I_T^{(0)}(m_3) \operatorname{Re} B^{(0)}(-im_3; m_1, m_2) + \sum_{i=1}^{3} \frac{I_T^{(1)}(m_i)}{(4\pi)^2}$$

$$+ \int_0^{\infty} \frac{dp\,dq\ pq\,n(\omega_1^p)n(\omega_2^q)}{32\pi^4 \omega_1^p \omega_2^q} \ln \left| \frac{(m_3^2 - m_1^2 - m_2^2 + 2pq)^2 - 4(\omega_1^p)^2(\omega_2^q)^2}{(m_3^2 - m_1^2 - m_2^2 - 2pq)^2 - 4(\omega_1^p)^2(\omega_2^q)^2} \right|$$

$$+ \int_0^{\infty} \frac{dp\,dq\ pq\,n(\omega_2^p)n(\omega_3^q)}{32\pi^4 \omega_2^p \omega_3^q} \ln \left| \frac{(m_1^2 - m_2^2 - m_3^2 + 2pq)^2 - 4(\omega_2^p)^2(\omega_3^q)^2}{(m_1^2 - m_2^2 - m_3^2 - 2pq)^2 - 4(\omega_2^p)^2(\omega_3^q)^2} \right|$$

$$+ \int_0^{\infty} \frac{dp\,dq\ pq\,n(\omega_3^p)n(\omega_1^q)}{32\pi^4 \omega_3^p \omega_1^q} \ln \left| \frac{(m_2^2 - m_3^2 - m_1^2 + 2pq)^2 - 4(\omega_3^p)^2(\omega_1^q)^2}{(m_2^2 - m_3^2 - m_1^2 - 2pq)^2 - 4(\omega_3^p)^2(\omega_1^q)^2} \right| \, ,$$

$$\text{(A.2.25)}$$

with $\omega_i^p = \sqrt{p^2 + m_i^2}$ and [114]

$$R(m_1^2, m_2^2, m_3^2) = \sqrt{m_1^4 + m_2^4 + m_3^4 - 2m_1^2 m_2^2 - 2m_1^2 m_3^2 - 2m_2^2 m_3^2} \, , \qquad \text{(A.2.26)}$$

$$L(m_1^2, m_2^2, m_3^2) = \operatorname{Li}_2 \left(-\frac{t_3 m_2}{m_1} \right) + \operatorname{Li}_2 \left(-\frac{t_3 m_1}{m_2} \right) + \frac{\pi^2}{6} + \frac{\ln^2 t_3}{2}$$

$$+ \frac{1}{2} \left[\ln \left(t_3 + \frac{m_2^2}{m_1^2} \right) - \ln \left(t_3 + \frac{m_1^2}{m_2^2} \right) + \frac{3}{4} \ln \left(\frac{m_1^2}{m_2^2} \right) \right] \ln \left(\frac{m_1^2}{m_2^2} \right) \, , \qquad \text{(A.2.27)}$$

$$t_3 = \frac{m_3^2 - m_1^2 - m_2^2 + R(m_1^2, m_2^2, m_3^2)}{2m_1 m_2} \, . \qquad \text{(A.2.28)}$$

In the effective potential the H-function is always multiplied by a factor $\sim g^2 m^2$, therefore the $\sim T^2$ term in the high-temperature expansion is sufficient to get the desired order $\sim g^2 m^2 T^2$. The high-temperature expansion is then [173, 174]

$$H(m_{b1}, m_{b2}, m_{b3}) = \frac{T^2}{(4\pi)^2} \left(\frac{1}{4\epsilon} - \ln \frac{m_{b1} + m_{b2} + m_{b3}}{\bar{\mu}} + \frac{1}{2} \right) + \mathcal{O} \left(\frac{\epsilon T^2}{\pi^2}, \frac{m_{bi} T}{\pi^3} \right) \, , \qquad \text{(A.2.29)}$$

$$H(m_{b1}, m_{f2}, m_{f3}) = \mathcal{O} \left(\frac{\epsilon T^2}{\pi^2}, \frac{m_{bi} T}{\pi^3} \right) \, . \qquad \text{(A.2.30)}$$

The contributions for the modified H-function are

$$H^{(-2)}(\underline{m_1}, m_2, m_3)$$
$$= \frac{3\left[m_1^2(m_1^2 + m_2^2 + m_3^2) + 2m_2^2 m_3^2\right]}{8(4\pi)^4} \ , \tag{A.2.31}$$

$$H^{(-1)}(\underline{m_1}, m_2, m_3)$$
$$= \frac{17m_1^2(m_1^2 + m_2^2 + m_3^2) + 22m_2^2 m_3^2}{16(4\pi)^4}$$
$$- \frac{3}{4(4\pi)^4}\left[m_1^4 \ln\left(\frac{m_1^2}{\bar\mu^2}\right) + m_2^2(m_1^2 + m_3^2)\ln\left(\frac{m_2^2}{\bar\mu^2}\right) + m_3^2(m_1^2 + m_2^2)\ln\left(\frac{m_3^2}{\bar\mu^2}\right)\right]$$
$$+ \frac{1}{(4\pi)^2}\left\{I_T^{(0)}(\underline{m_1}) + \frac{1}{3}\left[I_T^{(0)}(\underline{m_2}) + I_T^{(0)}(\underline{m_3})\right]\right\}$$
$$+ \frac{1}{4(4\pi)^2}\left[(m_2^2 - 3m_1^2 - 3m_3^2)I_T^{(0)}(m_2) + (m_3^2 - 3m_1^2 - 3m_2^2)I_T^{(0)}(m_3)\right] \ ,$$

$$H^{(0)}(\underline{m_1}, m_2, m_3)$$
$$= \frac{77\left[m_1^2(m_1^2 + m_2^2 + m_3^2) + 62m_2^2 m_3^2\right]}{32(4\pi)^4} + \frac{\pi^2\left[m_1^2(m_1^2 + m_2^2 + m_3^2) + 2m_2^2 m_3^2\right]}{16(4\pi)^4}$$
$$+ \frac{3}{8(4\pi)^4}\left[m_1^4 \ln^2\left(\frac{m_1^2}{\bar\mu}\right) + m_2^2(m_1^2 + m_3^2)\ln^2\left(\frac{m_2^2}{\bar\mu}\right) + m_3^2(m_1^2 + m_2^2)\ln^2\left(\frac{m_3^2}{\bar\mu}\right)\right]$$
$$- \frac{1}{8(4\pi)^4}\left[17m_1^4 \ln\left(\frac{m_1^2}{\bar\mu}\right) + m_2^2(17m_1^2 + 11m_3^2)\ln\left(\frac{m_2^2}{\bar\mu}\right)\right.$$
$$\left. + m_3^2(17m_1^2 + 11m_2^2)\ln\left(\frac{m_3^2}{\bar\mu}\right)\right]$$
$$+ \frac{1}{(4\pi)^4}\left\{\frac{3m_1^2}{8}\left[(m_1^2 + m_2^2 - m_3^2)\ln\left(\frac{m_1^2}{\bar\mu}\right)\ln\left(\frac{m_2^2}{\bar\mu}\right)\right.\right.$$
$$\left.+ (m_1^2 + m_3^2 - m_2^2)\ln\left(\frac{m_1^2}{\bar\mu}\right)\ln\left(\frac{m_3^2}{\bar\mu}\right) + (m_2^2 + m_3^2 - m_1^2)\ln\left(\frac{m_2^2}{\bar\mu}\right)\ln\left(\frac{m_3^2}{\bar\mu}\right)\right]$$
$$\left.+ \frac{3m_2^3 m_3^2}{4}\ln\left(\frac{m_2^2}{\bar\mu}\right)\ln\left(\frac{m_3^2}{\bar\mu}\right) - \frac{3m_1^2}{4}R(m_1^2, m_2^2, m_3^2)L(m_1^2, m_2^2, m_3^2)\right\}$$
$$+ I_T^{(0)}(\underline{m_1})\text{Re }B^{(0)}(-im_1; m_2, m_3)$$
$$+ I_T^{(0)}(\underline{m_2})\left\{\frac{R^2(m_1^2, m_2^2, m_3^2) + 3m_1^2 m_2^2}{3m_2^4}\text{Re }B^{(0)}(-im_2; m_3, m_1)\right.$$
$$+ \frac{1}{18m_2^4(4\pi)^2}\left[-6m_1^2(m_1^2 + m_2^2 - m_3^2)\ln\left(\frac{m_1^2}{\bar\mu}\right)\right.$$
$$+ 6m_3^2(m_1^2 + 2m_2^2 - m_3^2)\ln\left(\frac{m_3^2}{\bar\mu}\right) - 6m_1^4 + m_2^4 - 6m_3^4 - 9m_1^2 m_2^2$$
$$\left.\left.+ 12m_1^2 m_3^2 + 9m_2^2 m_3^2\right]\right\} + (2 \leftrightarrow 3)$$
$$+ I_T^{(0)}(m_2)\left\{\frac{R^2(m_1^2, m_2^2, m_3^2)}{4m_2^2}\text{Re }B^{(0)}(-im_2; m_3, m_1)\right.$$

$$
+ \frac{1}{4m_2^2(4\pi)^2}\left[m_1^2(m_1^2 + m_2^2 - m_3^2)\ln\left(\frac{m_1^2}{\bar\mu}\right) + m_3^2(-m_1^2 + m_2^2 + m_3^2)\ln\left(\frac{m_3^2}{\bar\mu}\right)\right.
$$

$$
\left.\left. - m_1^4 - m_3^4 - m_1^2 m_2^2 + 2m_1^2 m_3^2 - m_2^2 m_3^2 \right]\right\} + (2 \leftrightarrow 3)
$$

$$
+ \frac{1}{(4\pi)^2}\left\{ I_T^{(1)}(\underline{m_1}) + \frac{1}{3}\left[I_T^{(1)}(\underline{m_2}) + I_T^{(1)}(\underline{m_3})\right]\right\}
$$

$$
+ \frac{1}{4(4\pi)^2}\left[(m_2^2 - 3m_1^2 - 3m_3^2)I_T^{(1)}(m_2) + (m_3^2 - 3m_1^2 - 3m_2^2)I_T^{(1)}(m_3)\right]
$$

$$
+ \int_0^\infty \frac{dpdq\ p^3 q\, n(\omega_1^p) n(\omega_2^q)}{32\pi^4 \omega_1^p \omega_2^q} \ln\left| \frac{(m_3^2 - m_1^2 - m_2^2 + 2pq)^2 - 4(\omega_1^p)^2(\omega_2^q)^2}{(m_3^2 - m_1^2 - m_2^2 - 2pq)^2 - 4(\omega_1^p)^2(\omega_2^q)^2}\right|
$$

$$
+ \int_0^\infty \frac{dpdq\ p^3 q\, n(\omega_1^p) n(\omega_3^q)}{32\pi^4 \omega_1^p \omega_3^q} \ln\left| \frac{(m_2^2 - m_1^2 - m_3^2 + 2pq)^2 - 4(\omega_1^p)^2(\omega_3^q)^2}{(m_2^2 - m_1^2 - m_3^2 - 2pq)^2 - 4(\omega_1^p)^2(\omega_3^q)^2}\right|
$$

$$
+ \int_0^\infty \frac{dpdq\ p^2 q^2 n(\omega_2^p) n(\omega_3^q)}{4\pi^4 \omega_2^p \omega_3^q} \left\{ 1 + \frac{\omega_2^p \omega_3^q}{4pq}\ln\left| \frac{(m_1^2 - m_2^2 - m_3^2)^2 - 4(pq - \omega_2^p\omega_3^q)^2}{(m_1^2 - m_2^2 - m_3^2)^2 - 4(pq + \omega_2^p\omega_3^q)^2}\right|\right.
$$

$$
\left.+ \frac{(\omega_2^p)^2 + (\omega_3^q)^2 - m_1^2}{8pq}\ln\left| \frac{(m_1^2 - m_2^2 - m_3^2 + 2pq)^2 - 4(\omega_2^p)^2(\omega_3^q)^2}{(m_1^2 - m_2^2 - m_3^2 - 2pq)^2 - 4(\omega_2^p)^2(\omega_3^q)^2}\right|\right\}.
$$

$$(A.2.32)$$

The high-temperature limit is [175]

$$
H(\underline{m_{b1}}, m_{b2}, m_{b3}) = \frac{T^4}{72}\left[\frac{1}{4\epsilon} + \ln\left(\frac{\bar\mu e^{\gamma_E}}{2T}\right) - \frac{\zeta'(2)}{\zeta(2)}\right]
$$

$$
+ \frac{D-1}{2} I(0_b)\left[I_{n=0}(m_{b2}) + I_{n=0}(m_{b3})\right] + \frac{m_{b2}m_{b3}T^2}{(4\pi)^2}
$$

$$
- \frac{m_{b1}^2 T^2}{(4\pi)^2}\left[\frac{1}{4\epsilon} - \ln\frac{m_{b1} + m_{b2} + m_{b3}}{\bar\mu} + \frac{1}{2}\right] + \mathcal{O}\left(\epsilon T^4, \frac{m^2 T^2}{\pi^2}\right),
$$

$$(A.2.33)$$

$$
H(\underline{m_{b1}}, m_{f2}, m_{f3}) = \frac{T^4}{288}\left[\frac{1}{4\epsilon} + \ln\left(\frac{\bar\mu e^{\gamma_E}}{4T}\right) - \frac{\zeta'(2)}{\zeta(2)}\right] + \mathcal{O}\left(\epsilon T^4, \frac{m^2 T^2}{\pi^2}\right),
$$

$$(A.2.34)$$

$$
H(\underline{m_{f1}}, m_{f2}, m_{b3}) = -\frac{T^4}{144}\left[\frac{1}{4\epsilon} + \ln\left(\frac{\bar\mu e^{\gamma_E}}{T}\right) - \frac{3\ln 2}{2} - \frac{\zeta'(2)}{\zeta(2)}\right]
$$

$$
+ \frac{D-1}{2} I(0_f) I_{n=0}(m_{b3}) + \mathcal{O}\left(\epsilon T^4, \frac{m^2 T^2}{\pi^2}\right). \qquad (A.2.35)
$$

Here only the zero-modes of the I-function with non-zero argument have to be considered as explained in section 3.3. These so called linear terms $\sim mT^3$ are written in D dimensions as to check their D-dimensional cancellation in the full result (cf. the discussion at the end of section 3.1). The function $I_{n=0}(m)$ is given in eq. (1.3.15).

Appendix B

Two-Loop Diagrams

In this Appendix we list the expressions for all the diagrams contributing to the two-loop potential of the Inert Doublet Model as explained in section 3.2. Dropping some v-independent terms for simplicity the expressions read

$$
(sss) = -3v^2\lambda_1^2 \left[H(\widetilde{m}_h, \widetilde{m}_h, \widetilde{m}_h) + H(\widetilde{m}_h, \widetilde{m}_G, \widetilde{m}_G) \right]
$$

$$
- \frac{v^2}{4} \left[\lambda_L^2 H(\widetilde{m}_h, \widetilde{m}_H, \widetilde{m}_H) + \lambda_S^2 H(\widetilde{m}_H, \widetilde{m}_A, \widetilde{m}_A) \right]
$$

$$
- \frac{v^2}{4} \left[(\lambda_4 + \lambda_5)^2 H(\widetilde{m}_G, \widetilde{m}_H, \widetilde{m}_{H^\pm}) + (\lambda_4 - \lambda_5)^2 H(\widetilde{m}_G, \widetilde{m}_A, \widetilde{m}_{H^\pm}) \right]
$$

$$
- \frac{v^2}{2} \left[\lambda_3^2 H(\widetilde{m}_h, \widetilde{m}_{H^\pm}, \widetilde{m}_{H^\pm}) + \lambda_5^2 H(\widetilde{m}_G, \widetilde{m}_H, \widetilde{m}_A) \right] , \qquad \text{(B.0.1)}
$$

$$
(ss) = \frac{3\lambda_1}{4} \left[I^2(\widetilde{m}_h) + 2I(\widetilde{m}_h)I(\widetilde{m}_G) + 5I^2(\widetilde{m}_G) \right]
$$

$$
+ \frac{\lambda_2}{2} \left[I^2(\widetilde{m}_H) + I^2(\widetilde{m}_A) + 2I^2(\widetilde{m}_{H^\pm}) \right]
$$

$$
+ \frac{\lambda_2}{4} \left[I(\widetilde{m}_H) + I(\widetilde{m}_A) + 2I(\widetilde{m}_{H^\pm}) \right]^2
$$

$$
+ \frac{\lambda_L}{4} \left[I(\widetilde{m}_h)I(\widetilde{m}_H) + I(\widetilde{m}_G)I(\widetilde{m}_A) \right]
$$

$$
+ \frac{\lambda_S}{4} \left[I(\widetilde{m}_h)I(\widetilde{m}_A) + I(\widetilde{m}_G)I(\widetilde{m}_H) \right] + (\lambda_3 + \lambda_4)I(\widetilde{m}_G)I(\widetilde{m}_{H^\pm})
$$

$$
+ \frac{\lambda_3}{2}I(\widetilde{m}_h)I(\widetilde{m}_{H^\pm}) + \frac{\lambda_3}{2}I(\widetilde{m}_G)\left[I(\widetilde{m}_H) + I(\widetilde{m}_A) + I(\widetilde{m}_{H^\pm}) \right] , \quad \text{(B.0.2)}
$$

$$
(s) = \frac{1}{2}(\delta m_h^2 - \delta m_{\phi T}^2 - \widetilde{m}_h^2 \delta Z_\phi)I(\widetilde{m}_h) + \frac{3}{2}(\delta m_G^2 - \delta m_{\phi T}^2 - \widetilde{m}_G^2 \delta Z_\phi)I(\widetilde{m}_G)
$$

$$
+ \frac{1}{2}(\delta m_H^2 - \delta m_{\chi T}^2 - \widetilde{m}_H^2 \delta Z_\chi)I(\widetilde{m}_H)
$$

$$
+ \frac{1}{2}(\delta m_A^2 - \delta m_{\chi T}^2 - \widetilde{m}_A^2 \delta Z_\chi)I(\widetilde{m}_A)
$$

$$
+ (\delta m_{H^\pm}^2 - \delta m_{\chi T}^2 - \widetilde{m}_{H^\pm}^2 \delta Z_\chi)I(\widetilde{m}_{H^\pm}) , \qquad \text{(B.0.3)}
$$

$$
(ssv) = -\frac{3g_2^2}{8}\bigg[(\widetilde{m}_W^2 - 2\widetilde{m}_h^2 - 2\widetilde{m}_G^2)H(\widetilde{m}_W, \widetilde{m}_h, \widetilde{m}_G)
$$

$$
+ (\widetilde{m}_W^2 - 4\widetilde{m}_G^2)H(\widetilde{m}_W, \widetilde{m}_G, \widetilde{m}_G)
$$

$$
\begin{aligned}
&- \left[I(\widetilde{m}_h) + I(\widetilde{m}_G)\right] I(\widetilde{m}_G) + 2\left[I(\widetilde{m}_h) + 3I(\widetilde{m}_G)\right] I(\widetilde{m}_W) \\
&+ H(\underline{\widetilde{m}_W}, \widetilde{m}_h, \widetilde{m}_G) - 2H(\widetilde{m}_W, \underline{\widetilde{m}_h}, \widetilde{m}_G) - 2H(\widetilde{m}_W, \widetilde{m}_h, \underline{\widetilde{m}_G}) \\
&+ H(\underline{\widetilde{m}_W}, \widetilde{m}_G, \widetilde{m}_G) - 4H(\widetilde{m}_W, \underline{\widetilde{m}_G}, \widetilde{m}_G) \\
&- H(\underline{m_W}, \widetilde{m}_h, \widetilde{m}_G) + 2H(m_W, \underline{\widetilde{m}_h}, \widetilde{m}_G) + 2H(m_W, \widetilde{m}_h, \underline{\widetilde{m}_G}) \\
&- H(\underline{m_W}, \widetilde{m}_G, \widetilde{m}_G) + 4H(m_W, \underline{\widetilde{m}_G}, \widetilde{m}_G) \Bigg] \\
&- \frac{g_2^2}{8}\Bigg[(\widetilde{m}_W^2 - 2\widetilde{m}_H^2 - 2\widetilde{m}_A^2)H(\widetilde{m}_W, \widetilde{m}_H, \widetilde{m}_A) \\
&+ (\widetilde{m}_W^2 - 4\widetilde{m}_{H^\pm}^2)H(\widetilde{m}_W, \widetilde{m}_{H^\pm}, \widetilde{m}_{H^\pm}) \\
&+ 2(\widetilde{m}_W^2 - 2\widetilde{m}_H^2 - 2\widetilde{m}_{H^\pm}^2)H(\widetilde{m}_W, \widetilde{m}_H, \widetilde{m}_{H^\pm}) \\
&+ 2(\widetilde{m}_W^2 - 2\widetilde{m}_A^2 - 2\widetilde{m}_{H^\pm}^2)H(\widetilde{m}_W, \widetilde{m}_A, \widetilde{m}_{H^\pm}) \\
&- I(\widetilde{m}_H)I(\widetilde{m}_A) - \left[2I(\widetilde{m}_H) + 2I(\widetilde{m}_A) + I(\widetilde{m}_{H^\pm})\right]I(\widetilde{m}_{H^\pm}) \\
&+ 6\left[I(\widetilde{m}_H) + I(\widetilde{m}_A) + 2I(\widetilde{m}_{H^\pm})\right]I(\widetilde{m}_W) \\
&+ H(\underline{\widetilde{m}_W}, \widetilde{m}_H, \widetilde{m}_A) - 2H(\widetilde{m}_W, \underline{\widetilde{m}_H}, \widetilde{m}_A) - 2H(\widetilde{m}_W, \widetilde{m}_H, \underline{\widetilde{m}_A}) \\
&+ 2H(\underline{\widetilde{m}_W}, \widetilde{m}_H, \widetilde{m}_{H^\pm}) - 4H(\widetilde{m}_W, \underline{\widetilde{m}_H}, \widetilde{m}_{H^\pm}) - 4H(\widetilde{m}_W, \widetilde{m}_H, \underline{\widetilde{m}_{H^\pm}}) \\
&+ 2H(\underline{\widetilde{m}_W}, \widetilde{m}_A, \widetilde{m}_{H^\pm}) - 4H(\widetilde{m}_W, \underline{\widetilde{m}_A}, \widetilde{m}_{H^\pm}) - 4H(\widetilde{m}_W, \widetilde{m}_A, \underline{\widetilde{m}_{H^\pm}}) \\
&+ H(\underline{\widetilde{m}_W}, \widetilde{m}_{H^\pm}, \widetilde{m}_{H^\pm}) - 4H(\widetilde{m}_W, \underline{\widetilde{m}_{H^\pm}}, \widetilde{m}_{H^\pm}) \\
&- H(\underline{m_W}, \widetilde{m}_H, \widetilde{m}_A) + 2H(m_W, \underline{\widetilde{m}_H}, \widetilde{m}_A) + 2H(m_W, \widetilde{m}_H, \underline{\widetilde{m}_A}) \\
&- 2H(\underline{m_W}, \widetilde{m}_H, \widetilde{m}_{H^\pm}) + 4H(m_W, \underline{\widetilde{m}_H}, \widetilde{m}_{H^\pm}) + 4H(m_W, \widetilde{m}_H, \underline{\widetilde{m}_{H^\pm}}) \\
&- 2H(\underline{m_W}, \widetilde{m}_A, \widetilde{m}_{H^\pm}) + 4H(m_W, \underline{\widetilde{m}_A}, \widetilde{m}_{H^\pm}) + 4H(m_W, \widetilde{m}_A, \underline{\widetilde{m}_{H^\pm}}) \\
&- H(\underline{m_W}, \widetilde{m}_{H^\pm}, \widetilde{m}_{H^\pm}) + 4H(m_W, \underline{\widetilde{m}_{H^\pm}}, \widetilde{m}_{H^\pm}) \Bigg] , \qquad (\text{B.0.4})
\end{aligned}
$$

$$
\begin{aligned}
(\text{sv}) =\ & \frac{3g_2^2}{8}\left[I(\widetilde{m}_h) + 3I(\widetilde{m}_G)\right]\left[I(\widetilde{m}_W) + (D-1)I(m_W)\right] \\
&+ \frac{3g_2^2}{8}\left[I(\widetilde{m}_H) + I(\widetilde{m}_A) + 2I(\widetilde{m}_{H^\pm})\right]\left[I(\widetilde{m}_W) + (D-1)I(m_W)\right] ,
\end{aligned}
$$
$$(\text{B.0.5})$$

$$
(\text{svv}) = -\frac{3g_2^2 m_W^2}{4}\left[H(\widetilde{m}_h, \widetilde{m}_W, \widetilde{m}_W) + (D-1)H(\widetilde{m}_h, m_W, m_W)\right] , \qquad (\text{B.0.6})
$$

$$
(\text{sgg}) = -\frac{3g_2^2 m_W^2}{4}\left[H(\widetilde{m}_h, m_W, m_W) - 2H(\widetilde{m}_G, m_W, m_W)\right] , \qquad (\text{B.0.7})
$$

$$
\begin{aligned}
(\text{vvv}) =\ & -\frac{3g_2^2}{2}(D-1)\Bigg[(\widetilde{m}_W^2 - 4m_W^2)H(\widetilde{m}_W, m_W, m_W) \\
&+ \left[4I(\widetilde{m}_W) - I(m_W)\right]I(m_W) \\
&+ H(\underline{\widetilde{m}_W}, m_W, m_W) - 4H(\widetilde{m}_W, \underline{m_W}, m_W) + 3H(\underline{m_W}, m_W, m_W) \Bigg] \\
&+ \frac{3g_2^2}{2}\Big[-H(\underline{m_W}, \widetilde{m}_W, \widetilde{m}_W) + 4H(m_W, \underline{\widetilde{m}_W}, \widetilde{m}_W) \\
&- 3H(\underline{m_W}, m_W, m_W)\Big] , \qquad (\text{B.0.8})
\end{aligned}
$$

$$(\text{ggv}) = -\frac{3g_2^2}{2}\bigg[(2m_W^2 - \widetilde{m}_W^2)H(\widetilde{m}_W, m_W, m_W) + [I(m_W) - 2I(\widetilde{m}_W)]\,I(m_W)$$
$$- H(\underline{\widetilde{m}_W}, m_W, m_W) + 4H(\widetilde{m}_W, \underline{m_W}, m_W) - H(\underline{m_W}, m_W, m_W)\bigg]\,,$$
$$(\text{B.0.9})$$

$$(\text{vv}) = \frac{3g_2^2}{2}(D-1)\left[2I(\widetilde{m}_W) + (D-2)I(m_W)\right]I(m_W)\,, \qquad\qquad (\text{B.0.10})$$

$$(\text{v}) = \frac{3}{2}\bigg[\delta Z_\xi\left[I(\widetilde{m}_W) - I(\underline{m_W})\right] + (D-1)m_W^2(\delta Z_{g^2} + \delta Z_\phi)I(m_W)$$
$$+ \left[\widetilde{m}_W^2\delta Z_\xi - m_{\text{E2}}^2\delta Z_A + m_W^2(\delta Z_{g^2} + \delta Z_\phi)\right]I(\widetilde{m}_W)\bigg] - \frac{3}{2}m_{\text{E2}}^2 I(\widetilde{m}_W)\,,$$
$$(\text{B.0.11})$$

$$(\text{g}) = -3m_W^2\left(\delta Z_\xi + \delta Z_{g^2} + \frac{\delta Z_\phi + \delta Z_v}{2}\right)I(m_W)\,, \qquad\qquad (\text{B.0.12})$$

$$(\text{sff}) = -\frac{3g_2^2}{2}\bigg[(\widetilde{m}_h^2 - 4m_t^2)H(\widetilde{m}_h, m_t, m_t) + \widetilde{m}_G H(\widetilde{m}_G, m_t, m_t)$$
$$+ 2(\widetilde{m}_G^2 - m_t^2)H(\widetilde{m}_G, m_t, 0_f) - 2\left[I(m_t) + I(0_f)\right]I(m_t)$$
$$+ 2I(\widetilde{m}_h)I(m_t) + 2I(\widetilde{m}_G)\left[I(0_f) + 2I(m_t)\right]\bigg]\,, \qquad\qquad (\text{B.0.13})$$

$$(\text{gff}) = \frac{3g_2^2}{8}\bigg[(\widetilde{m}_W^2 - 2m_t^2)H(\widetilde{m}_W, m_t, m_t)$$
$$- (D-1)(m_W^2 - 2m_t^2)H(m_W, m_t, m_t)$$
$$+ (D-2)I^2(m_t) + 2\left[I(\widetilde{m}_W) - (D-1)I(m_W)\right]I(m_t)$$
$$- H(\underline{m_W}, m_t, m_t) + 4H(m_W, \underline{m_t}, m_t)$$
$$+ 2H(\underline{\widetilde{m}_W}, m_t, m_t) - 4H(\widetilde{m}_W, \underline{m_t}, m_t)\bigg]$$
$$+ \frac{3g_2^2}{2}\bigg[(\widetilde{m}_W^2 - m_t^2)H(\widetilde{m}_W, m_t, 0_f) - (D-1)(m_W^2 - m_t^2)H(m_W, m_t, 0_f)$$
$$+ (D-2)I(m_t)I(0_f) + \left[I(\widetilde{m}_W) - (D-1)I(m_W)\right]\left[I(m_t) + I(0_f)\right]$$
$$- 2H(\underline{m_W}, m_t, 0_f) + 2H(m_W, \underline{m_t}, 0_f) + 2H(m_W, m_t, \underline{0_f})$$
$$+ 2H(\underline{\widetilde{m}_W}, m_t, 0_f) - 2H(\widetilde{m}_W, \underline{m_t}, 0_f) - 2H(\widetilde{m}_W, m_t, \underline{0_f})\bigg]$$
$$+ \frac{3(8n_G - 5)g_2^2}{8}\bigg[\widetilde{m}_W^2 H(\widetilde{m}_W, 0_f, 0_f) - (D-1)m_W^2 H(m_W, 0_f, 0_f)$$
$$+ (D-2)I^2(0_f) + 2\left[I(\widetilde{m}_W) - (D-1)I(m_W)\right]I(0_f)$$
$$- 2H(\underline{m_W}, 0_f, 0_f) + 4H(m_W, \underline{0_f}, 0_f)$$
$$+ 2H(\underline{\widetilde{m}_W}, 0_f, 0_f) - 4H(\widetilde{m}_W, \underline{0_f}, 0_f)\bigg]$$
$$+ 4g_3^2\bigg[(m_{\text{E3}}^2 - 4m_t^2)H(m_{\text{E3}}, m_t, m_t)$$

$$+ (D-2)I^2(m_t) + 2\left[I(m_{\mathrm{E3}}) - (D-1)I(0_b)\right]I(m_t)$$
$$- 2H(\underline{0_b}, m_t, m_t) + 4H(0_b, \underline{m_t}, m_t)$$
$$+ 2H(\underline{m_{\mathrm{E3}}}, m_t, m_t) - 4H(m_{\mathrm{E3}}, \underline{m_t}, m_t)\Bigg] ,\qquad\qquad\text{(B.0.14)}$$

$$\text{(f)} = -6m_t^2(\delta Z_\phi + \delta Z_{h_t^2})I(m_t) .\qquad\qquad\text{(B.0.15)}$$

Appendix C

Pole Masses

In this Appendix we list the counterterms of the Inert Doublet Model and state their relation to the renormalization group equations. Furthermore, we show the expressions for the one-loop on-shell self-energies. Using these expressions and the pole mass relations we can then write the couplings of the Inert Doublet Model in terms of the pole masses, i.e. physical parameters. We derive the input parameters for our numerical evaluation of the effective potential by solving the system of expressions for the couplings in a self-consistent way as described in section 3.3.

C.1 Counterterms

The bare coupling constants of the Lagrangian of the Inert Doublet Model are expressed as

$$\mu_{iB}^2 = \mu_i^2(1 + \delta Z_{\mu_i^2}) \ , \quad \lambda_{iB} = \lambda_i(1 + \delta Z_{\lambda_i}) \ ,$$
$$g_{iB}^2 = g_i^2(1 + \delta Z_{g_i^2}) \ , \quad h_{tB}^2 = h_t^2(1 + \delta Z_{h_t^2}) \ . \tag{C.1.1}$$

We also need to renormalize certain unphysical quantities, i.e. wave functions and the gauge fixing parameter:

$$\phi_B^\dagger \phi_B = \phi^\dagger \phi(1 + \delta Z_\phi) \ , \quad \chi_B^\dagger \chi_B = \chi^\dagger \chi(1 + \delta Z_\chi) \ ,$$
$$A_{\mu B}^a A_{\nu B}^a = A_\mu^a A_\nu^a(1 + \delta Z_A) \ , \quad \xi_B = \xi(1 + \delta Z_\xi) \ . \tag{C.1.2}$$

The renormalization of the background field (cf. discussion in section 3.1) is given through

$$v_B = v(1 + \delta Z_v) \ . \tag{C.1.3}$$

The computation of the counterterms for the couplings is a standard calculation, presented e.g. in ref. [176]. The wave function counterterms have to cancel the momentum dependent terms in the two-point functions and the background field v is renormalized through the gauge-fixing interaction term given in eq. (3.1.9). The results of the counterterms are

$$\delta Z_{\mu_1^2} = \frac{1}{(4\pi)^2 \epsilon} \left[3h_t^2 - \frac{9g_2^2}{4} + 6\lambda_1 + \frac{\mu_2^2}{\mu_1^2}(2\lambda_3 + \lambda_4) \right] \ , \tag{C.1.4}$$

$$\delta Z_{\mu_2^2} = \frac{1}{(4\pi)^2\epsilon}\left[-\frac{9g_2^2}{4} + 6\lambda_2 + \frac{\mu_1^2}{\mu_2^2}(2\lambda_3 + \lambda_4)\right] , \tag{C.1.5}$$

$$\delta Z_{\lambda_1} = \frac{1}{(4\pi)^2\epsilon}\left[6h_t^2 - \frac{9g_2^2}{2} + \frac{9g_2^4}{16\lambda_1} - \frac{3h_t^2}{\lambda_1} + 12\lambda_1 + \frac{2\lambda_3^2 + 2\lambda_3\lambda_4 + \lambda_4^2 + \lambda_5^2}{2\lambda_1}\right] , \tag{C.1.6}$$

$$\delta Z_{\lambda_2} = \frac{1}{(4\pi)^2\epsilon}\left[-\frac{9g_2^2}{2} + \frac{9g_2^4}{16\lambda_2} + 12\lambda_2 + \frac{2\lambda_3^2 + 2\lambda_3\lambda_4 + \lambda_4^2 + \lambda_5^2}{2\lambda_2}\right] , \tag{C.1.7}$$

$$\delta Z_{\lambda_3} = \frac{1}{(4\pi)^2\epsilon}\left[3h_t^2 - \frac{9g_2^2}{2} + \frac{9g_2^4}{8\lambda_3} + 6(\lambda_1 + \lambda_2) + 2\lambda_3 + \frac{2(\lambda_1 + \lambda_2)\lambda_4 + \lambda_4^2 + \lambda_5^2}{\lambda_3}\right] , \tag{C.1.8}$$

$$\delta Z_{\lambda_4} = \frac{1}{(4\pi)^2\epsilon}\left[3h_t^2 - \frac{9g_2^2}{2} + 2(\lambda_1 + \lambda_2) + 4\lambda_3 + 2\lambda_4 + \frac{4\lambda_5}{\lambda_4}\right] , \tag{C.1.9}$$

$$\delta Z_{\lambda_5} = \frac{1}{(4\pi)^2\epsilon}\left[3h_t^2 - \frac{9g_2^2}{2} + 2(\lambda_1 + \lambda_2) + 4\lambda_3 + 6\lambda_4\right] , \tag{C.1.10}$$

$$\delta Z_{g_2^2} = \frac{g_2^2}{(4\pi)^2\epsilon}\left[\frac{4n_G}{3} - 7\right] , \tag{C.1.11}$$

$$\delta Z_{g_3^2} = \frac{g_3^2}{(4\pi)^2\epsilon}\left[\frac{4n_G}{3} - 11\right] , \tag{C.1.12}$$

$$\delta Z_{h_t^2} = \frac{1}{(4\pi)^2\epsilon}\left[\frac{9h_t^2}{2} - \frac{9g_2^2}{4} - 8g_3^2\right] , \tag{C.1.13}$$

$$\delta Z_\phi = \frac{1}{(4\pi)^2\epsilon}\left[-3h_t^2 + 3g_2^2\right] , \tag{C.1.14}$$

$$\delta Z_v = \frac{1}{(4\pi)^2\epsilon}\left[3h_t^2 + \frac{5g_2^2}{2}\right] , \tag{C.1.15}$$

$$\delta Z_\chi = \frac{1}{(4\pi)^2\epsilon}\frac{3g_2^2}{2} , \tag{C.1.16}$$

$$\delta Z_A = \delta Z_\xi = \frac{g_2^2}{(4\pi)^2\epsilon}\left[3 - \frac{3n_G}{4}\right] . \tag{C.1.17}$$

The renormalization group β-functions are fixed by the counterterms through

$$\bar{\mu}\frac{d\lambda_i}{d\bar{\mu}} = 2\lambda_i\epsilon \ \delta Z_{\lambda_i} + \mathcal{O}(\lambda_i^3) , \tag{C.1.18}$$

and likewise for the other couplings.

C.2   Pole masses

To calculate the one-loop on-shell self-energies in the Higgs broken phase we need to compute the corrections to the two-point functions. The topologies of all the diagrams contributing to the two-point function are shown in figure C.1, where the blob is a counterterm.

The computations are carried out for all the scalars, gauge bosons and the top quark. The results are given in terms of the vacuum master integrals given in Appendix A.1. The resulting expressions for the one-loop on-shell self-energies $\Pi(K;\bar{\mu})$ are
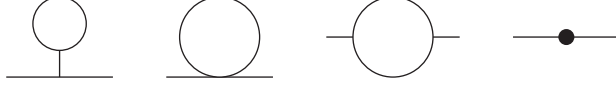
Figure C.1: Topologies contributing to the pole masses.

$$\Pi_h(-im_h;\bar{\mu})$$

$$= m_h^2 \delta Z_{\mu_1^2} + 12h_t^2 A(m_t) - 6\lambda_1 A(m_h) + \left(\frac{3(1-d)}{2}g_2^2 - 6\lambda_1\right)A(m_W)$$

$$- 2\lambda_3 A(m_{H^\pm}) - \lambda_L A(m_H) - \lambda_S A(m_A)$$

$$+ 3h_t^2(4m_t^2 - m_h^2)B(-im_h;m_t,m_t) - 9\lambda_1 m_h^2 B(-im_h;m_h,m_h)$$

$$+ \left(\frac{3}{2}g_2^2\left[(1-d)m_W^2 + m_h^2\right] - 3\lambda_1 m_h^2\right)B(-im_h;m_W,m_W)$$

$$- \lambda_3^2 v_0^2 B(-im_h;m_{H^\pm},m_{H^\pm}) - \frac{1}{2}\lambda_L^2 v_0^2 B(-im_h;m_H,m_H)$$

$$- \frac{1}{2}\lambda_S^2 v_0^2 B(-im_h;m_A,m_A) , \tag{C.2.1}$$

$$\Pi_W^{(T)}(-im_W;\bar{\mu})$$

$$= m_W^2\left(\delta Z_{g_2^2} - \delta Z_{\lambda_1} + \delta Z_{\mu_1^2}\right) + g_2^2\Bigg(\left[\frac{6m_t^2}{m_h^2} - \frac{3}{2}\right]A(m_t) - \frac{A(m_h)}{2}$$

$$+ \left[\frac{3(d-1)m_W^2}{2m_h^2} + 2d - 4\right]A(m_W) + \left[\frac{1}{2} - \frac{\lambda_3 v_0^2}{2m_h^2}\right]A(m_{H^\pm})$$

$$+ \left[\frac{1}{4} - \frac{\lambda_L v_0^2}{4m_h^2}\right]A(m_H) + \left[\frac{1}{4} - \frac{\lambda_S v_0^2}{4m_h^2}\right]A(m_A)$$

$$+ 6m_W^2 B(-im_W;m_W,m_W) - m_W^2 B(-im_W;m_W,m_h)$$

$$+ \frac{3(m_t^2 - m_W^2)}{2}B(-im_W;0,m_t) + \left(\frac{3}{2} - 2n_G\right)m_W^2 B(-im_W;0,0)$$

$$+ (7 - 4d)D^{(T)}(-im_W;m_W,m_W) - D^{(T)}(-im_W;m_W,m_h)$$

$$- D^{(T)}(-im_W;m_{H^\pm},m_H) - D^{(T)}(-im_W;m_{H^\pm},m_A)$$

$$+ 6D^{(T)}(-im_W;0,m_t) + (8n_G - d)D^{(T)}(-im_W;0,0)\Bigg), \tag{C.2.2}$$

$$2[\Sigma_S(-im_t;\bar{\mu}) - \Sigma_V(-im_t;\bar{\mu})] = \delta Z_{h_t^2} - \delta Z_{\lambda_1} + \delta Z_{\mu_1^2}$$

$$+ \frac{1}{m_t^2}\Bigg(12h_t^2 A(m_t) - 6\lambda_1 A(m_h) + \left[\frac{3(d-1)g_2^2}{2} - 6\lambda_1\right]A(m_W)$$

$$- 2\lambda_3 A(m_{H^\pm})1\lambda_L A(m_H) - \lambda_S A(m_A)\Bigg)$$

$$+ \frac{8dg_3^2}{3}B(-im_t;0,m_t) + h_t^2\left[B(-im_t;m_W,m_t) - B(-im_t;m_h,m_t)\right]$$

$$+ \frac{8(d-2)g_3^2}{3}C(-im_t;0,m_t)$$

$$+ \frac{(d-2)g_2^2}{4}\left[2C(-im_t;m_W,0)+C(-im_t;m_W,m_t)\right]$$
$$+ h_t^2\left[C(-im_T;m_h,m_t)+C(-im_t;m_W,m_t)+C(-im_t;m_h,m_t)\right] \ .$$
$$(C.2.3)$$

For the on-shell self-energies of the inert scalars we use $n_3 = n_4 = -n_5 = 1$ and obtain

$$\Pi_H(-im_H;\bar{\mu})$$

$$= \mu_2^2 \delta Z_{\mu_2^2} + \sum_{i=3,4,5} \frac{\lambda_i v_0^2}{2}(\delta Z_{lai} + \delta Z_{\mu_1^2} - \delta Z_{la1})$$

$$+ \frac{12\lambda_L m_t^2}{m_h^2}A(m_t) - \lambda_L A(m_h)$$

$$+ \left[\frac{3(1-d)\lambda_L m_W^2}{m_h^2} + \frac{3(d-2)g_2^2}{4} - \lambda_4 - 2\lambda_5\right]A(m_W)$$

$$+ \left[3\lambda_2 - \frac{\lambda_L^2 v_0^2}{2m_h^2}\right]A(m_H)$$

$$+ \left[\lambda_2 + \frac{g_2^2}{4} + \frac{\lambda_5^2 v_0^2 - (\lambda_3+\lambda_4)^2 v_0^2}{2m_h^2}\right]A(m_A)$$

$$+ \left[2\lambda_2 + \frac{g_2^2}{2} - \frac{\lambda_3\lambda_L v_0^2}{m_h^2}\right]A(m_{H^\pm}) - \Lambda_L^2 v_0^2 B(-im_H;m_h,m_H)$$

$$- \left[\lambda_5^2 v_0^2 + \frac{(m_W^2 - 2m_H^2 - 2m_A^2)g_2^2}{4}\right]B(-im_H;m_W,m_A)$$

$$- \left[\frac{(\lambda_4+\lambda_5)^2 v_0^2}{2} + \frac{(m_W^2 - 2m_H^2 - 2m_{H^\pm})g_2^2}{2}\right]B(-im_H;m_W,m_{H^\pm}) \ ,$$
$$(C.2.4)$$

$$\Pi_A(-im_A;\bar{\mu})$$

$$= \mu_2^2 \delta Z_{\mu_2^2} + \sum_{i=3,4,5} \frac{n_i\lambda_i v_0^2}{2}(\delta Z_{\lambda_i} + \delta Z_{\mu_1^2} - \delta Z_{\lambda_1})$$

$$+ \frac{12\lambda_S m_t^2}{m_h^2}A(m_t) - \lambda_S A(m_h)$$

$$+ \left[\frac{3(1-d)\lambda_S m_W^2}{m_h^2} + \frac{3(d-2)g_2^2}{4} - \lambda_4 + 2\lambda_5\right]A(m_W)$$

$$+ \left[3\lambda_2 - \frac{\lambda_S^2 v_0^2}{2m_h^2}\right]A(m_A)$$

$$+ \left[\lambda_2 + \frac{g_2^2}{4} + \frac{\lambda_5^2 v_0^2 - (\lambda_3+\lambda_4)^2 v_0^2}{2m_h^2}\right]A(m_H)$$

$$+ \left[2\lambda_2 + \frac{g_2^2}{2} - \frac{\lambda_3\lambda_S v_0^2}{m_h^2}\right]A(m_{H^\pm}) - \Lambda_S^2 v_0^2 B(-im_A;m_h,m_A)$$

$$- \left[\lambda_5^2 v_0^2 + \frac{(m_W^2 - 2m_H^2 - 2m_A^2)g_2^2}{4}\right]B(-im_A;m_W,m_H)$$

$$-\left[\frac{(\lambda_4-\lambda_5)^2 v_0^2}{2}+\frac{(m_W^2-2m_A^2-2m_{H^\pm})g_2^2}{2}\right]B(-im_A;m_W,m_{H^\pm})\ ,$$

$$(C.2.5)$$

$\Pi_{H^\pm}(-im_{H^\pm};\bar\mu)$

$$=\mu_2^2\delta Z_{\mu_2^2}+\frac{\lambda_3 v_0^2}{2}(\delta Z_{\lambda_3}+\delta Z_{\mu_1^2}-\delta Z_{\lambda_1})$$

$$+\frac{12\lambda_3 m_t^2}{m_h^2}A(m_t)-\lambda_3 A(m_h)$$

$$+\left[\frac{3(1-d)\lambda_3 m_W^2}{m_h^2}+\frac{3(d-2)g_2^2}{4}+\lambda_4\right]A(m_W)$$

$$+\left[\lambda_2+\frac{g_2^2}{4}-\frac{\lambda_3\lambda_L v_0^2}{2m_h^2}\right]A(m_H)$$

$$+\left[\lambda_2+\frac{g_2^2}{4}-\frac{\lambda_3\lambda_S v_0^2}{2m_h^2}\right]A(m_A)$$

$$+\left[4\lambda_2+\frac{g_2^2}{4}-\frac{\lambda_3^2 v_0^2}{m_h^2}\right]A(m_{H^\pm})-\Lambda_3^2 v_0^2 B(-im_{H^\pm};m_h,m_{H^\pm})$$

$$-\left[\frac{(\lambda_4+\lambda_5)^2 v_0^2}{4}+\frac{(m_W^2-2m_H^2-2m_{H^\pm})g_2^2}{4}\right]B(-im_{H^\pm};m_W,m_H)$$

$$-\left[\frac{(\lambda_4-\lambda_5)^2 v_0^2}{4}+\frac{(m_W^2-2m_A^2-2m_{H^\pm})g_2^2}{4}\right]B(-im_{H^\pm};m_W,m_A)$$

$$-\frac{(m_W^2-4m_{H^\pm})g_2^2}{4}B(-im_{H^\pm};m_W,m_{H^\pm})\ .\qquad(C.2.6)$$

We want to check that all the divergences are canceled by the counterterms given in eqs. (C.1.4) - (C.1.17). To do so we use the tree-level vacuum expectation value v_0 which can be approximated within the one-loop expressions as

$$v_0^2=-\frac{\mu_1^2}{\lambda_1}\approx\frac{m_h^2}{2\lambda_1}\approx\frac{4m_W^2}{g^2}\ .\qquad(C.2.7)$$

We collect all the terms proportional to $[(4\pi)^2\epsilon]^{-1}$ in $\Pi_h(-im_h;\bar\mu)$ for both counterterms and the loop expressions. Using the tree-level mass relations from table 3.1 in chapter 3 and the expressions for the master integrals we get

ct : $m_h^2\left(3h_t^2-\frac{9g_2^2}{4}+6\lambda_1+\frac{\mu_2^2}{\mu_1^2}(2\lambda_3+\lambda_4)\right)=$

$$=m_h^2\left(3h_t^2-\frac{9g_2^2}{4}+6\lambda_1\right)-2\mu_2^2(2\lambda_3+\lambda_4)\ ,\qquad(C.2.8)$$

loops : $-12h_t^2 m_t^2+6\lambda_1 m_h^2-\left(\frac{3(1-d)}{2}g_2^2-6\lambda_1\right)m_W^2+2\lambda_3 m_{H^\pm}^2+\lambda_L m_H^2+\lambda_S m_A^2$

$$+3h_t^2(4m_t^2-m_h^2)-9\lambda_1 m_h^2+\frac{3}{2}g_2^2\left[(1-d)m_W^2+m_h^2\right]-3\lambda_1 m_h^2$$

$$-\lambda_3^2 v_0^2-\frac{1}{2}\lambda_L^2 v_0^2-\frac{1}{2}\lambda_S^2 v_0^2$$

$$=-6\lambda_1 m_h^2+2\mu_2^2(2\lambda_3+\lambda_4)-3h_t^2 m_h^2+\frac{9g_2^2}{4}m_h^2\ .\qquad(C.2.9)$$

Taking now the sum over both $1/\epsilon$ contributions we see that they vanish and thus all the divergences are canceled. Similarly all divergences cancel in the expressions for the other self-energies.

Using these expressions we can write the one-loop corrected masses in the form $m_h = -2\mu_1^2 + \mathrm{Re}\ \Pi_h$, where the couplings and self-energies are understood to be taken at the scale $\bar{\mu} = m_Z$. We can invert these relations to get a set of equations for the different couplings:

$$\mu_1^2(\bar{\mu}) = -\frac{m_h^2}{2}\left[1 - \frac{\mathrm{Re}\ \Pi_h(-im_h;\bar{\mu})}{m_h^2}\right] , \tag{C.2.10}$$

$$\mu_2^2(\bar{\mu}) = m_H^2\left[1 - \frac{\mathrm{Re}\ \Pi_H(-im_H;\bar{\mu})}{m_H^2}\right] - \frac{2\lambda_L m_W^2}{g_0^2}\left[1 - \frac{\delta g_2^2}{g_0^2} - \frac{\mathrm{Re}\ \Pi_W^{(T)}(-im_W;\bar{\mu})}{m_W^2}\right] , \tag{C.2.11}$$

$$\lambda_1(\bar{\mu}) = \frac{g_0^2 m_h^2}{8m_W^2}\left[1 + \frac{\delta g_2^2(\bar{\mu})}{g_0^2} + \frac{\mathrm{Re}\ PiW}{m_W^2} - \frac{\mathrm{Re}\ \Pi_h(-im_h;\bar{\mu})}{m_h^2}\right] , \tag{C.2.12}$$

$$h_t^2(\bar{\mu}) = \frac{g_0^2 m_t^2}{2m_W^2}\left[1 + \frac{\delta g_2^2(\bar{\mu})}{g_0^2} + \frac{\mathrm{Re}\ \Pi_W^{(T)}(-im_W;\bar{\mu})}{m_W^2} - 2(\Sigma_S - \Sigma_V)(-im_t;\bar{\mu})\right] , \tag{C.2.13}$$

$$\begin{aligned}
\lambda_3(\bar{\mu}) = &\frac{g_0^2 m_{H^\pm}^2}{2m_W^2}\left[1 + \frac{\delta g_2^2(\bar{\mu})}{g_0^2} + \frac{\mathrm{Re}\ \Pi_W^{(T)}(-im_W;\bar{\mu})}{m_W^2} - \frac{\mathrm{Re}\ \Pi_{H^\pm}(-im_{H^\pm};\bar{\mu})}{m_{H^\pm}^2}\right] \\
&- \frac{g_0^2 m_H^2}{2m_W^2}\left[1 + \frac{\delta g_2^2(\bar{\mu})}{g_0^2} + \frac{\mathrm{Re}\ \Pi_W^{(T)}(-im_W;\bar{\mu})}{m_W^2} - \frac{\mathrm{Re}\ \Pi_H(-im_H;\bar{\mu})}{m_H^2}\right] \\
&+ \lambda_L(\bar{\mu})\left[1 - \frac{\delta g_2^2(\bar{\mu})}{g_0^2} - \frac{\mathrm{Re}\ \Pi_W^{(T)}(-im_W;\bar{\mu})}{m_W^2}\right] ,
\end{aligned} \tag{C.2.14}$$

$$\begin{aligned}
\lambda_4(\bar{\mu}) = &\frac{g_0^2 m_H^2}{4m_W^2}\left[1 + \frac{\delta g_2^2(\bar{\mu})}{g_0^2} + \frac{\mathrm{Re}\ \Pi_W^{(T)}(-im_W;\bar{\mu})}{m_W^2} - \frac{\mathrm{Re}\ \Pi_H(-im_H;\bar{\mu})}{m_H^2}\right] \\
&+ \frac{g_0^2 m_A^2}{4m_W^2}\left[1 + \frac{\delta g_2^2(\bar{\mu})}{g_0^2} + \frac{\mathrm{Re}\ \Pi_W^{(T)}(-im_W;\bar{\mu})}{m_W^2} - \frac{\mathrm{Re}\ \Pi_A(-im_A;\bar{\mu})}{m_A^2}\right] \\
&- \frac{g_0^2 m_{H^\pm}^2}{2m_W^2}\left[1 + \frac{\delta g_2^2(\bar{\mu})}{g_0^2} + \frac{\mathrm{Re}\ \Pi_W^{(T)}(-im_W;\bar{\mu})}{m_W^2} - \frac{\mathrm{Re}\ \Pi_{H^\pm}(-im_{H^\pm};\bar{\mu})}{m_{H^\pm}^2}\right] \\
&+ \frac{\lambda_L(\bar{\mu})}{2}\left[\frac{\delta g_2^2(\bar{\mu})}{g_0^2} + \frac{\mathrm{Re}\ \Pi_W^{(T)}(-im_W;\bar{\mu})}{m_W^2}\right] ,
\end{aligned} \tag{C.2.15}$$

$$\begin{aligned}
\lambda_5(\bar{\mu}) = &\frac{g_0^2 m_H^2}{4m_W^2}\left[1 + \frac{\delta g_2^2(\bar{\mu})}{g_0^2} + \frac{\mathrm{Re}\ \Pi_W^{(T)}(-im_W;\bar{\mu})}{m_W^2} - \frac{\mathrm{Re}\ \Pi_H(-im_H;\bar{\mu})}{m_H^2}\right] \\
&- \frac{g_0^2 m_A^2}{4m_W^2}\left[1 + \frac{\delta g_2^2(\bar{\mu})}{g_0^2} + \frac{\mathrm{Re}\ \Pi_W^{(T)}(-im_W;\bar{\mu})}{m_W^2} - \frac{\mathrm{Re}\ \Pi_A(-im_A;\bar{\mu})}{m_A^2}\right] \\
&+ \frac{\lambda_L(\bar{\mu})}{2}\left[\frac{\delta g_2^2(\bar{\mu})}{g_0^2} + \frac{\mathrm{Re}\ \Pi_W^{(T)}(-im_W;\bar{\mu})}{m_W^2}\right] ,
\end{aligned} \tag{C.2.16}$$

where $\delta g_2^2(\bar{\mu}) = g_2^2(\bar{\mu}) - g_0^2$. The constant g_0^2 is related to the Fermi constant G_μ as $g_0^2 = 4\sqrt{2}G_\mu m_W^2$ and the Fermi constant is defined in terms of the muon lifetime [177, 178].

Bibliography

[1] M. Laine and M. Meyer, "Standard Model thermodynamics across the electroweak crossover," JCAP **1507** (2015) no.07, 035 [arXiv:1503.04935 [hep-ph]].

[2] M. Laine, M. Meyer and G. Nardini, "Thermal phase transition with full 2-loop effective potential," Nucl. Phys. B **920** (2017) 565 [arXiv:1702.07479 [hep-ph]].

[3] S. L. Glashow, "Partial Symmetries of Weak Interactions," Nucl. Phys. **22** (1961) 579.

[4] S. Weinberg, "A Model of Leptons," Phys. Rev. Lett. **19** (1967) 1264.

[5] A. Salam, "Weak and Electromagnetic Interactions," Conf. Proc. C **680519** (1968) 367.

[6] F. Englert and R. Brout, "Broken Symmetry and the Mass of Gauge Vector Mesons," Phys. Rev. Lett. **13** (1964) 321.

[7] P. W. Higgs, "Spontaneous Symmetry Breakdown without Massless Bosons," Phys. Rev. **145** (1966) 1156.

[8] A. H. Guth, "The Inflationary Universe: A Possible Solution to the Horizon and Flatness Problems," Phys. Rev. D **23** (1981) 347.

[9] A. D. Linde, "A New Inflationary Universe Scenario: A Possible Solution of the Horizon, Flatness, Homogeneity, Isotropy and Primordial Monopole Problems," Phys. Lett. **108B** (1982) 389.

[10] A. Albrecht and P. J. Steinhardt, "Cosmology for Grand Unified Theories with Radiatively Induced Symmetry Breaking," Phys. Rev. Lett. **48** (1982) 1220.

[11] A. D. Linde, "Inflationary Cosmology," Lect. Notes Phys. **738** (2008) 1 [arXiv:0705.0164 [hep-th]].

[12] A. A. Penzias and R. W. Wilson, "A Measurement of excess antenna temperature at 4080-Mc/s," Astrophys. J. **142** (1965) 419.

[13] C. L. Bennett *et al.* [WMAP Collaboration], "Nine-Year Wilkinson Microwave Anisotropy Probe (WMAP) Observations: Final Maps and Results," Astrophys. J. Suppl. **208** (2013) 20 [arXiv:1212.5225 [astro-ph.CO]].

[14] G. Hinshaw *et al.* [WMAP Collaboration], "Nine-Year Wilkinson Microwave Anisotropy Probe (WMAP) Observations: Cosmological Parameter Results," Astrophys. J. Suppl. **208** (2013) 19 [arXiv:1212.5226 [astro-ph.CO]].

[15] P. A. R. Ade *et al.* [Planck Collaboration], "Planck 2015 results. XIII. Cosmological parameters," Astron. Astrophys. **594** (2016) A13 [arXiv:1502.01589 [astro-ph.CO]].

[16] N. Aghanim *et al.* [Planck Collaboration], "Planck 2015 results. XI. CMB power spectra, likelihoods, and robustness of parameters," Astron. Astrophys. **594** (2016) A11 [arXiv:1507.02704 [astro-ph.CO]].

[17] S. Sarkar, "Measuring the baryon content of the universe: BBN versus CMB," astro-ph/0205116.

[18] R. V. Wagoner, W. A. Fowler and F. Hoyle, "On the Synthesis of elements at very high temperatures," Astrophys. J. **148** (1967) 3.

[19] H. Reeves, J. Andouze, W. A. Fowler and D. N. Schramm, "On The Origin Of Light Elements," Astrophys. J. **179** (1973) 909.

[20] A. G. Cohen, A. De Rujula and S. L. Glashow, "A Matter - antimatter universe?," Astrophys. J. **495** (1998) 539 [astro-ph/9707087].

[21] A. D. Sakharov, "Violation of CP Invariance, c Asymmetry, and Baryon Asymmetry of the Universe," Pisma Zh. Eksp. Teor. Fiz. **5** (1967) 32 [JETP Lett. **5** (1967) 24] [Sov. Phys. Usp. **34** (1991) 392] [Usp. Fiz. Nauk **161** (1991) 61].

[22] M. Dine and A. Kusenko, "The Origin of the matter - antimatter asymmetry," Rev. Mod. Phys. **76** (2003) 1 [hep-ph/0303065].

[23] D. E. Morrissey and M. J. Ramsey-Musolf, "Electroweak baryogenesis," New J. Phys. **14** (2012) 125003 [arXiv:1206.2942 [hep-ph]].

[24] P. Minkowski, "$\mu \to e\gamma$ at a Rate of One Out of 10^9 Muon Decays?," Phys. Lett. **67B** (1977) 421.

[25] M. Fukugita and T. Yanagida, "Baryogenesis Without Grand Unification," Phys. Lett. B **174** (1986) 45.

[26] I. Affleck and M. Dine, "A New Mechanism for Baryogenesis," Nucl. Phys. B **249** (1985) 361.

[27] D. A. Kirzhnits and A. D. Linde, "Symmetry Behavior in Gauge Theories," Annals Phys. **101** (1976) 195.

[28] A. A. Belavin, A. M. Polyakov, A. S. Schwartz and Y. S. Tyupkin, "Pseudoparticle Solutions of the Yang-Mills Equations," Phys. Lett. **59B** (1975) 85.

[29] S. S. Chern and J. Simons, "Characteristic forms and geometric invariants," Annals Math. **99** (1974) 48.

[30] E. Witten, "Topological Quantum Field Theory," Commun. Math. Phys. **117** (1988) 353.

[31] G. 't Hooft, "Symmetry Breaking Through Bell-Jackiw Anomalies," Phys. Rev. Lett. **37** (1976) 8.

[32] M. E. Shaposhnikov, "Baryon Asymmetry of the Universe in Standard Electroweak Theory," Nucl. Phys. B **287** (1987) 757.

[33] W. Buchmuller, Z. Fodor and A. Hebecker, "Gauge invariant treatment of the electroweak phase transition," Phys. Lett. B **331** (1994) 131 [hep-ph/9403391].

[34] H. H. Patel and M. J. Ramsey-Musolf, "Baryon Washout, Electroweak Phase Transition, and Perturbation Theory," JHEP **1107** (2011) 029 [arXiv:1101.4665 [hep-ph]].

[35] N. K. Nielsen, "On the Gauge Dependence of Spontaneous Symmetry Breaking in Gauge Theories," Nucl. Phys. B **101** (1975) 173.

[36] R. Fukuda and T. Kugo, "Gauge Invariance in the Effective Action and Potential," Phys. Rev. D **13** (1976) 3469.

[37] M. Quiros, "Finite temperature field theory and phase transitions," hep-ph/9901312.

[38] J. I. Kapusta and C. Gale, "Finite-temperature field theory: Principles and applications,"

[39] M. Laine and A. Vuorinen, "Basics of Thermal Field Theory," Lect. Notes Phys. **925** (2016) pp.1 [arXiv:1701.01554 [hep-ph]].

[40] T. Matsubara, "A New approach to quantum statistical mechanics," Prog. Theor. Phys. **14** (1955) 351.

[41] R. Kubo, "Statistical mechanical theory of irreversible processes. 1. General theory and simple applications in magnetic and conduction problems," J. Phys. Soc. Jap. **12** (1957) 570.

[42] P. C. Martin and J. S. Schwinger, "Theory of many particle systems. 1.," Phys. Rev. **115** (1959) 1342.

[43] R. R. Parwani, "Resummation in a hot scalar field theory," Phys. Rev. D **45** (1992) 4695 Erratum: [Phys. Rev. D **48** (1993) 5965] [hep-ph/9204216].

[44] P. B. Arnold and O. Espinosa, "The Effective potential and first order phase transitions: Beyond leading-order," Phys. Rev. D **47** (1993) 3546 Erratum: [Phys. Rev. D **50** (1994) 6662] [hep-ph/9212235].

[45] M. E. Carrington, "The Effective potential at finite temperature in the Standard Model," Phys. Rev. D **45** (1992) 2933.

[46] G. Aad *et al.* [ATLAS Collaboration], "Observation of a new particle in the search for the Standard Model Higgs boson with the ATLAS detector at the LHC," Phys. Lett. B **716** (2012) 1 [arXiv:1207.7214 [hep-ex]].

[47] S. Chatrchyan *et al.* [CMS Collaboration], "Observation of a new boson at a mass of 125 GeV with the CMS experiment at the LHC," Phys. Lett. B **716** (2012) 30 [arXiv:1207.7235 [hep-ex]].

[48] G. Aad *et al.* [ATLAS and CMS Collaborations], "Combined Measurement of the Higgs Boson Mass in *pp* Collisions at $\sqrt{s}$ = 7 and 8 TeV with the ATLAS and CMS Experiments," Phys. Rev. Lett. **114** (2015) 191803 [arXiv:1503.07589 [hep-ex]].

[49] K. Kajantie, M. Laine, K. Rummukainen and M. E. Shaposhnikov, "Is there a hot electroweak phase transition at m(H) larger or equal to m(W)?," Phys. Rev. Lett. **77** (1996) 2887 [hep-ph/9605288].

[50] K. Rummukainen, M. Tsypin, K. Kajantie, M. Laine and M. E. Shaposhnikov, "The Universality class of the electroweak theory," Nucl. Phys. B **532** (1998) 283 [hep-lat/9805013].

[51] K. Kajantie, M. Laine, K. Rummukainen and M. E. Shaposhnikov, "The Electroweak phase transition: A Nonperturbative analysis," Nucl. Phys. B **466** (1996) 189 [hep-lat/9510020].

[52] F. Csikor, Z. Fodor and J. Heitger, "Endpoint of the hot electroweak phase transition," Phys. Rev. Lett. **82** (1999) 21 [hep-ph/9809291].

[53] F. Karsch, T. Neuhaus, A. Patkos and J. Rank, "Critical Higgs mass and temperature dependence of gauge boson masses in the SU(2) gauge Higgs model," Nucl. Phys. Proc. Suppl. **53** (1997) 623 [hep-lat/9608087].

[54] Y. Aoki, "Four-dimensional simulation of the hot electroweak phase transition with the SU(2) gauge Higgs model," Phys. Rev. D **56** (1997) 3860 [hep-lat/9612023].

[55] M. Gurtler, E. M. Ilgenfritz and A. Schiller, "Where the electroweak phase transition ends," Phys. Rev. D **56** (1997) 3888 [hep-lat/9704013].

[56] M. Laine and K. Rummukainen, "What's new with the electroweak phase transition?," Nucl. Phys. Proc. Suppl. **73** (1999) 180 [hep-lat/9809045].

[57] M. D'Onofrio and K. Rummukainen, "Standard model cross-over on the lattice," Phys. Rev. D **93** (2016) no.2, 025003 [arXiv:1508.07161 [hep-ph]].

[58] G. Steigman, B. Dasgupta and J. F. Beacom, "Precise Relic WIMP Abundance and its Impact on Searches for Dark Matter Annihilation," Phys. Rev. D **86** (2012) 023506 [arXiv:1204.3622 [hep-ph]].

[59] M. D'Onofrio, K. Rummukainen and A. Tranberg, "Sphaleron Rate in the Minimal Standard Model," Phys. Rev. Lett. **113** (2014) no.14, 141602 [arXiv:1404.3565 [hep-ph]].

[60] M. D'Onofrio, K. Rummukainen and A. Tranberg, "The Sphaleron Rate through the Electroweak Cross-over," JHEP **1208** (2012) 123 [arXiv:1207.0685 [hep-ph]].

[61] L. Canetti, M. Drewes, T. Frossard and M. Shaposhnikov, "Dark Matter, Baryogenesis and Neutrino Oscillations from Right Handed Neutrinos," Phys. Rev. D **87** (2013) 093006 [arXiv:1208.4607 [hep-ph]].

[62] K. Kajantie, M. Laine, K. Rummukainen and M. E. Shaposhnikov, "Generic rules for high temperature dimensional reduction and their application to the standard model," Nucl. Phys. B **458** (1996) 90 [hep-ph/9508379].

[63] A. D. Linde, "Infrared Problem in Thermodynamics of the Yang-Mills Gas," Phys. Lett. **96B** (1980) 289.

[64] D. J. Gross, R. D. Pisarski and L. G. Yaffe, "QCD and Instantons at Finite Temperature," Rev. Mod. Phys. **53** (1981) 43.

[65] P. H. Ginsparg, "First Order and Second Order Phase Transitions in Gauge Theories at Finite Temperature," Nucl. Phys. B **170** (1980) 388.

[66] T. Appelquist and R. D. Pisarski, "High-Temperature Yang-Mills Theories and Three-Dimensional Quantum Chromodynamics," Phys. Rev. D **23** (1981) 2305.

[67] M. Laine, "The Renormalized gauge coupling and nonperturbative tests of dimensional reduction," JHEP **9906** (1999) 020 [hep-ph/9903513].

[68] A. Gynther and M. Vepsalainen, "Pressure of the standard model at high temperatures," JHEP **0601** (2006) 060 [hep-ph/0510375].

[69] A. Gynther and M. Vepsalainen, "Pressure of the standard model near the electroweak phase transition," JHEP **0603** (2006) 011 [hep-ph/0512177].

[70] E. Braaten and A. Nieto, "Effective field theory approach to high temperature thermodynamics," Phys. Rev. D **51** (1995) 6990 [hep-ph/9501375].

[71] A. Vuorinen, "Four-loop Feynman diagrams in three dimensions," Master's Thesis (2001)
`http://ethesis.helsinki.fi/julkaisut/mat/fysii/pg/vuorinen/`
`fourloop.pdf`

[72] M. Laine and A. Rajantie, "Lattice continuum relations for 3-D SU(N) + Higgs theories," Nucl. Phys. B **513** (1998) 471 [hep-lat/9705003].

[73] M. Laine and Y. Schroder, "Quark mass thresholds in QCD thermodynamics," Phys. Rev. D **73** (2006) 085009 [hep-ph/0603048].

[74] C. Grojean, G. Servant and J. D. Wells, "First-order electroweak phase transition in the standard model with a low cutoff," Phys. Rev. D **71** (2005) 036001 [hep-ph/0407019].

[75] P. Huang, A. Joglekar, B. Li and C. E. M. Wagner, "Probing the Electroweak Phase Transition at the LHC," Phys. Rev. D **93** (2016) no.5, 055049 [arXiv:1512.00068 [hep-ph]].

[76] N. G. Deshpande and E. Ma, "Pattern of Symmetry Breaking with Two Higgs Doublets," Phys. Rev. D **18** (1978) 2574.

[77] E. Ma, "Verifiable radiative seesaw mechanism of neutrino mass and dark matter," Phys. Rev. D **73** (2006) 077301 [hep-ph/0601225].

[78] R. Barbieri, L. J. Hall and V. S. Rychkov, "Improved naturalness with a heavy Higgs: An Alternative road to LHC physics," Phys. Rev. D **74** (2006) 015007 [hep-ph/0603188].

[79] L. Lopez Honorez, E. Nezri, J. F. Oliver and M. H. G. Tytgat, "The Inert Doublet Model: An Archetype for Dark Matter," JCAP **0702** (2007) 028 [hep-ph/0612275].

[80] M. Gustafsson, E. Lundstrom, L. Bergstrom and J. Edsjo, "Significant Gamma Lines from Inert Higgs Dark Matter," Phys. Rev. Lett. **99** (2007) 041301 [astro-ph/0703512 [ASTRO-PH]].

[81] T. Hambye and M. H. G. Tytgat, "Electroweak symmetry breaking induced by dark matter," Phys. Lett. B **659** (2008) 651 [arXiv:0707.0633 [hep-ph]].

[82] P. Agrawal, E. M. Dolle and C. A. Krenke, "Signals of Inert Doublet Dark Matter in Neutrino Telescopes," Phys. Rev. D **79** (2009) 015015 [arXiv:0811.1798 [hep-ph]].

[83] S. Andreas, M. H. G. Tytgat and Q. Swillens, "Neutrinos from Inert Doublet Dark Matter," JCAP **0904** (2009) 004 [arXiv:0901.1750 [hep-ph]].

[84] T. Hambye, F.-S. Ling, L. Lopez Honorez and J. Rocher, "Scalar Multiplet Dark Matter," JHEP **0907** (2009) 090 Erratum: [JHEP **1005** (2010) 066] [arXiv:0903.4010 [hep-ph]].

[85] C. Arina, F. S. Ling and M. H. G. Tytgat, "IDM and iDM or The Inert Doublet Model and Inelastic Dark Matter," JCAP **0910** (2009) 018 [arXiv:0907.0430 [hep-ph]].

[86] E. M. Dolle and S. Su, "The Inert Dark Matter," Phys. Rev. D **80** (2009) 055012 [arXiv:0906.1609 [hep-ph]].

[87] L. Lopez Honorez and C. E. Yaguna, "The inert doublet model of dark matter revisited," JHEP **1009** (2010) 046 [arXiv:1003.3125 [hep-ph]].

[88] L. Lopez Honorez and C. E. Yaguna, "A new viable region of the inert doublet model," JCAP **1101** (2011) 002 [arXiv:1011.1411 [hep-ph]].

[89] A. Goudelis, B. Herrmann and O. Stål, "Dark matter in the Inert Doublet Model after the discovery of a Higgs-like boson at the LHC," JHEP **1309** (2013) 106 [arXiv:1303.3010 [hep-ph]].

[90] M. Klasen, C. E. Yaguna and J. D. Ruiz-Alvarez, "Electroweak corrections to the direct detection cross section of inert higgs dark matter," Phys. Rev. D **87** (2013) 075025 [arXiv:1302.1657 [hep-ph]].

[91] A. Arhrib, Y. L. S. Tsai, Q. Yuan and T. C. Yuan, "An Updated Analysis of Inert Higgs Doublet Model in light of the Recent Results from LUX, PLANCK, AMS-02 and LHC," JCAP **1406** (2014) 030 [arXiv:1310.0358 [hep-ph]].

[92] K. P. Modak and D. Majumdar, "Confronting Galactic and Extragalactic γ-rays Observed by Fermi-lat With Annihilating Dark Matter in an Inert Higgs Doublet Model," Astrophys. J. Suppl. **219** (2015) no.2, 37 [arXiv:1502.05682 [hep-ph]].

[93] F. S. Queiroz and C. E. Yaguna, "The CTA aims at the Inert Doublet Model," JCAP **1602** (2016) no.02, 038 [arXiv:1511.05967 [hep-ph]].

[94] C. Garcia-Cely, M. Gustafsson and A. Ibarra, "Probing the Inert Doublet Dark Matter Model with Cherenkov Telescopes," JCAP **1602** (2016) no.02, 043 [arXiv:1512.02801 [hep-ph]].

[95] S. Banerjee and N. Chakrabarty, "A revisit to scalar dark matter with radiative corrections," arXiv:1612.01973 [hep-ph].

[96] I. F. Ginzburg, K. A. Kanishev, M. Krawczyk and D. Sokolowska, "Evolution of Universe to the present inert phase," Phys. Rev. D **82** (2010) 123533 [arXiv:1009.4593 [hep-ph]].

[97] T. A. Chowdhury, M. Nemevsek, G. Senjanovic and Y. Zhang, "Dark Matter as the Trigger of Strong Electroweak Phase Transition," JCAP **1202** (2012) 029 [arXiv:1110.5334 [hep-ph]].

[98] D. Borah and J. M. Cline, "Inert Doublet Dark Matter with Strong Electroweak Phase Transition," Phys. Rev. D **86** (2012) 055001 [arXiv:1204.4722 [hep-ph]].

[99] G. Gil, P. Chankowski and M. Krawczyk, "Inert Dark Matter and Strong Electroweak Phase Transition," Phys. Lett. B **717** (2012) 396 [arXiv:1207.0084 [hep-ph]].

[100] J. M. Cline and K. Kainulainen, "Improved Electroweak Phase Transition with Subdominant Inert Doublet Dark Matter," Phys. Rev. D **87** (2013) no.7, 071701 [arXiv:1302.2614 [hep-ph]].

[101] N. Blinov, J. Kozaczuk, D. E. Morrissey and C. Tamarit, "Electroweak Baryogenesis from Exotic Electroweak Symmetry Breaking," Phys. Rev. D **92** (2015) no.3, 035012 [arXiv:1504.05195 [hep-ph]].

[102] N. Blinov, S. Profumo and T. Stefaniak, "The Electroweak Phase Transition in the Inert Doublet Model," JCAP **1507** (2015) no.07, 028 [arXiv:1504.05949 [hep-ph]].

[103] P. Basler, M. Krause, M. Muhlleitner, J. Wittbrodt and A. Wlotzka, "Strong First Order Electroweak Phase Transition in the CP-Conserving 2HDM Revisited," JHEP **1702** (2017) 121 [arXiv:1612.04086 [hep-ph]].

[104] D. Land and E. D. Carlson, "Two stage phase transition in two Higgs models," Phys. Lett. B **292** (1992) 107 [hep-ph/9208227].

[105] A. Hammerschmitt, J. Kripfganz and M. G. Schmidt, "Baryon asymmetry from a two stage electroweak phase transition?," Z. Phys. C **64** (1994) 105 [hep-ph/9404272].

[106] S. Inoue, G. Ovanesyan and M. J. Ramsey-Musolf, "Two-Step Electroweak Baryogenesis," Phys. Rev. D **93** (2016) 015013 [arXiv:1508.05404 [hep-ph]].

[107] M. Sperling, D. Stöckinger and A. Voigt, "Renormalization of vacuum expectation values in spontaneously broken gauge theories," JHEP **1307** (2013) 132 [arXiv:1305.1548 [hep-ph]].

[108] M. Sperling, D. Stöckinger and A. Voigt, "Renormalization of vacuum expectation values in spontaneously broken gauge theories: Two-loop results," JHEP **1401** (2014) 068 [arXiv:1310.7629 [hep-ph]].

[109] G. C. Wick, "The Evaluation of the Collision Matrix," Phys. Rev. **80** (1950) 268.

[110] J. C. Collins, "Renormalization : An Introduction to Renormalization, The Renormalization Group, and the Operator Product Expansion,"

[111] M. Laine and M. Losada, "Two loop dimensional reduction and effective potential without temperature expansions," Nucl. Phys. B **582** (2000) 277 [hep-ph/0003111].

[112] S. Groote, J. G. Korner and A. A. Pivovarov, "On the evaluation of sunset - type Feynman diagrams," Nucl. Phys. B **542** (1999) 515 [hep-ph/9806402].

[113] G. Passarino, "An Approach toward the numerical evaluation of multiloop Feynman diagrams," Nucl. Phys. B **619** (2001) 257 [hep-ph/0108252].

[114] M. Caffo, H. Czyz, S. Laporta and E. Remiddi, "The Master differential equations for the two loop sunrise selfmass amplitudes," Nuovo Cim. A **111** (1998) 365 [hep-th/9805118].

[115] S. R. Coleman and E. J. Weinberg, "Radiative Corrections as the Origin of Spontaneous Symmetry Breaking," Phys. Rev. D **7** (1973) 1888.

[116] M. E. Peskin and T. Takeuchi, "A New constraint on a strongly interacting Higgs sector," Phys. Rev. Lett. **65** (1990) 964.

[117] M. E. Peskin and T. Takeuchi, "Estimation of oblique electroweak corrections," Phys. Rev. D **46** (1992) 381.

[118] A. Barroso, P. M. Ferreira, I. P. Ivanov and R. Santos, "Metastability bounds on the two Higgs doublet model," JHEP **1306** (2013) 045 [arXiv:1303.5098 [hep-ph]].

[119] N. Chakrabarty, D. K. Ghosh, B. Mukhopadhyaya and I. Saha, "Dark matter, neutrino masses and high scale validity of an inert Higgs doublet model," Phys. Rev. D **92** (2015) no.1, 015002 [arXiv:1501.03700 [hep-ph]].

[120] N. Khan and S. Rakshit, "Constraints on inert dark matter from metastability of electroweak vacuum," arXiv:1503.03085 [hep-ph].

[121] B. Swiezewska, "Inert scalars and vacuum metastability around the electroweak scale," JHEP **1507** (2015) 118 [arXiv:1503.07078 [hep-ph]].

[122] P. M. Ferreira and B. Swiezewska, "One-loop contributions to neutral minima in the inert doublet model," JHEP **1604** (2016) 099 [arXiv:1511.02879 [hep-ph]].

[123] Q. H. Cao, E. Ma and G. Rajasekaran, "Observing the Dark Scalar Doublet and its Impact on the Standard-Model Higgs Boson at Colliders," Phys. Rev. D **76** (2007) 095011 [arXiv:0708.2939 [hep-ph]].

[124] E. Lundstrom, M. Gustafsson and J. Edsjo, "The Inert Doublet Model and LEP II Limits," Phys. Rev. D **79** (2009) 035013 [arXiv:0810.3924 [hep-ph]].

[125] E. Dolle, X. Miao, S. Su and B. Thomas, "Dilepton Signals in the Inert Doublet Model," Phys. Rev. D **81** (2010) 035003 [arXiv:0909.3094 [hep-ph]].

[126] M. Gustafsson, S. Rydbeck, L. Lopez-Honorez and E. Lundstrom, "Status of the Inert Doublet Model and the Role of multileptons at the LHC," Phys. Rev. D **86** (2012) 075019 [arXiv:1206.6316 [hep-ph]].

[127] A. Arhrib, R. Benbrik and N. Gaur, "$H \to \gamma\gamma$ in Inert Higgs Doublet Model," Phys. Rev. D **85** (2012) 095021 [arXiv:1201.2644 [hep-ph]].

[128] M. Krawczyk, D. Sokolowska, P. Swaczyna and B. Swiezewska, "Constraining Inert Dark Matter by $R_{\gamma\gamma}$ and WMAP data," JHEP **1309** (2013) 055 [arXiv:1305.6266 [hep-ph]].

[129] G. C. Dorsch, S. J. Huber, K. Mimasu and J. M. No, "Echoes of the Electroweak Phase Transition: Discovering a second Higgs doublet through $A_0 \to ZH_0$," Phys. Rev. Lett. **113** (2014) no.21, 211802 [arXiv:1405.5537 [hep-ph]].

[130] G. Belanger, B. Dumont, A. Goudelis, B. Herrmann, S. Kraml and D. Sengupta, "Dilepton constraints in the Inert Doublet Model from Run 1 of the LHC," Phys. Rev. D **91** (2015) no.11, 115011 [arXiv:1503.07367 [hep-ph]].

[131] A. Ilnicka, M. Krawczyk and T. Robens, "Inert Doublet Model in light of LHC Run I and astrophysical data," Phys. Rev. D **93** (2016) no.5, 055026 [arXiv:1508.01671 [hep-ph]].

[132] N. Blinov, J. Kozaczuk, D. E. Morrissey and A. de la Puente, "Compressing the Inert Doublet Model," Phys. Rev. D **93** (2016) no.3, 035020 [arXiv:1510.08069 [hep-ph]].

[133] M. A. Díaz, B. Koch and S. Urrutia-Quiroga, "Constraints to Dark Matter from Inert Higgs Doublet Model," Adv. High Energy Phys. **2016** (2016) 8278375 [arXiv:1511.04429 [hep-ph]].

[134] M. Hashemi, M. Krawczyk, S. Najjari and A. F. Żarnecki, "Production of Inert Scalars at the high energy e^+e^- colliders," JHEP **1602** (2016) 187 [arXiv:1512.01175 [hep-ph]].

[135] P. Poulose, S. Sahoo and K. Sridhar, "Exploring the Inert Doublet Model through the dijet plus missing transverse energy channel at the LHC," Phys. Lett. B **765** (2017) 300 [arXiv:1604.03045 [hep-ph]].

[136] S. Kanemura, M. Kikuchi and K. Sakurai, "Testing the dark matter scenario in the inert doublet model by future precision measurements of the Higgs boson couplings," Phys. Rev. D **94** (2016) no.11, 115011 [arXiv:1605.08520 [hep-ph]].

[137] A. Datta, N. Ganguly, N. Khan and S. Rakshit, "Exploring collider signatures of the inert Higgs doublet model," Phys. Rev. D **95** (2017) no.1, 015017 [arXiv:1610.00648 [hep-ph]].

[138] M. Hashemi and S. Najjari, "Observability of Inert Scalars at the LHC," arXiv:1611.07827 [hep-ph].

[139] A. Belyaev, G. Cacciapaglia, I. P. Ivanov, F. Rojas and M. Thomas, "Anatomy of the Inert Two Higgs Doublet Model in the light of the LHC and non-LHC Dark Matter Searches," arXiv:1612.00511 [hep-ph].

[140] I. P. Ivanov, "Minkowski space structure of the Higgs potential in 2HDM," Phys. Rev. D **75** (2007) 035001 [Phys. Rev. D **76** (2007) 039902] [hep-ph/0609018].

[141] B. W. Lee, C. Quigg and H. B. Thacker, "Weak Interactions at Very High-Energies: The Role of the Higgs Boson Mass," Phys. Rev. D **16** (1977) 1519.

[142] I. P. Ivanov, "Minkowski space structure of the Higgs potential in 2HDM. II. Minima, symmetries, and topology," Phys. Rev. D **77** (2008) 015017 [arXiv:0710.3490 [hep-ph]].

[143] A. Arhrib, "Unitarity constraints on scalar parameters of the standard and two Higgs doublets model," hep-ph/0012353.

[144] I. F. Ginzburg and I. P. Ivanov, "Tree-level unitarity constraints in the most general 2HDM," Phys. Rev. D **72** (2005) 115010 [hep-ph/0508020].

[145] J. S. Schwinger, "A Theory of the Fundamental Interactions," Annals Phys. **2** (1957) 407.

[146] A. Castillo, R. A. Diaz, J. Morales and C. G. Tarazona, "Study of vacuum behavior for inert models with discrete Z_2-like and abelian $U(1)$ symmetries," arXiv:1510.00494 [hep-ph].

[147] M. Baak, M. Goebel, J. Haller, A. Hoecker, D. Ludwig, K. Moenig, M. Schott and J. Stelzer, "Updated Status of the Global Electroweak Fit and Constraints on New Physics," Eur. Phys. J. C **72** (2012) 2003 [arXiv:1107.0975 [hep-ph]].

[148] G. Belanger, F. Boudjema, A. Pukhov and A. Semenov, "MicrOMEGAs 2.0: A Program to calculate the relic density of dark matter in a generic model," Comput. Phys. Commun. **176** (2007) 367 [hep-ph/0607059].

[149] A. Vicente, "Computer tools in particle physics," arXiv:1507.06349 [hep-ph].

[150] F. Staub, "Sarah," arXiv:0806.0538 [hep-ph].

[151] W. Porod and F. Staub, "SPheno 3.1: Extensions including flavour, CP-phases and models beyond the MSSM," Comput. Phys. Commun. **183** (2012) 2458 [arXiv:1104.1573 [hep-ph]].

[152] M. Laine and K. Rummukainen, "Two Higgs doublet dynamics at the electroweak phase transition: A Nonperturbative study," Nucl. Phys. B **597** (2001) 23 [hep-lat/0009025].

[153] M. Laine, G. Nardini and K. Rummukainen, "Lattice study of an electroweak phase transition at m_h 126 GeV," JCAP **1301** (2013) 011 [arXiv:1211.7344 [hep-ph]].

[154] G. D. Moore and K. Rummukainen, "Electroweak bubble nucleation, nonperturbatively," Phys. Rev. D **63** (2001) 045002 [hep-ph/0009132].

[155] K. Kokkotas, "Gravitational Wave Physics,"
`http://www.tat.physik.uni-tuebingen.de/~kokkotas/Teaching/`
`NS.BH.GW_files/GW_Physics.pdf`

[156] M. Kamionkowski, A. Kosowsky and M. S. Turner, "Gravitational radiation from first order phase transitions," Phys. Rev. D **49** (1994) 2837 [astro-ph/9310044].

[157] S. J. Huber and T. Konstandin, "Gravitational Wave Production by Collisions: More Bubbles," JCAP **0809** (2008) 022 [arXiv:0806.1828 [hep-ph]].

[158] M. Hindmarsh, S. J. Huber, K. Rummukainen and D. J. Weir, "Gravitational waves from the sound of a first order phase transition," Phys. Rev. Lett. **112** (2014) 041301 [arXiv:1304.2433 [hep-ph]].

[159] M. Hindmarsh, S. J. Huber, K. Rummukainen and D. J. Weir, "Numerical simulations of acoustically generated gravitational waves at a first order phase transition," Phys. Rev. D **92** (2015) no.12, 123009 [arXiv:1504.03291 [astro-ph.CO]].

[160] C. Caprini, R. Durrer and G. Servant, "The stochastic gravitational wave background from turbulence and magnetic fields generated by a first-order phase transition," JCAP **0912** (2009) 024 [arXiv:0909.0622 [astro-ph.CO]].

[161] C. Caprini *et al.*, "Science with the space-based interferometer eLISA. II: Gravitational waves from cosmological phase transitions," JCAP **1604**, no. 04, 001 (2016) [arXiv:1512.06239 [astro-ph.CO]].

[162] D. Bodeker and G. D. Moore, "Electroweak Bubble Wall Speed Limit," JCAP **1705** (2017) no.05, 025 [arXiv:1703.08215 [hep-ph]].

[163] H. Audley *et al.*, "Laser Interferometer Space Antenna," arXiv:1702.00786 [astro-ph.IM].

[164] W. T. Ni, "Gravitational waves, dark energy and inflation," Mod. Phys. Lett. A **25** (2010) 922 [arXiv:1003.3899 [astro-ph.CO]].

[165] W. T. Ni, "Gravitational wave detection in space," Int. J. Mod. Phys. D **25** (2016) no.14, 1630001 [arXiv:1610.01148 [astro-ph.IM]].

[166] G. M. Harry [LIGO Scientific Collaboration], "Advanced LIGO: The next generation of gravitational wave detectors," Class. Quant. Grav. **27** (2010) 084006.

[167] J. Aasi *et al.* [LIGO Scientific Collaboration], "Advanced LIGO," Class. Quant. Grav. **32** (2015) 074001 [arXiv:1411.4547 [gr-qc]].

[168] B. P. Abbott *et al.* [LIGO Scientific and Virgo Collaborations], "Observation of Gravitational Waves from a Binary Black Hole Merger," Phys. Rev. Lett. **116** (2016) no.6, 061102 [arXiv:1602.03837 [gr-qc]].

[169] B. P. Abbott *et al.* [LIGO Scientific and Virgo Collaborations], "GW151226: Observation of Gravitational Waves from a 22-Solar-Mass Binary Black Hole Coalescence," Phys. Rev. Lett. **116** (2016) no.24, 241103 [arXiv:1606.04855 [gr-qc]].

[170] B. P. Abbott *et al.* [LIGO Scientific and VIRGO Collaborations], "GW170104: Observation of a 50-Solar-Mass Binary Black Hole Coalescence at Redshift 0.2," Phys. Rev. Lett. **118** (2017) no.22, 221101 [arXiv:1706.01812 [gr-qc]].

[171] K. Danzmann *et al.* "Laser Interferometer Space Antenna," [arXiv:1702.00786 [astro-ph.IM]]

[172] J. Crowder and N. J. Cornish, "Beyond LISA: Exploring future gravitational wave missions," Phys. Rev. D **72** (2005) 083005 [gr-qc/0506015].

[173] P. B. Arnold and C. X. Zhai, "The Three loop free energy for pure gauge QCD," Phys. Rev. D **50** (1994) 7603 [hep-ph/9408276].

[174] P. B. Arnold and C. x. Zhai, "The Three loop free energy for high temperature QED and QCD with fermions," Phys. Rev. D **51** (1995) 1906 [hep-ph/9410360].

[175] M. Nishimura and Y. Schroder, "IBP methods at finite temperature," JHEP **1209** (2012) 051 [arXiv:1207.4042 [hep-ph]].

[176] M. E. Peskin and D. V. Schroeder, "An Introduction to quantum field theory," Reading, USA: Addison-Wesley (1995) 842 p

[177] A. Sirlin, "Radiative Corrections in the $SU(2)_L \times U(1)$ Theory: A Simple Renormalization Framework," Phys. Rev. D **22** (1980) 971.

[178] A. Sirlin, "On the $\mathcal{O}(\alpha^2)$ Corrections to τ_μ, m_W, m_Z in the $SU(2)_L \times U(1)$ Theory," Phys. Rev. D **29** (1984) 89.

Erklärung

gemäss Art. 28 Abs. 2 RSL 05

Name, Vorname: Meyer, Manuel

Matrikelnummer: 08-113-631

Studiengang: Theoretische Physik

                    Bachelor ☐   Master ☐   Dissertation ☒

Titel der Arbeit: Electroweak Phase Transition in the Standard
                    Model and its Inert Higgs Doublet Extension

Leiter der Arbeit: Prof. Dr. Mikko Laine

Ich erkläre hiermit, dass ich diese Arbeit selbständig verfasst und keine anderen als die angegebenen Quellen benutzt habe. Alle Stellen, die wörtlich oder sinngemäss aus Quellen entnommen wurden, habe ich als solche gekennzeichnet. Mir ist bekannt, dass andernfalls der Senat gemäss Artikel 36 Absatz 1 Buchstabe r des Gesetztes vom 5. September 1996 über die Universität zum Entzug des auf Grund dieser Arbeit verliehenen Titels berechtigt ist.

Ich gewähre hiermit Einsicht in diese Arbeit.

Bern, 08.08.2017

Manuel Meyer

Curriculum Vitae

Personal Information

Name	Manuel Meyer
Date of birth	26. April 1988
Contact	maenu.meyer@bluewin.ch

Education

08/1995–07/2004	Primary school in Grosshöchstetten
08/2004–07/2007	High school Burgdorf, specializing in physics and mathematics
09/2008–09/2011	B.Sc. in physics, Universität Bern Bachelor thesis: *Dirac Algebra in Mathematica* Supervisor: Prof. Dr. Thomas Becher
09/2011–05/2013	M.Sc. in theoretical physics, Universität Bern Master thesis: *Maxwell Fields on Branes* Supervisor: Prof. Dr. Jean-Pierre Derendinger
09/2013–08/2017	Ph.D. in theoretical physics, Universität Bern Attended schools in Göttingen, Erice (awarded for best theoretical new talent presentation) and Schladming and conferences in Lausanne (SEWM 2014), Munich (MIAPP Baryogenesis 2016) and Stavanger (SEWM 2016)